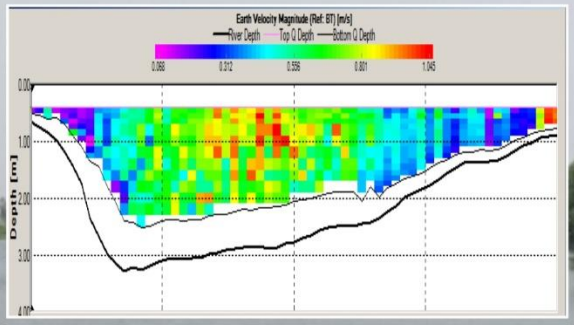
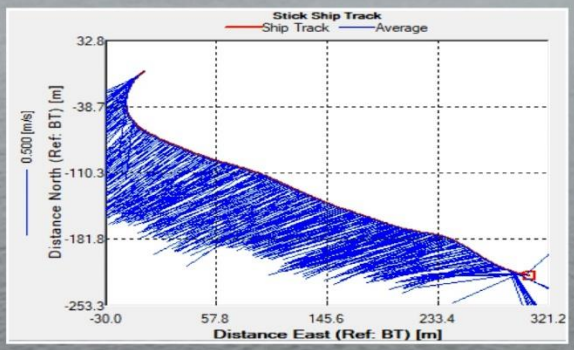
PCRWR

unesco

JICA

Hydro-Morphology of the Tributaries and Active Flood Plains of the River Indus







Manzoor Ahmad Malik
Muhammad Ashraf

Pakistan Council of Research in Water Resources (PCRWR)
2021

Citation:

Malik, M.A., M. Ashraf (2021). Hydro-Morphology of the Tributaries and Active Flood Plains of the River Indus. Pakistan Council of Research in Water Resources (PCRWR). pp 80.

© All rights reserved by PCRWR. The authors encourage fair use of this material for non-commercial purposes with proper citation.

ISBN: 978-969-8469-78-1

Disclaimer:

The views expressed in this report are those of the authors and not necessarily those of the institution. Where trade names are used, it does not imply endorsement of, or discrimination against, any product.

Hydro-Morphology of the Tributaries and Active Flood Plains of the River Indus

Manzoor Ahmad Malik
Muhammad Ashraf

Pakistan Council of Research in Water Resources
2021

Table of Contents

FOREWORD v
Executive Summary vii
Acknowledgements ix
1. Introduction 1
1.1. Theory and literature 2
1.2. Boat tracking for making measurements 4
1.3. Compass calibration 5
1.4. Moving bed test 5
1.5. Riverbed material sampling 6
1.6. Description of the study area 6
2. Methodology 9
2.1. Measurement of river flow and morphology 9
2.2. Measurement of the seepage rate 11
2.3. Riverbed sediment sampling and analysis 13
2.4. Measurement of infiltration rates and determining soil texture 14
3. Results and discussions 16
3.1. Coverage of measurements at river sections 16
3.2. Evaluation of flow measurements 17
3.3 Compass calibration 29
3.4 Moving bed test 30
3.5 Point seepage rates 30
3.6 Infiltration rates 33
3.6.1 Spatial coverage of Horton's steady state infiltration rates 33
3.7 Soil texture classes 38
3.8. Bed material of eastern rivers 43
3.8.1 Bed material profile of the river Jhelum 43
3.8.2. Bed material profile of the river Chenab 44
3.8.3. Bed material profile of the river Ravi 45
3.8.4. Bed material profile of the river Sutlej 46
3.9. Soil moisture retention characteristics and allied parameters 48
4. Major Findings 52
References 53
ANNEXURES 57

List of Tables

Table 1: Attributes of the Indus river system and its eastern tributaries 8

Table 2: River wise distribution of surveyed river cross sections 17

Table 3: Compass calibration results at the selected river sections 29

Table 4: Moving bed test results of the selected river sections 30

Table 5: Spatial coverage percentages of different soil classes in the surface, middle and bottom layers of soil pits in active flood plains along the banks of the eastern tributaries..... 39

Table 6: Descriptive statistics of soil physical and hydraulic parameters along the 50 selected sections of the eastern tributaries of the river Indus..... 51

List of Figures

Figure 1: Unmeasured areas in ADCP measurement cross section (Simpson, 2001). 4

Figure 2: Field operation of ADCP River Ray tethered to boat and real time monitoring of the transect on the host laptop..... 9

Figure 3: A view of the measurement of distance of the end of the transect to the riverbank with laser range finder..... 11

Figure 4: Assembly and operation of seepage meter for measurement of seepage rate 12

Figure 5: A view of the seepage meter installed in the river for measurement of seepage rate 13

Figure 6: US BMH-53 bed material sediment sampler used for river bed sampling 15

Figure 7: Field setup for double ring infiltration test 15

Figure 8: Spatial distribution of survey sites on all the four eastern tributaries of the river Indus..... 16

Figure 9: ADCP based measurement of discharge of the river Jhelum in chronological order of measurement dates 20

Figure 10: ADCP based measurement of discharge of the river Jhelum in the order of upstream to downstream measurement sections..... 21

Figure 11: ADCP measured section profile of the river Jhelum at section JEH-14..... 21

Figure 12: ADCP based measurement of discharge of the river Chenab in chronological order of measurement dates 22

Figure 13: ADCP based measurement of discharge of the river Chenab in the order of upstream to downstream measurement sections..... 23

Figure 14: PID infographic showing the rivers and canals discharges for October 24, 2017 (source: www.irrigation.punjab.gov.pk)..... 24

Figure 15: A view of the ADCP measurements being made at upstream of Trimmu barrage..... 25

Figure 16: ADCP based measurement of discharge of the river Ravi in chronological order of measurement dates 26

Figure 17: ADCP based measurement of discharge of the river Ravi in the order of upstream to downstream measurement sections 27

Figure 18: ADCP based measurement of discharge of the river Sutlej in chronological order of measurement dates 28

Figure 19: ADCP based measurement of discharge of the river Sutlej in the order of upstream to downstream measurement sections 29

Figure 20: Seepage rates at the sections of discharge measurement in all the eastern rivers..... 32

Figure 21: Comparison of R^2 of fitting cumulative infiltration data on Philip and Horton equations 34
Figure 22: Spatial coverage of Horton's steady state infiltration rates in the surface layer of active flood plains (20 km each side) of the eastern rivers 35
Figure 23: Spatial coverage of Horton's steady state infiltration rates in the middle layer of active flood plains (20 km each side) of the eastern rivers 36
Figure 24: Spatial coverage of Horton's steady state infiltration rates in the bottom layer of active flood plains (20 km each side) of the eastern rivers 37
Figure 25: Spatial coverage percentages of different ranges of infiltration rates at the surface, middle and bottom layers along the banks of the eastern tributaries 38
Figure 26: Spatial coverage of soil classes in the surface layer of active flood plains (20 km each side) of the eastern rivers 40
Figure 27: Spatial coverage of soil classes in the middle layer of active flood plains (20 km each side) of the eastern rivers 41
Figure 28: Spatial coverage of soil classes in the bottom layer of active flood plains (20 km each side) of the eastern rivers 42
Figure 29: Bed material uniformity coefficient and mean particle size from upstream to downstream reach on both the banks of the river Jhelum 44
Figure 30: Bed material uniformity coefficient and mean particle size from upstream to downstream reach on both the banks of the river Chenab 45
Figure 31: Bed material uniformity coefficient and mean particle size from upstream to downstream reach on both the banks of the river Ravi 46
Figure 32: Bed material uniformity coefficient and mean particle size from upstream to downstream reach on both the banks of the river Sutlej 47
Figure 33: A view of the river Sutlej without any water at Bahawalpur Bridge 47
Figure 34: Soil moisture-retention curves for representative soil types of river banks 50

FOREWORD

The growing climate change impacts on the hydrological extremes are well accepted by the scientific community and Pakistan is amongst the worst hit by it. After the devastating historical flood of 2010, dire need of upgrading flood forecasting capacity of the country was felt. UNESCO and JICA closely worked together to provide financial and technical support under the umbrella project titled “Strategic Strengthening of Flood Warning and Management Capacity of Pakistan”. Given the scarcity of data to calibrate and validate forecasting models, a key challenge was to collect and collate local data of hydro-morphological features of rivers and physico-hydraulic characteristics of the Indus Basin soils. This data was later used for Integrated Flood Forecasting System (IFS model) for the River Indus and its tributaries. Pakistan Council of Research in Water Resources (PCRWR) was entrusted with this task under the project using state of the art Acoustic Doppler Current Profiler (ADCP) for measurement of river flow regimes and morphological profiles. PCRWR also immensely contributed towards capacity building of local professionals in its usage.

I am pleased to note that PCRWR indigenously developed equipment for measurement of seepage rates was instrumental in collecting data on bed material profiles along the rivers. A well-equipped laboratory was established for the analysis of soil physico-hydraulic properties using georeferenced samples collected from the field. The overall volume and quality of data collected and collated as well as building capacity of PCRWR professionals has been outstanding and fully met International Standards.

This research report pertains to the hydro-morphological features of the eastern tributaries of the River Indus. These tributaries pass through the terrain which is well populated as well as had vast agricultural fields. These data sets have already helped improve the early warning and flood management system of Pakistan and in future will also contribute towards better water resources management, disaster risk reduction and agricultural productivity enhancement. I sincerely hope this report becomes a key reference for models and modellers working on improved understanding of climate change impacts and devising adaptations for the sustainable water sector growth of the country, a key aim of the United Nations Sustainable Development Goals especially SDGs 6 and 13.

Professor Dr Shahbaz Khan
Director and UNESCO Representative to the People’s Republic of China, the Democratic People’s Republic of Korea, Japan, Mongolia and the Republic of Korea

Executive Summary

The River Indus Basin is amongst the regions most vulnerable to climate change, its eastern tributaries are frequently inundated during monsoon. Past few decades have seen increased frequency and intensity of floods which are anticipated to exacerbate. The region is thickly populated and intensely cultivated. Recent floods played havoc with life and property. Disaster risk reduction demands improved flood forecasting. That requires updated primary data for modeling tools. River flow regimes, river morphology and soil physico-hydraulic features are key inputs for such models.

In this study, we carried out measurements of river flow regimes, cross-sectional profiles, bed material, seepage rates, and soil physico-hydraulic properties of the active flood plains on both sides of the tributaries. For river flow regimes and morphological features, Acoustic Doppler Current Profiler (ADCP) was used. Bed material was collected and analyzed for mean particle size and uniformity coefficient. Locally developed seepage meter was used for seepage rate measurements. Improved double ring infiltrometer for infiltration rate, hydrometer method for soil texture, and pressure plate and hanging table extractors were used for soil-moisture retention characteristics.

The ADCP can generate reliable data of river flow regime and morphology if usage guidelines are followed properly. Bed material mean particle size decreases towards downstream reaches of the rivers Jhelum, Chenab and Ravi in conformity with Sternberg's law, but is vice versa in case of river Sutlej. Uniformity coefficient of bed material shows no systematic trends. Seepage rates also have mixed trends, but are generally more in upper reaches in line with bed material mean particle sizes.

Silt loam, loam and sandy loam are dominant soils in three horizons up to 1.0 m depth in the active flood plains, but coverage of sand dominant classes increase with depth. Infiltration data fitted better on Horton's model than Philip's. Dominant range of steady-state infiltration rate is 15-30 mm/hr that increases towards 60-90 mm/hr at the deeper layer. Average bulk density up to 1 m depth profile is 1.44 - 1.45 mg/cm^3 with coefficient of variability (CV) in low range of 8.68 - 9.31%. Average Horton's steady-state infiltration varied from 0.45-76.75 mm/hr with high CV in the range of 135 - 158%; van Genuchten Θs average values are 0.45 - 0.46 cm^3/cm^3 with CV in the low range; Θr is 0.05 - 0.06 cm^3/cm^3 with CV in the medium range; α ranges 0.01 - 0.02 cm^{-1} with medium CV; and n have average values of 1.06 -1.90 with CV in the medium range. Average organic matter is 0.68 -1.27% with medium variability in the three horizons up to 1.0 m depth.

Acknowledgements

This report is an outcome of the study “Characterizing Hydrology of the Eastern Rivers of the Indus Plain” under the umbrella project “Strategic Strengthening of Flood Warning and Management Capacity of Pakistan”. This key study was conducted with the financial and technical support provided by Japan International Cooperation Agency (JICA) and United Nations Educational, Scientific and Cultural Organization (UNESCO). The authors would like to thank Professor Dr. Shahbaz Khan, the then Director, Regional Science Bureau for Asia and the Pacific, Jakarta, Indonesia; Ms. Vibeke Jensen, the then Country Director, UNESCO Pakistan; Dr. Ai Sugiura, Science Programme Specialist, Policy Capacity Building, UNESCO House, Jakarta, Indonesia and Mr. Raza Shah, Programme Officer UNESCO, Pakistan for their continuous support to PCRWR.

The authors would also like to thank their colleagues Engr. Faizan ul Hasan, Director; Engr. Ali Bahzad, Deputy Director; Engr. Ibtisam Asmat, Deputy Director; Engr. Muhammad Aleem, Engr. Muhammad Abbas, Engr. Sajid Hussain, and Mr. Faizan Sabir; Research Associates for assistance and contribution in data collection, field sampling, laboratory analysis and results compilation. Thanks are also due to Engr. Muhammad Umar, Assistant Director for proof reading. The contributions in persistently formatting the manuscript by Mr. Tariq Mahmood, Assistant Private Secretary and Mr. Zeeshan Munawar, Assistant, in designing the title page are thankfully acknowledged.

1. Introduction

Hydrological cycle is one of the most important systems on the planet earth to sustain life. It spreads thousands cubic kilometers of water on terrestrial land for providing wide variety of ecosystem services. Water from hydrological cycle interacts with land mass and subsequently makes its way into rivers and streams.

Temporal and spatial distribution of water by the hydrological cycle is highly erratic and is not demand driven. Rather droughts and floods are peculiar feature of the cycle. This feature is becoming more prominent owing to climate change, which is now an accepted reality (Wetherald and Manabe, 2002). When water enters into rivers and streams, it becomes the most important component of the hydrological cycle for human interaction and intervention. That is why civilizations flourished in the proximity of rivers for meeting their food, fiber and other demands. At the same time, it makes them vulnerable to damages caused by the excess and shortage of water.

The water in rivers and streams gave rise to the discipline of water resources management, which is science of dealing with the excess and shortage of water. River systems can be better managed only if their flow regimes, fluvial processes, morphological features and physico-hydraulic characteristics are well understood. This knowledge is essential, inter-alia, for design of water related structures (reservoirs, bridges, flood dikes, drainage schemes, groundwater recharge wells etc.); flood warning systems and mitigation measures; assessing and developing hydropower potential; ecological health of water ways and wetlands, etc. It is also important for navigation and recreational sites; policy measures and legislation for water diversion; distribution and control; seawater intrusion and preventive measures; disaster risk reduction, etc (Loucks and van Beek, 2017).

The importance of data regarding the most critical component of the cycle has increased manifold due to implications of climate change and population stress. Although total quantum of water resources is same but it has to meet the demand of highest population that the planet earth has ever seen. Therefore, purpose of this study was to provide reliable database of river flow regime, fluvial processes, morphological features and surface-groundwater interaction using state of the art tools and techniques. The data so generated will be useful for the hydrological modellers, water resources managers, policy makers and other stakeholders for better management of water resources under the changing climatic conditions and rising water demand. This is important especially for the Indus Basin of Pakistan, which is habitat of more than 200 million people. The basin has the world's largest irrigation system, where floods and droughts are common feature.

Better management of the Indus Basin is, therefore, key to sustainable growth and socio-economic uplift of the country.

Apropos, this study was conducted on the eastern tributaries of the river Indus with the objectives:

(i) To evaluate the reported flow regimes with those measured with state of the art Acoustic Doppler Current Profiler (ADCP).

(ii) To characterize morphological features of the river system.

(iii) To characterize soil physical and hydraulic properties of the active flood plains.

1.1. Theory and literature

Acoustic Doppler Current Profiler (ADCP) is the latest tool for discharge measurement that uses Doppler effect principle. The Doppler principle is the dependence of sound frequency shift on the relative velocity between the sound transmitter and receiver and was named after the physicist John Doppler who discovered it. According to the principle, frequency of sound decreases when relative velocity between the transmitter and the receiver increases and vice versa.

In flow measurement, ADCP transmits sound waves in water and receives the waves reflected back from the sediments moving with water. Fundamental assumption in its application is that the suspended sediments travel with velocity of water. Sound waves used for the purpose are ultrasonic and commonly applied frequencies for flow measurements range from 300 to 3000 kHz (Mueller *et al.,* 2013). The change in frequency of the sound waves reflected back from sediments moving with water determines its velocity.

ADCPs are classified according to their mounting, which are side-looking (horizontal) and downward or upward looking (vertical). Side looking are mounted on the side and upward looking at the bottom of a regular section of water channel to determine average velocity. Downward looking are on tethered boat, which is traversed across the water channel from bank to bank. ADCPs are further categorized into “narrowband” and “broadband”. A narrowband ADCP transmits a single long pulse and compare its returned signal with itself to determine the frequency shift. Whereas, a broadband transmits multiple phase coded short pulses and compare the returned signal of one pulse with the other one for determining frequency shift. Narrowband is simple and easy to process but involves more random error due to time and space resolution limitations of a single pulse. Broadband requires complex background calculations but has improved accuracy due to better time

and space resolution between multiple pulses (Simpson and Oltmann, 1993; Brumly *et al.,* 1991).

Limitations of the instrument are that water must neither be too clear nor too muddy as in flood conditions. In the former case, back scattered sound energy would be too meager to detect for determining velocity of water. In case of the latter, attenuation of the sound waves would be too high for accurate measurements. These limitations are qualitative and depend on sediment characteristics and water depth. However, low frequency sound has more penetration capacity to carry out measurements in water carrying heavy load of sediments than in case of vice versa (Mueller *et al.,* 2013).

ADCP measures discharge by traversing across the river from bank to bank which is called transect. During each transect, ADCP divides measurement sections into horizontal segments of specified width called ensembles. Each ensemble is further divided into vertical segments, which are called bins or depth cells. Size and number of depth cells are determined in the instrument configuration based on the water depth recorded by its software (RDI, 2001).

The ensemble width is determined as the product of the boat speed and time between ensembles. ADCP determines velocity for each bin, then calculate for each ensemble and subsequently for the transect comprising measured ensembles. However, ADCP cannot measure velocity profiles for the entire transect. The unmeasured zones include instrument draft, blanking distance, side-lobe and riverbanks, which are shown in Figure 1 (Simpson, 2001).

In the unmeasured zones, draft depth is the depth of water above the bottom of ADCP up to which it remains submerged in water. Blanking distance is the depth of water below ADCP to which measurements remain unrealized due to technical reasons of pinging resonance. Similarly, side lobes interference further keeps some part as unmeasured zone in the bottom of the stream. Theoretical details of blanking distance and side lobes interference are beyond the scope of this report. Interested readers are referred to Mueller *et al*. (2013).

The discharges of unmeasured zones are determined by configuration based extrapolations. For extrapolation, measurements of at least two bins are required. Therefore, each transect is terminated near the point of transect where discharge measurements of at least two bins remain available. This is carried out by real time monitoring the measurement window displayed by the data processing software on the laptop during measurements. The distance from the point of transect termination to the bank shore is determined and entered in the data processing software which estimate discharges of unmeasured banks shore.

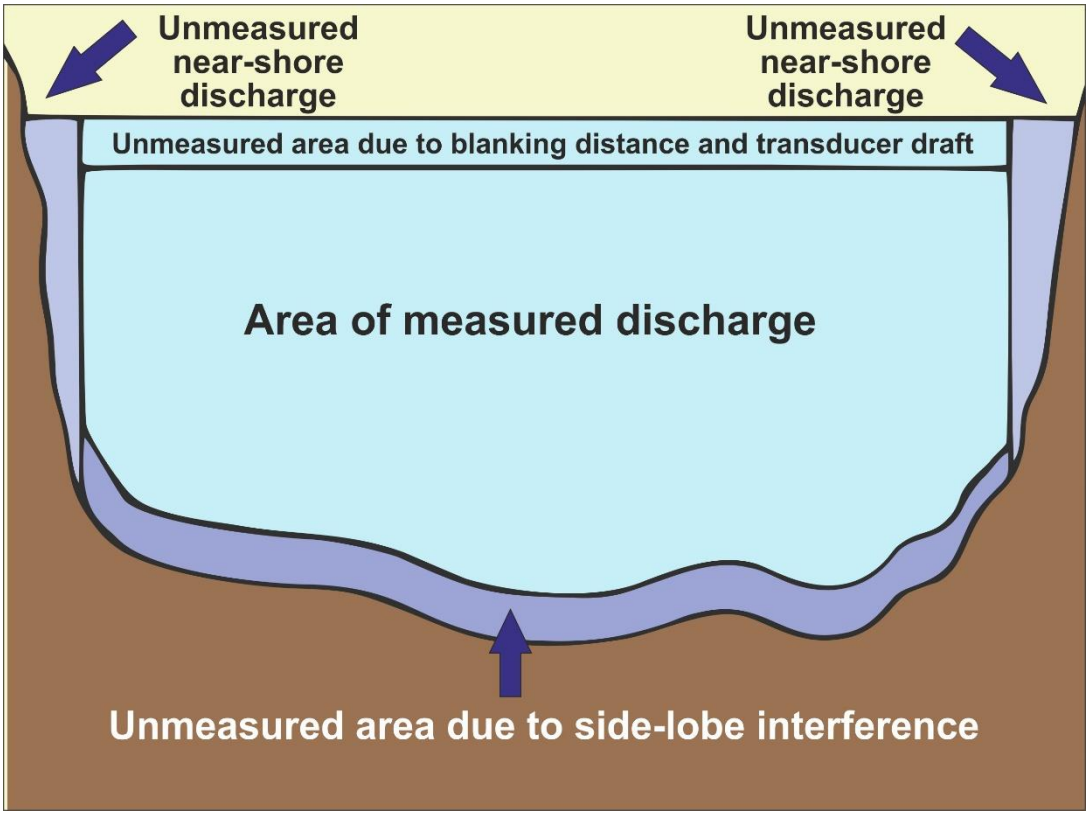


Figure 1: Unmeasured areas in ADCP measurement cross section (Simpson, 2001).

1.2. Boat tracking for making measurements

ADCP measurements rely on determining the boat positions with reference to which boat and water velocities are calculated. For that purpose, it works on either GPS tracking or bottom tracking (BT) mode. In GPS mode, position is determined with reference to magnetic north using fluxgate compass. Errors in the compass reading substantially affect the velocity and discharge measurement. Potential sources of compass error are ferromagnetic materials attached with the boat, compass displacement owing to sudden acceleration, or deceleration of the boat and local magnetic declination (also called variation). Magnitudes of geographic location based magnetic declinations are available on relevant websites (www.interpex.com/magfield.htm, www.resurgentsoftware.com/GeoMag.html). In addition, magnetic deviation caused by local magnetic fields are also required to be accounted for along with magnetic declination. Pertinent to mention is that, the magnetic declination is point-to-point changes in the magnetic north from true north and is determined from computer models such as Geomagix, GeoMag, etc. However, magnetic deviations are local phenomena and effects of both are required to be accounted for if GPS based boat tracking is to be used as it affects magnitude as well as direction of the velocity vectors and hence discharge (Mueller *et al.,* 2013).

Under the conditions where site-specific magnetic deviation is significant due to bridges, buildings or power transmission lines, bottom-tracking mode is preferred. However, BT mode has its own limitations. In BT mode, boat velocity is determined with reference to the riverbed if it is stationary. For assessing riverbed condition, various methods are available, which measure bed movement and make moving-bed corrections accordingly.

If neither GPS tracking nor bottom tracking warrants application, then VTG (Velocity Tracking and speed on Ground) tracking mode for determining the boat velocity can be used. In VTG mode, Doppler shift of the satellite signals is used to determine boat velocity. For details of all these methods, the readers are referred to Mueller *et al.* (2013).

1.3. Compass calibration

Compass calibration is essential in particular when GPS mode of boat tracking and loop method for correcting discharge owing to moving-bed conditions are used, and in general for other modes of tracking (Mueller and Wagner, 2006). The calibration corrects earth's magnetic field distortions due to magnetic material near the ADCP. These corrections are necessary for avoiding error in headings measurements. However, large structures such as bridges, piles etc., near the measurement location may still cause heading error and require consideration while selecting measurement section. ADCP user's guide is referred to for compass calibration, as it requires configuration for the specific compass installed. WinRiver II software used with Teledyne ADCP automatically detects installed compass and configure it for calibration (Teledyne, 2015). After calibration, compass error should be less than 1 degree. If the error is greater than the given range even after repeated calibrations, it will require special care for minimizing causes of potential compass errors such as irregular ship track and directional bias (Mueller and Wagner, 2006).

1.4. Moving bed test

As mentioned earlier, the ADCP reports boat velocity by three methods namely: i) bottom tracking; ii) GGA NMEA (National Marine Electronic Association) sentence mode and iii) VTG NMEA sentence mode. In bottom tracking mode, it calculates boat velocity by Doppler shift of acoustic pulses from bottom of the river assuming that the riverbed is stationary, which very often is not the case. In rivers having heavy sediment load, bed material remains moving what is called moving-bed condition. Under such conditions, ADCP underestimates water velocity and hence discharge. Therefore, moving bed test is crucial for reliable measurement of discharge. Various methods of moving bed test are available such as stationary boat without GPS, stationary boat with GPS and loop test. Whatever the method adopted, moving bed condition exists if the moving-bed velocity is

greater than 1% of the average water velocity. Mueller *et al.* (2013) have given details of carrying out moving bed test and criteria for considering the bed as moving or stationary.

1.5. Riverbed material sampling

Riverbed sediment distribution is important for determining sediment transportation, riverbed stability, channel roughness, river management, design of hydraulic structures, reservoir sedimentation, calibration and validation of numerical models and movement of contaminants. Toxic chemicals are adsorbed on and transported with fine sediments and affect the water quality and aquatic life. Management practices include improving watershed vegetative cover and slope stabilization. Assessment of baseline, or evaluation of management practices, requires determining sediment size distribution of the river bed material.

Sediment particles have vertical stratification in rivers having gravel beds. The top two layers of stratification in such beds are pavement and sub pavement, which are significant for determining river bed characteristics. The largest particles determine thickness of each of the layers, wherein fine particles remain embedded in the large particles. Under such conditions, sampling technique determines what population of particles would be sampled. Bed Material sampling is usually carried out during low flow periods. Bed load and suspended sediment sampling can, however, be conducted during any flow but preferably during high flows or floods (Diplas *et al.,* 2008). Bulk volume samples are typically collected and sieve-analysis is carried out for requisite parameters (Peter *et al.,* 1989). Equipment such as drag-sampler, scoop sampler, US BM-54 and US MH-53 are typically used for sample collection. The former two are less accurate than the latter, whereas US BM-54 is too heavy to be carriage friendly. US BMH-53 is designed for sampling by wading in shallow waters (Peter *et al.,* 1989).

1.6. Description of the study area

The rivers Jhelum, Chenab, Ravi and Sutlej are the eastern tributaries of the Indus river. Of these, the rivers Ravi and Sutlej are called the left bank eastern whereas the rivers Jhelum and Chenab are the left bank western tributaries. The river Sutlej is the longest and the Jhelum is the shortest of all the four. Annual average discharges and attributes of these rivers are given in Table 1.

Mangla dam is located on the upstream of the River Jhelum near Mirpur, Azad Jammu and Kashmir. Rasul barrage is the only barrage located on this river until its confluence with the river Chenab at Trimmu. Barrages on the river Chenab from upstream to downstream are at Marrala, Khanki and Trimmu. It receives waters from the Ravi and the Sutlej rivers at Panjnad (locally means junction of five streams).

The Chenab is the second largest tributary of the river Indus and collects waters of all the other tributaries but retains its own name until mergence with the river Indus. The river Ravi enters into Pakistan territory near Ravi Syphon and have Balloki and Sidhnai barrages at its upstream and downstream reaches, respectively. The river Sutlej enters into Pakistan near Bhedian Kalan district Kasur. The barrages on it from upstream to downstream are Sulemanki, Islam and Mailsi. It drains into the river Chenab near Uch Sharif and forms together the river Panjnad, which flows over a reach of 70 km until it drains near Mithankot into the river Indus.

Tarbela dam is Pakistan's largest reservoir near Swabi on the river Indus. The barrages at the upstream of Mithankot on the river Indus are Jinnah, Chashma and Taunsa. Whereas, Guddu, Sukkur and Kotri are the barrages at the downstream of Mithankot until the main Indus river drains into the Arabian Sea.

The Indus river System supplies water to the world's largest contiguous irrigation system comprising three large dams, 45 canal commands, 12 inter link canals, 22 barrages and head works, 60,000 km length of canals, more than 100,000 water courses and about 1.2 million tube wells. (The system irrigates about 18 million hectares of land that forms the fourth largest chunk of irrigated agriculture contributing 19.5% of country's GDP.) The system originates from the world's highest mountain ranges of Karakorum, Hindukush and Himalaya, which have the largest frozen water reserves after polar region. The share of glacial melt, snowmelt and rainfall are 51, 22 and 27% respectively (MoWR, 2018; Ashraf, 2019).

Table 1: Attributes of the Indus river system and its eastern tributaries

River	Origin	Path	Length / annual flow	Tributaries	Glaciated area (%)
Indus (main)	Mansarowar lake, Tibet	Kashmir, Skardu, Tarbella, Multan and Arabian Sea	2880 km / 100 BCM	Hunza and Gilgit at Raikot, Kabul at Attock and Chenab at Mithankot	12
Jhelum	Verinag spring, Indian Kashmir (Indian illegally occupied Jammu and Kashmir)	Wular Lake, Muzzaffarabad, Mangla and Trimmu	820 km / 28 BCM	Neelum and Kunhar at Muzzaffarabad and Chenab at Trimmu	1
Chenab	Himachal Pradesh (India)	Kishtwar, Marala Panjnad, Mithankot	1361 km / 28 BCM	Jhelum at Trimmu, Ravi at Ahmadpur Sial, Sutlej at Panjnad	13
Ravi	Rohtang Pass in Kangra (India)	Chamba, Madhopur, Lahore, Ahmadpur Sial	894 km / 7.8 BCM	Chenab at Ahmadpur Sial	3
Beas	Rohtang Pass in Kulu (India)	Kangra, Singbol, Hoshiarpur, Talwara	467 km / 15.6 BCM	Sutlej at Harike	5
Sutlej	Lake Rakshastel Western Tibet	Ludhiana, Ferozpur, Bahawalpur	1542 km / 16.64 BCM	Chenab at Panjnad	11
Kabul	Kabul, Afghanistan	Chitral, Kabul, Warsak, Nowshehra	480 km / 21.4 BCM	Indus at Attock	-

Source: Fahlbusch and Thathe (2004), and Ashraf (2019)

2. Methodology

2.1. Measurement of river flow and morphology

For measurement of flow regimes and cross sections profile, Acoustic Doppler Current Profiler (ADCP) was used. As mentioned before, the ADCP works on the principle of the Doppler Effect. It can measure multiple parameters, inter-alia, river discharge, point as well as average flow velocity, width and cross sectional area of the channel. Additionally, the ADCP computes a complete depth profile at the cross section, hence giving shape of river morphology.

For measurement of these parameters, River Ray ADCP of Teledyne was used, fifty sites were selected along the Indus river eastern tributaries namely the rivers Jhelum, Chenab, Ravi and Sutlej. An approximate interval of 40 km was maintained between the selected sections. For selection of a river section, due consideration was given to the technical requirements and accessibility. Therefore, preferred sections were those, which were logistically approachable, reasonably straight, and had little turbulence or eddies. All measurements were taken using ADCP tethered parallel to the boat as shown in Figure 2.



Figure 2: Field operation of ADCP River Ray tethered to boat and real time monitoring of the transect on the host laptop.

Prior to the measurements, the ADCP was duly configured and the boat speed was kept as low as possible. Since almost all the measurements were taken in lean flow period, difficulties were faced in maintaining boat speed lower than the average velocity of water flow as per USGS guidelines (Mueller *et al.,* 2013). Before carrying out each measurement, moving-bed test was carried out. Owing to the measurements made over the lean flow period, moving bed conditions exceeding the permissible limits of 1-2% of the average flow velocity were not observed. However, composite (GGA) mode option for velocity profile, river cross section and the discharge calculations with WinRiver-II software was used for getting the data both in bottom tracking (BT) and GPS tracking systems. The software displays the real time data on the windows of the host laptop carried on-board by the survey team. A member of the team monitored speed of the boat while observing stability of the ADCP. Due care was taken that the boat slowly takes start and maintain almost uniform speed as per USGS Guidelines (Mueller *et al.,* 2013).

It was ensured that the right (R) or the left (L) bank were duly marked. Measurements were started from one bank and carried out to the next until recording of at least two bins remained available close to each bank. For measurement of distance from the start/stop position to the actual bank of the river, laser range finder as shown in Figure 3 was used and entered accordingly in the transect. A trial first measurement was usually taken to become acquainted with the river section, boat stability and any untoward condition in the section. A transect was not accounted for in the measurements if any anomaly in it was detected such as missing ensemble. Almost 4-8 transects were recorded at every river section and took the average of those four, or more, transects having relative residual (RR) within maximum permissible relative residual (MPRR), or fall reasonably close to that (Mueller *et al.,* 2013). Furthermore, the same number of left to right and right to left transects were tried to maintain for avoiding directional bias or other systematic errors.



Figure 3: A view of the measurement of distance of the end of the transect to the riverbank with laser range finder.

2.2. Measurement of the seepage rate

For measurement of the seepage rate, a meter based on the Idaho University concept available in literature was developed. The seepage meter, as shown in Figure 4, comprises a seepage bell of 60 cm diameter cylinder having depth of 50 cm. A 13 mm nozzle was welded to a hole drilled on top of the bell. The nozzle was connected to the threaded cap of a flexible plastic bag. The cap of the bag could be screw-tightened and unscrewed when required. It was ensured that the entire setup became air-tight on tightening the cap on the mouth of the plastic bag. Provision was made to change the size of the bag keeping in view the expected seepage rate at any section. Small bag was thermal-massage bag and the large bag was the thermal-pillow bag in terms of their medical usage.

For driving the seepage bell into the riverbed, crossbar and hammering anvil were prepared separately. For logistic convenience, the seepage bell, cross bar and hammering anvil were made to be assembled together and disassembled when required. For driving into the riverbed, the bell was placed in the bed having water depth not more than 1 m. The cross bar was then placed on the bell-top and the hammering anvil was fixed over the cross bar. After assembling the seepage meter, the anvil was hammered

with 4-5 kg hammer until 20-30 cm of the seepage meter bell drove into the riverbed. The sides of the bell were then plastered with bentonite clay for avoiding lateral flow.

The attached plastic pipe was then allowed to fill with river water. The thermal plastic bottle semi filled with water was weighed and carefully screw-tightened with the plastic pipe. The plastic bottle was allowed to float on the surface of the river water such that the same water head remained inside and outside the bottle. An angle-iron bar was provided at the side of the bell for fastening the plastic bottle to avoid dragging away by the flowing water. The bar was also used to pull out the seepage meter after finishing the seepage test. This airtight arrangement took as much water from the plastic bag as much seeped from the seepage bell into the riverbed.

Three seepage measurements were simultaneously carried out at each of the river sections. For this purpose, three seepage meters were installed simultaneously. Each seepage test was conducted for at least 24 hours. After that the plastic bag was carefully removed and loss in weight of water over the lapsed time was recorded by difference in weights of water-filled bag before and after the test. The water lost due to seepage was divided by the cross sectional area of the seepage bell and the time lapped for the test that gave point seepage rate. Average of the three trials was taken as representative seepage rate at each river section. The assembly of the seepage meter and its installation steps in the field are given in Figure 4. A view of the meter installed in the river for measurement of seepage rate is shown in Figure 5.



Figure 4: Assembly and operation of seepage meter for measurement of seepage rate

.



Figure 5: *A view of the seepage meter installed in the river for measurement of seepage rate*

2.3. Riverbed sediment sampling and analysis

Riverbed sediment samples using vacuum type US BMH-53 Rickly Sediment Sampler (Figure 6) were collected. This sampler comprises a cylinder and piston. The sampler-driving handle is telescopic type comprising hollow outer tube and solid inner bar. The inner bar is attached to the piston inside the cylinder. When cylinder is driven into the riverbed, the piston inside it starts retreating backward. This backward movement of the piston becomes visible from ejection of the inner bar at the driving end. In this way, the sediments trapped inside the cylinder remain under suction and do not wash out when the sediment sampler is pulled out of the riverbed under running water conditions. After pulling out the sampler from water, the inner telescopic bar is pushed to remove the sediments sample from the cylinder for collection in a plastic bag. In this way, little water is carried with the sediment sample.

Three sediment samples, each of 5 cm diameter and 5 cm length, were collected from each bank of the selected river section and made a composite sample for analysis. The composite samples were duly coded for each section of the river. These samples were

brought to the laboratory and air-cum oven dried. Sieve analysis of the oven dried samples were carried out and developed S-curves. From the S-curves, mean particle diameter and uniformity coefficient were determined. Uniformity coefficient (Cu) is defined as the ratio of sieve sizes through which 60% of the material by weight passes to that which allows passage of 10%. It is given by Equation 1.

$$\text{Uniformity Coefficient (Cu)} = D_{60}/D_{10} \quad (1)$$

Where:

D_{60} is sieve aperture size that passes 60% of the sample.

D_{10} is the sieve aperture size that passes 10% of the sample.

2.4. Measurement of infiltration rates and determining soil texture

The improved methodology for double ring infiltrometers as described in detail by Malik *et al.* (2019) was used for measurement of infiltration at surface, middle (0.5 m) and bottom (1.0 m) layers of the soil pits in the active flood plains on each bank of the selected river sections. Briefly, the methodology involved pouring of water from a water-can into infiltrometer rings through a funnel-pipe arrangement while keeping the funnel totally detached from the water-can. Water release from the water-can was manually controlled with a tap in such a way that a constant head was maintained in both the rings. The constant water head in both the rings was monitored by placing a hooked bar on the rings. The constant head was maintained by ensuring that the tips of the hooks remain merely touching the water surface. This arrangement facilitated keeping the same and constant head in each infiltration test. Amount of water infiltrated in specified time intervals recorded with digital watch was determined by weighing feeding-can on an electronic balance. A field set up of the infiltration test arrangement is shown in Figure 7. Infiltration data analysis and parameter studied were also adopted from Malik *et al.* (2019). Similarly, the procedure of the same authors was followed for collecting soil samples from the pits and their texture analysis carried out with Hydrometer method. The results of analysis are given in Annexures B-I to B-IV.

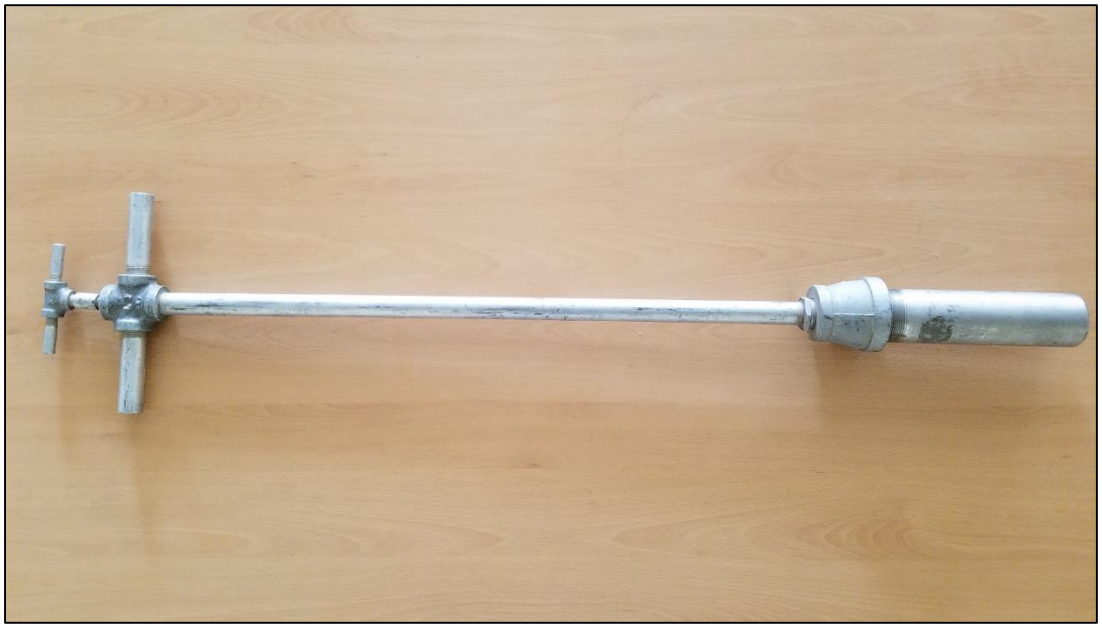


Figure 6: US BMH-53 bed material sediment sampler used for river bed sampling

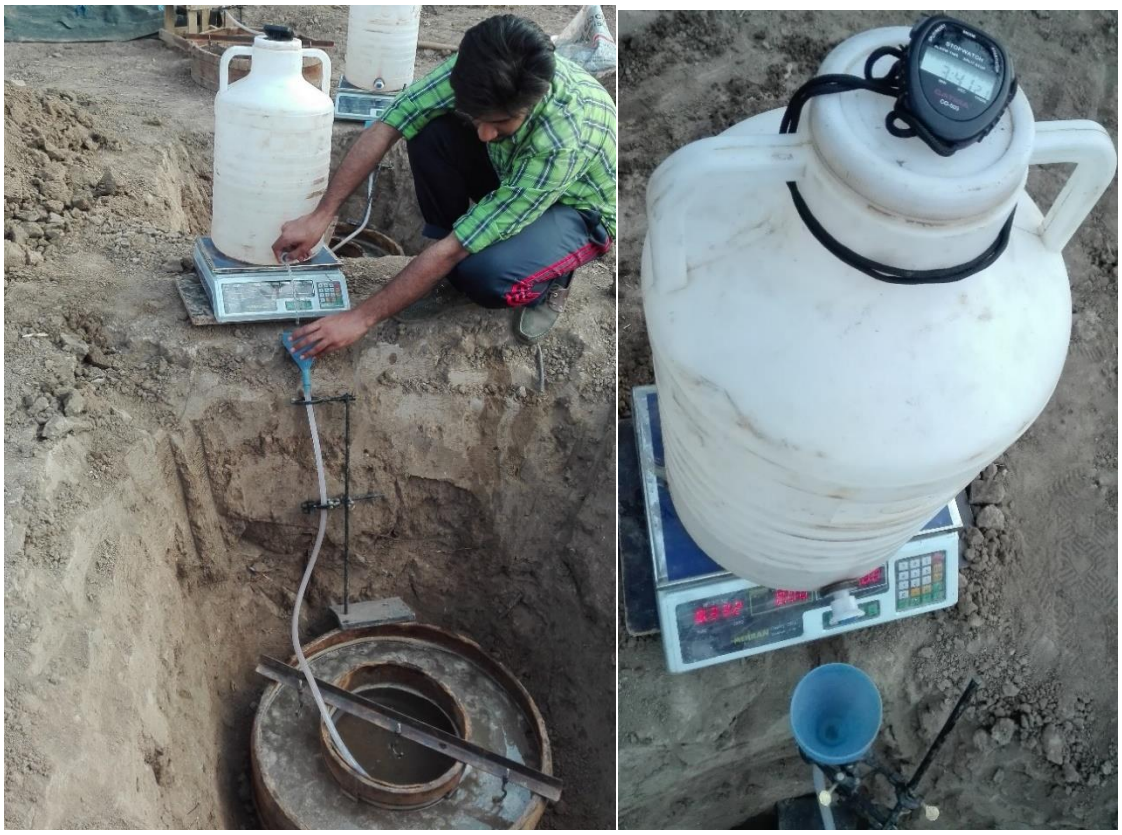


Figure 7: Field setup for double ring infiltration test

3. Results and discussions

3.1. Coverage of measurements at river sections

Coverage of the river cross sections on the eastern tributaries of the river Indus together with section codes and dates of the sites surveyed are given in Figure 8. Distribution of the coverage on each of the rivers is given in Table 2. The results of discharge measurements both in chronological order and in terms of the sectional sequence from upstream to downstream of the river Jhelum are given in Figures 9 and 10, respectively.

These discharges were measured in composite (GGA) mode. The composite mode in WinRiver-II has the provision to record the discharge measurements based on bottom tracking (BT) and Global Position System (GPS) tracking modes separately but simultaneously. It has the edge that transects in both the modes in each measurement can be compared for detection of distortions, if any, and the reliable quality measurement can be adopted. The graphs also show the available discharge data of Federal Flood Commission at the nearest gauging stations of the upstream, or downstream, of the measured sections alongside ADCP measurements-based river widths.

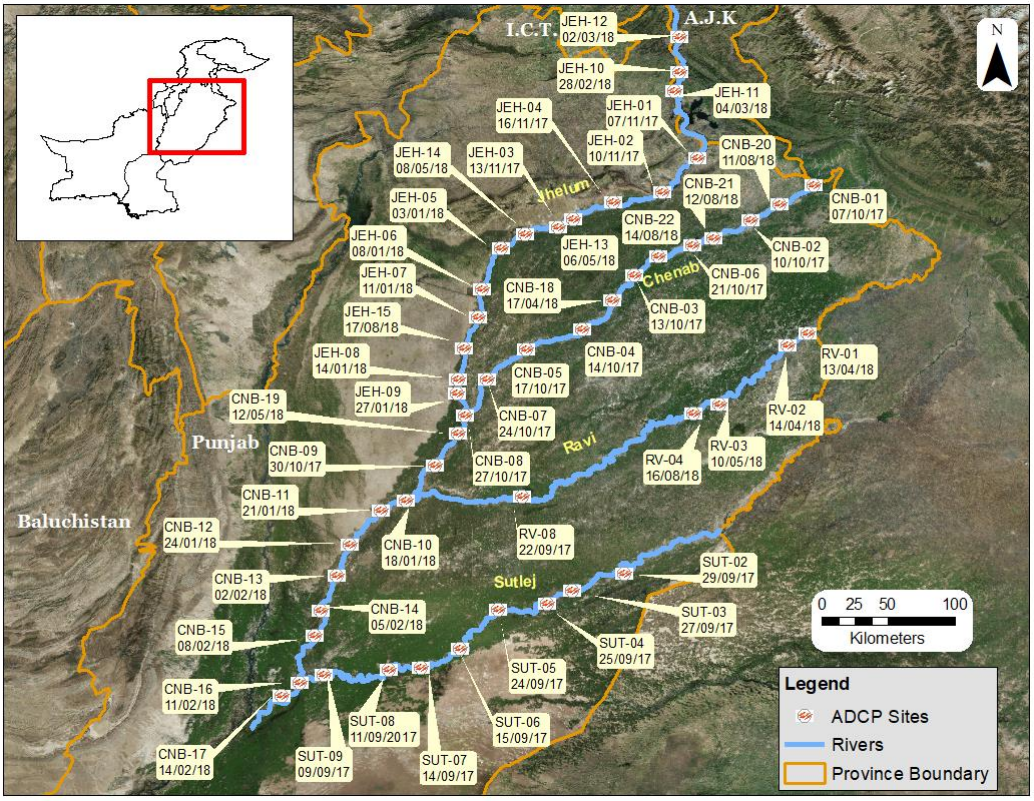


Figure 8: Spatial distribution of survey sites on all the four eastern tributaries of the river Indus

Table 2: River wise distribution of surveyed river cross sections

River	No. of discharge measurement sections
Jhelum River	15
Chenab River	22
Ravi River	5
Sutlej River	8
Total	50

3.2. Evaluation of flow measurements

Since the discharge data pertain to neither the same section nor the same date on any of the rivers, therefore the flows can be assessed neither as steady nor uniform. Furthermore, all the river sections have barrages for canal diversions and the diversion rates vary from day to day based on demands raised by the provincial authorities. The river Jhelum has Mangla dam of 11 BCM (9 MAF) capacity on its upstream with hydel power generation capacity of 1000 MW. The reservoir operation depends on provincial indents of irrigation water, release of water for power generation, time of the year and anticipated inflow.

The sequence of the measurements was neither from upstream to downstream or vice versa, nor was it practical due to field limitations in a trip. Therefore, the trend development under such conditions of random data becomes difficult. Nevertheless, the trends still exist to a certain extent. For instance, sites 5, 6, 7, 8 and 9 (Figure 9) on various sections of the river Jhelum were covered in January, 2017, which is lean flow period and hence measured discharges are the lowest compared with all the other sections.

The sections 1, 2, 3 and 4 in Figure 9 pertain to the measurements made in November, 2017 downstream Mangla Dam in the upper reaches of the river Jhelum. November is normally dry month of the year, but Mangla dam is filled in the preceding monsoon season and is reserved for the forthcoming “Rabi” season for wheat sowing. November is the time of first irrigation of the wheat crop. Therefore, water is released from Mangla Reservoir for meeting the demands tendered by provincial irrigation departments.

The sites 13 and 14 were surveyed in the month of May, 2017 when snowmelt contributions increase the river discharge and so is visible in Figures-9 and 10. Therefore, the river section width increase along with the discharges depending on the site. River

width is determined by the local gradient of the river and geographical features. The measured river spans are almost consistent with discharges except for section 14 of the river Jhelum. The section 14 falls at the piedmont of the Salt Range and is controlled by mountainous guide wall from the right-bank. That guide wall reduced the river span thereby increasing its depth to almost 4 m as shown in Figure 11, which reflects the cross sectional depth profile of the river.

A comparison of BT mode measurements with GGA mode shows that none of those is persistently and systematically higher, or lower, than the other (Gilja *et al.,* 2011). Although, results of both the modes of measurements are almost in close conformity, but most of the GGA measurements are higher than BT mode. The reason is evidently the moving bed, which remains unaccounted for if it is less than threshold value. Whereas, moving bed always cause a negative error in the measured discharge.

The discharge measurements along with quality evaluation in terms of total transects in each measurement and outliers thereof in either of the modes is given in Figure 10 for the river Jhelum. Quality assurance demands that each measurement should have at least four transects comprising half of those from left to right-bank and the other half from right to left. Each of the four transects is considered quality assured if it's relative residual (RR) is less than maximum permissible relative residual (MPRR) which is ±5 in case of four transacts. (Teledyne, 2015; Mueller *et al.,* 2013). The RR is given by Equation 2.

$$RR = (Qi-Qm)/Qm \quad (2)$$

Where Qi is discharge of the selected individual transect and Qm is mean discharge of all the selected transects in the measurement. The value of MPRR increases almost proportionally with increase in number of selected quality transects. A transect is considered outlier if RR > MPRR. It was endeavored to carry out more than four transects in each measurement if site conditions warranted. That facilitates to sort out the requisite number of quality transects if possible.

Figure 10 shows that six measurements (Nos.1, 4, 6, 7, 10, and 11) have no outliers in either of the modes while meeting requisite transects criteria of four or more. All the other measurements have outliers either in BT or GPS mode. Amongst the compromised quality measurements, four BT mode (section Nos 3, 8, 12, and 15) have outliers viz-a-viz eight GPS mode (section Nos. 2, 3, 5, 9, 12, 13, 14, 15) contain outliers. It is important to mention that sources of errors due to magnetic declination and deviation are always more in GPS mode than the BT mode. These sections also fall in mountainous upper reach of the river where multipath errors may also become dominant in GPS mode. Moving bed condition is the major source of error in BT mode, which in this case was almost non-existent due to low-flow conditions.

Regarding comparison with the discharges reported by the Federal Flood Commission (FFC), two of the discharge data at the sections 1 and 2 became available. The BT, GGA and FFC discharges at section 2 are 484, 494 and 557 m^3/s, respectively. The measurement section was about 3 km downstream of Rasul Barrage. The FFC data is reported in the early morning whereas in this study, measurements were taken mostly in the afternoon due to time required for logistics and equipment deployment. At section 1, the BT, GGA and FFC discharges are 699, 705 and 773 m^3/s, respectively. The site at this section was 35 km downstream of Mangla. Therefore, FFC discharge was calculated by deducting reported diversion (PID, 2017) to Upper Jhelum Canal (218 m^3/s) out of the reported release (991 m^3/s) of FFC downstream Mangla on the said date (7-11-2017).

The results of discharge measurements both in chronological order and in terms of the sectional sequence from upstream to downstream of the river Chenab are given in Figures-12 and 13, respectively. Almost similar trends are found for discharge measurement records of the river Chenab. The FFC reported discharges are moderately higher than the ADCP recorded measurements. The major discrepancy is regarding the section-8 measured on 27-10-2017, where FFC reported discharge (113 m^3/s) is much less than ADCP measured (BT = 450: GPS = 456 m^3/s). The BT and GPS mode discharges and river width for this section are compatible. The measurement at this section is average of six transects without any outlier as shown in secondary horizontal and vertical axis of Figure 13 and therefore, meets the quality criteria of the best measurement.

The ADCP measurement at section-8 was carried out upstream of Trimmu Barrage and downstream of the confluence of the rivers Jhelum and Chenab. On the upstream is the Rasul Barrage, whereas Chashma Jhelum Link (CJL) Canal drains into the reach between the two Barrages. Punjab Irrigation Department (PID) updates discharges of rivers and canals on daily basis on a comprehensive infographic on its website (irrigation.punjab.gov.pk). The infographic of the said date is given in Figure 14. It shows that on the date in question, neither there was any release downstream of Rasul Barrage, nor any contribution from CJL canal. The release downstream Qadirabad Barrage was also nil. Despite nil contributions from upstream sources, the inflow and outflow at Trimmu Barrage is 113 m^3/s (3973 cusec) on the date, which does not meet inflow-outflow balance criteria at the node of Trimmu Barrage. The ADCP measurement as mentioned above is much higher. A snap of the river section of the said date is given in Figure 15, which gives a reflection of the quantum of flow at the time of ADCP measurement and raises question on FFC reported value. The discharges at sections 20, 21 and 22 of the River Chenab were measured in August 2018 during flood. The measurement discrepancies over the

flood conditions are common feature of the ADCP due to high sediment load, moving bed conditions and misdetections of the riverbed (Mueller *et al.,* 2013).

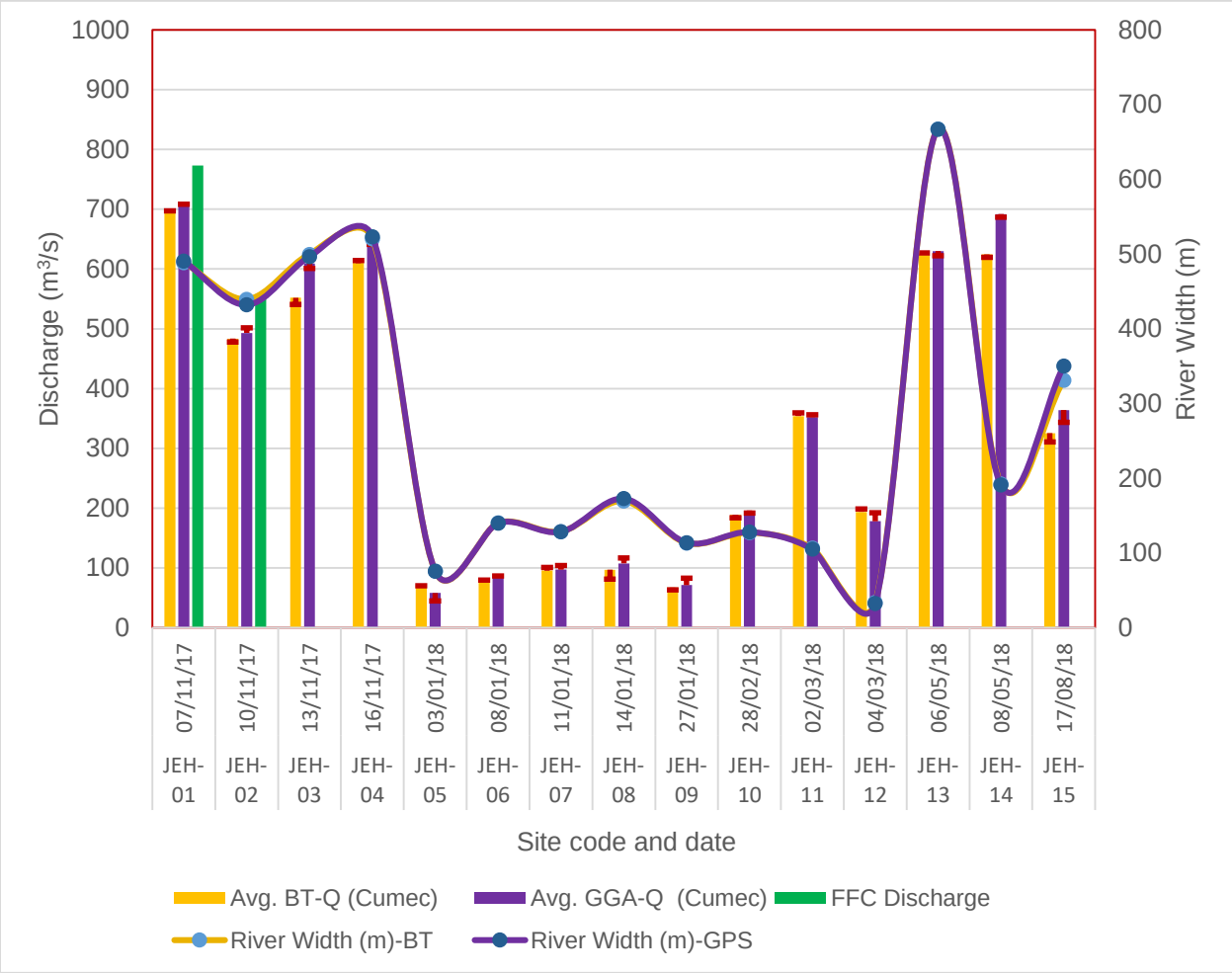


Figure 9: ADCP based measurement of discharge of the river Jhelum in chronological order of measurement dates

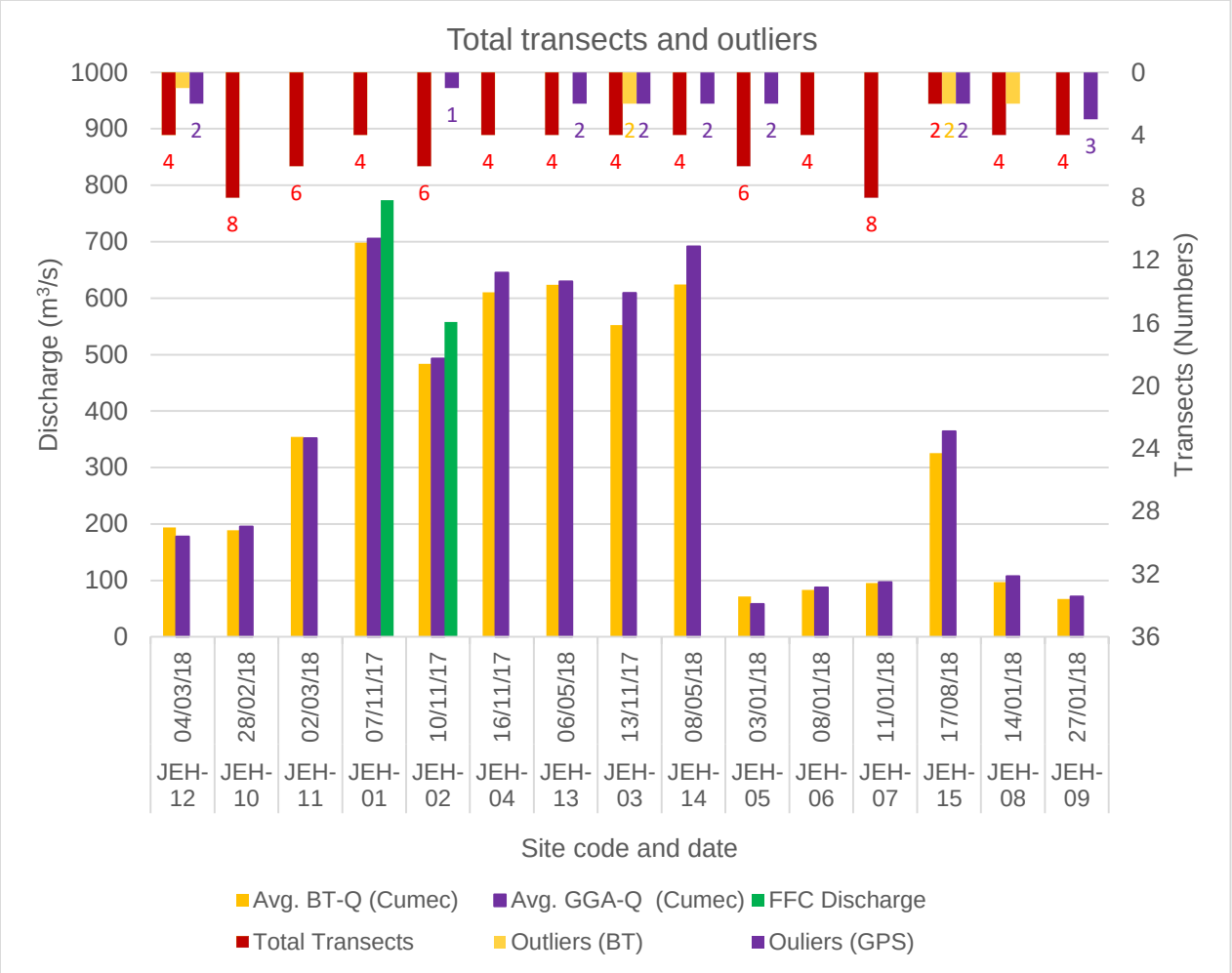


Figure 10: ADCP based measurement of discharge of the river Jhelum in the order of upstream to downstream measurement sections

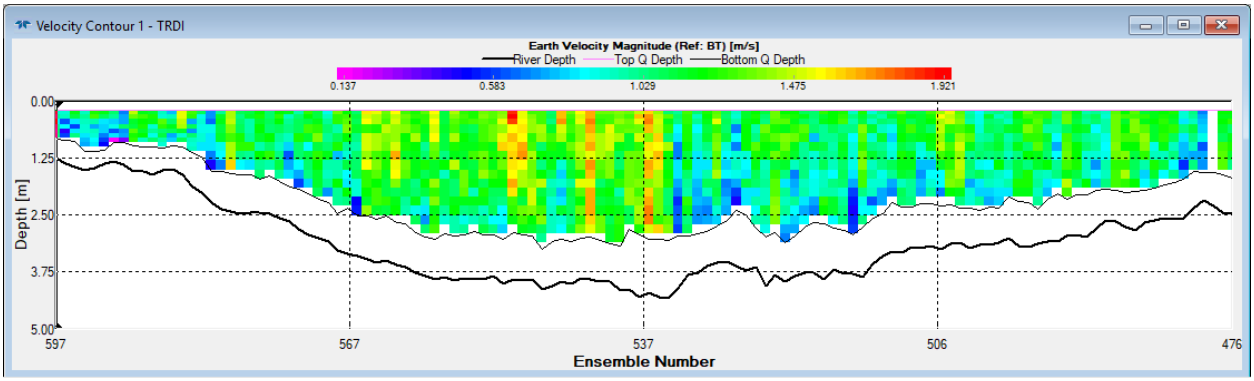


Figure 11: ADCP measured section profile of the river Jhelum at section JEH-14

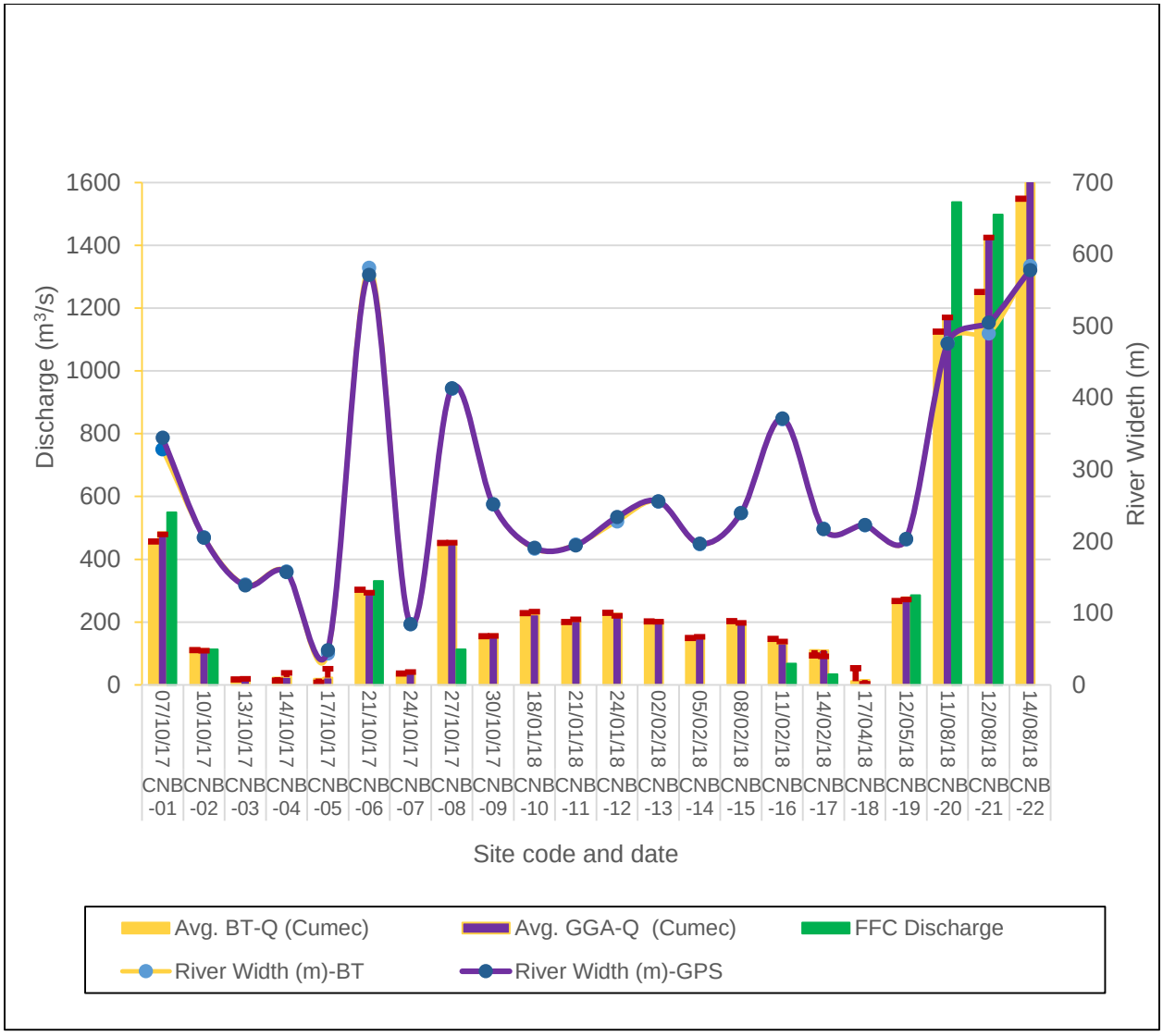


Figure 12: ADCP based measurement of discharge of the river Chenab in chronological order of measurement dates

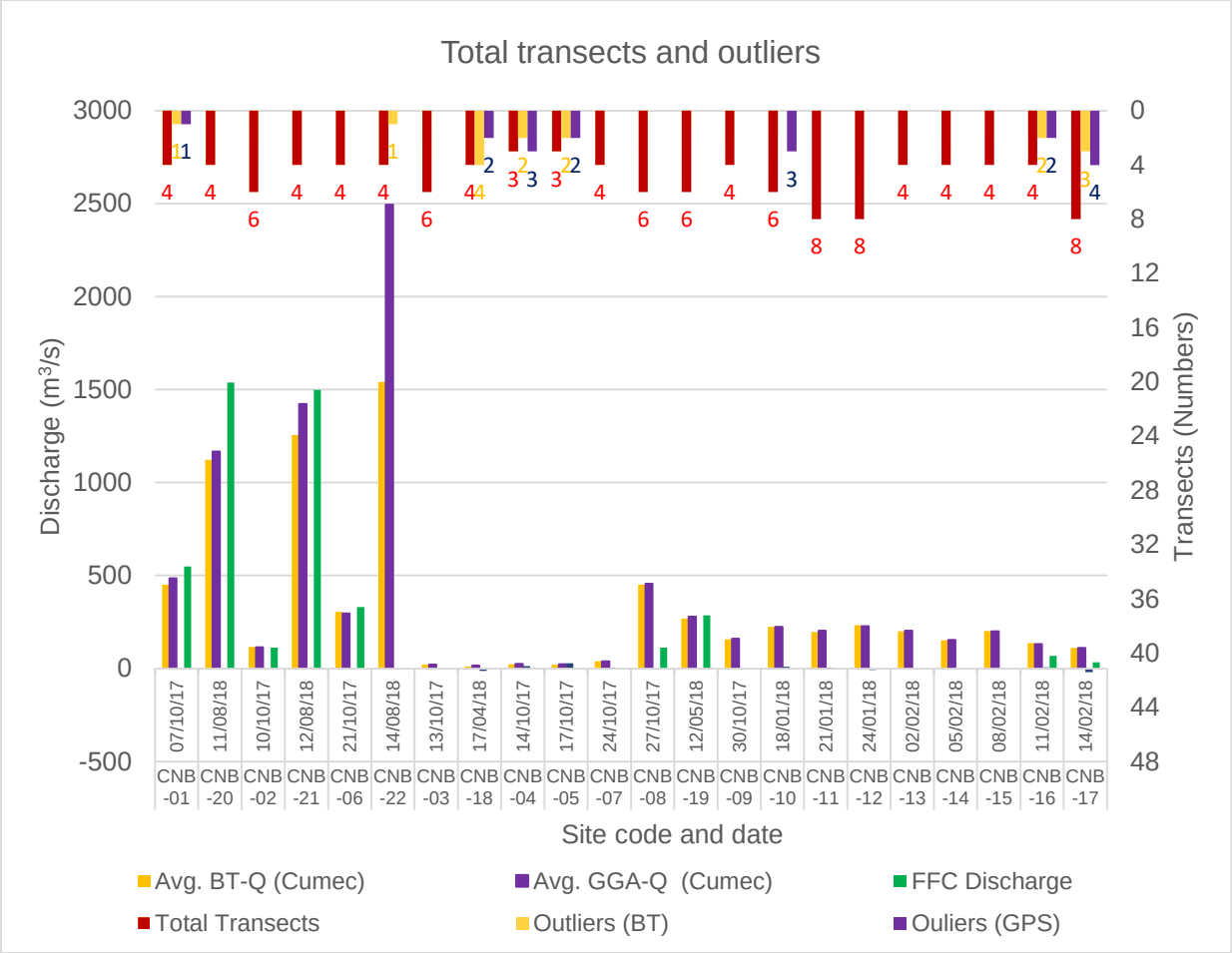


Figure 13: ADCP based measurement of discharge of the river Chenab in the order of upstream to downstream measurement sections

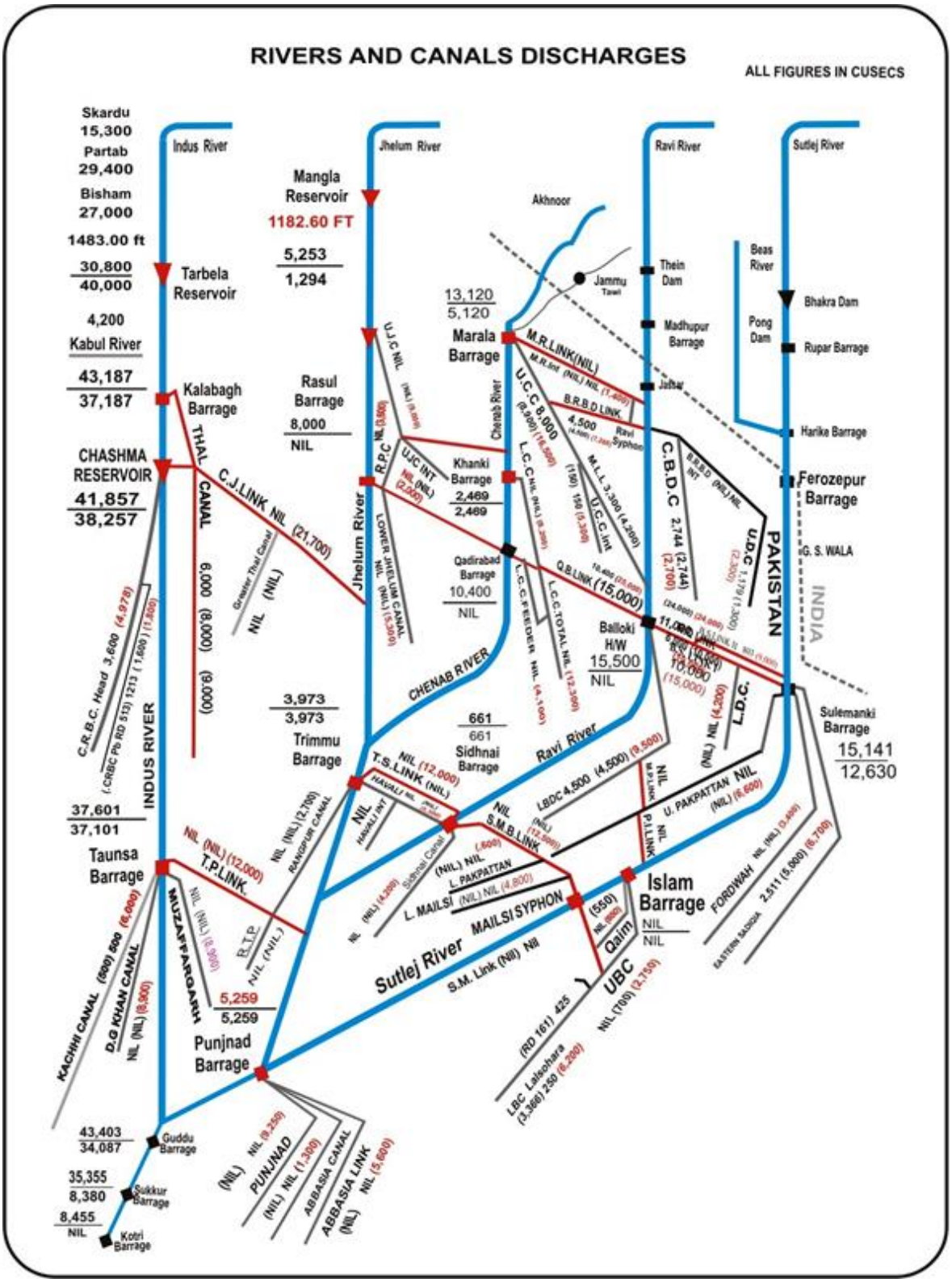


Figure 14: PID infographic showing the rivers and canals discharges for October 24, 2017 (source: www.irrigation.punjab.gov.pk)



Figure 15: A view of the ADCP measurements being made at upstream of Trimmu barrage

The results of discharge measurements both in chronological order and in terms of the sectional sequence from upstream to downstream of the river Ravi are given in Figures 16 and 17, respectively. Measurement at the river Ravi was one of the difficult tasks. Under the Indus Water Treaty (World Bank, 1960), water rights of the rivers Ravi and Sutlej were given to India. Therefore, the rivers remain dry round the year except some water during the monsoon season. Cities falling at the river banks dispose off their sewage into the river Ravi. At the downstream of Lahore, the river virtually becomes a sewage drain. Therefore, the use of ADCP was too difficult. Even then some measurements were taken. The river Ravi has no dam on it in Pakistan's territory. However, some link canals offtake from the river Chenab and drain water into the Ravi. The first diversion structure on the Ravi in Pakistan's Territory is Balloki Barrage from where Upper Bari canal offtakes. The section-3 on the Ravi is on the upstream of the Balloki Barrage where Qadirabad-Balloki link canal drains into it and hence the measurement became possible due to water supplied through the link canal.

Comparison with the FFC data for the river Ravi (Figures-16 and 17) shows that the reported data is persistently less but reasonably close to ADCP measurements. It might be due to disposal of municipal wastewater into the river Ravi as well as poor quality of water hindering accurate ADCP measurements.

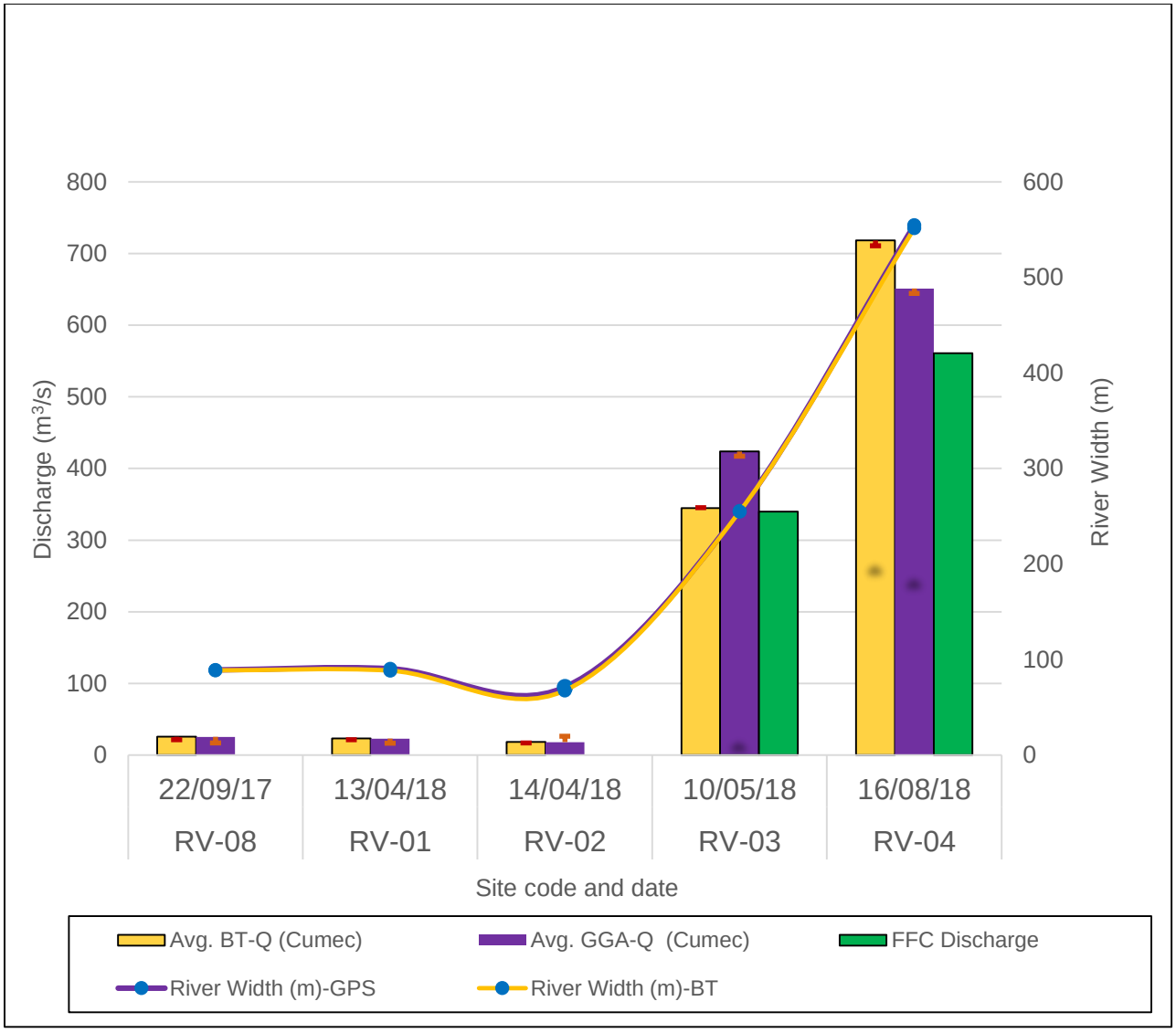


Figure 16: ADCP based measurement of discharge of the river Ravi in chronological order of measurement dates

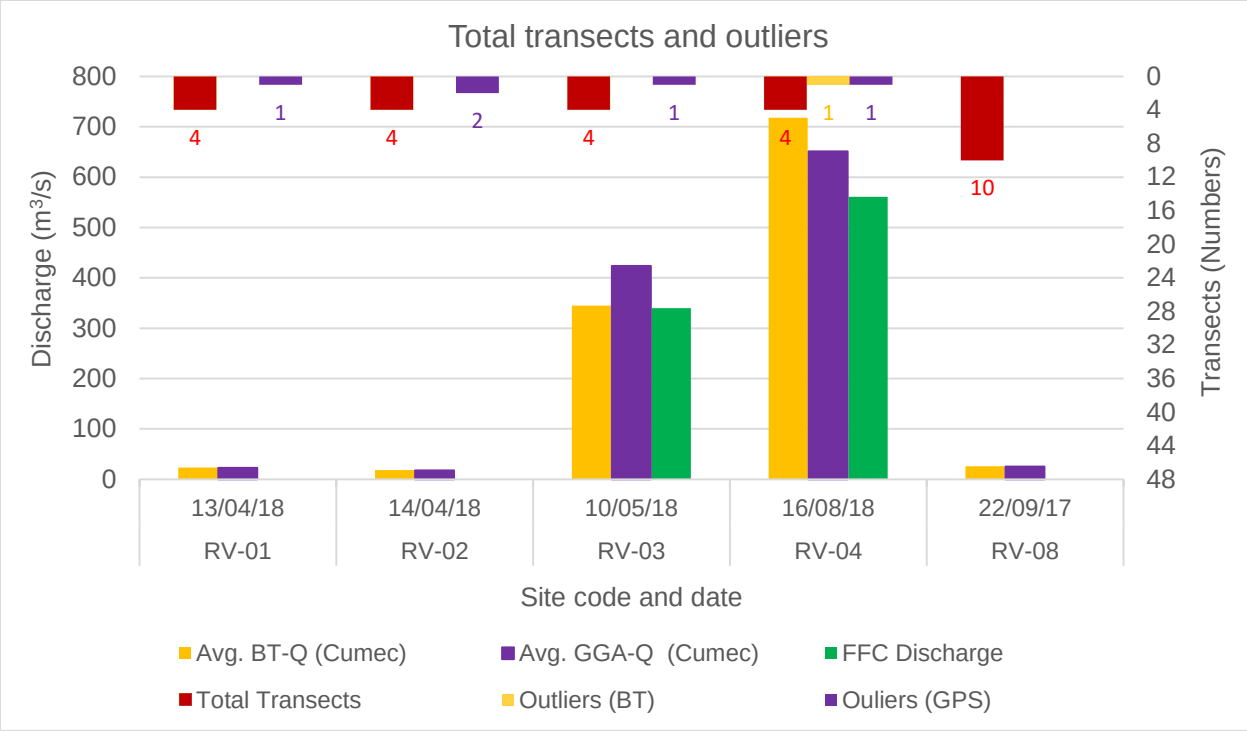


Figure 17: ADCP based measurement of discharge of the river Ravi in the order of upstream to downstream measurement sections

The results of discharge measurements in chronological order and in terms of the sectional sequence from upstream to downstream of the river Sutlej are given in Figures-18 and 19, respectively. Waters diverted from western tributaries (the Jhelum and Chenab) supply water to the river Sutlej from where it is diverted to irrigate area on its left bank. The measurements on the river Sutlej were made in the downstream reaches in early September when seasonal link canals carry enough water owing to the preceding monsoon season to make it available at the downstream reaches. Therefore, the measurements at the sections 6, 7, 8 and 9 became possible. However, subsequent measurements in the second half of the September, 2017 were virtually in shallow stream, which could be crossed by wading as these were on the upstream of the river. The data pertaining to the measurements on all the sections of the four rivers are given in Annexures A-I to A-III. The data were post-processed using magnetic declination given in the annexure and draft depth of 0.1 m in the playback configuration of WinRiver II.

For the river Sutlej, FFC reported discharges at two sections downstream of Islam Barrage are shown alongside the ADCP measurements in the Figures. The reported discharges are available pertaining to dates of the measurements at section-8 and section-9 only. These sections fall at the far downstream reach of the river Sutlej near its confluence with the river Chenab. The maximum depth of the river at section-8 was less

than 1.5 m, which was mostly around 0.75 m. Under that situation, ADCP ensembles frequently lost and measured discharge came out less than that could be. The measurements at the section-9 were further downstream where some field configuration regarding orientation of the river banks (interchange of left with right bank by mistake) added error that made the data unreliable.

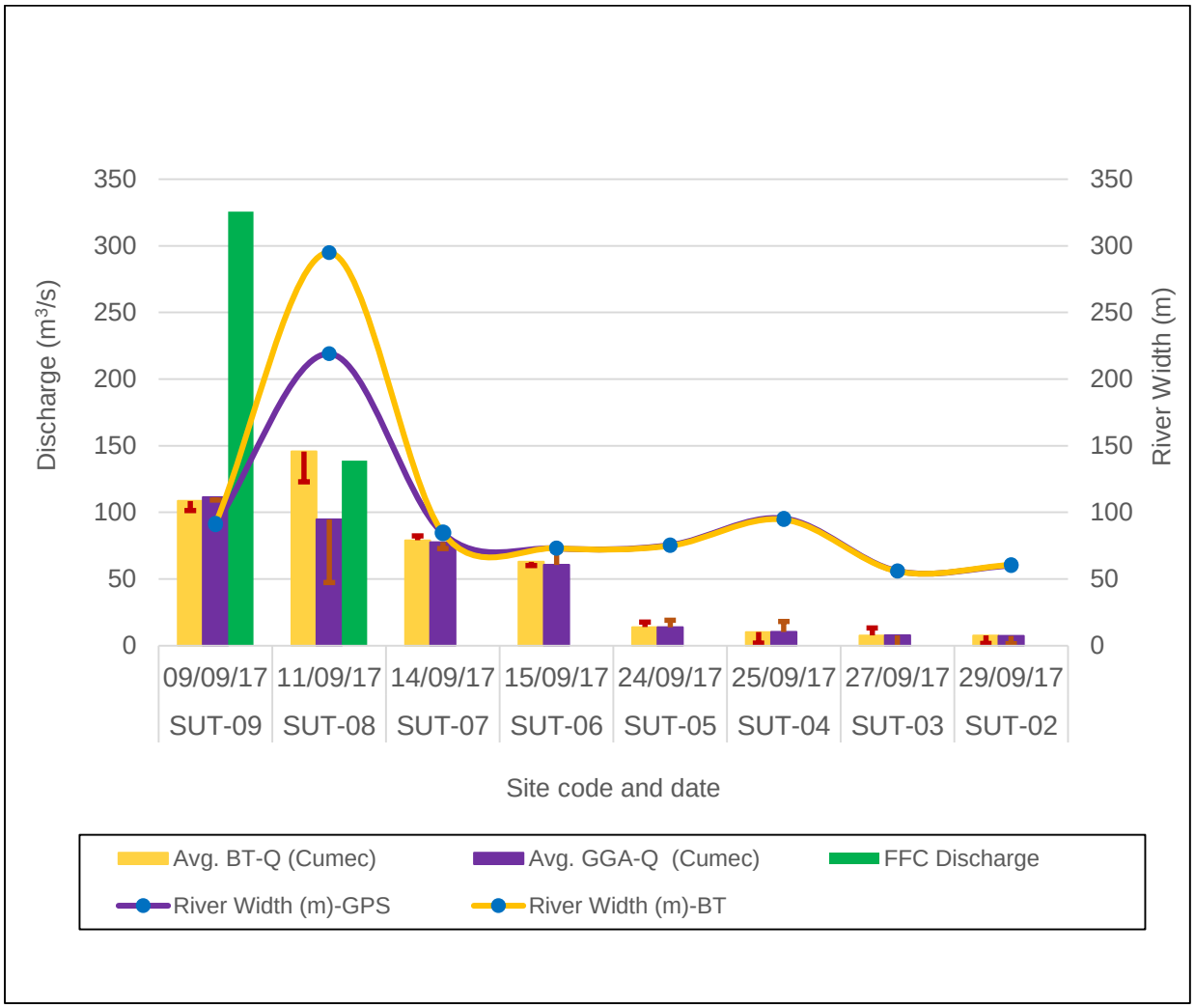


Figure 18: ADCP based measurement of discharge of the river Sutlej in chronological order of measurement dates

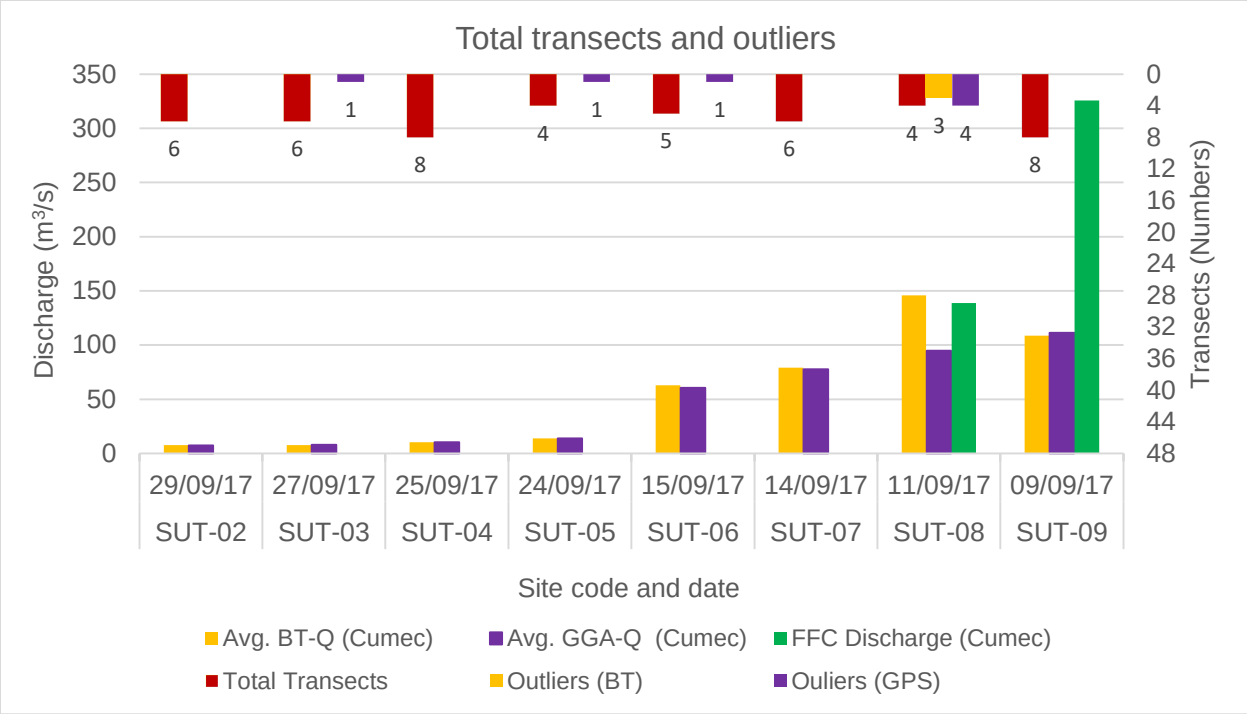


Figure 19: ADCP based measurement of discharge of the river Sutlej in the order of upstream to downstream measurement sections

3.3 Compass calibration

Compass calibration is preferred for all the ADCPs having internal magnetic compass but is necessary only when GPS mode is used as reference for boat velocity (Mueller and Wagner, 2006). The measurements in the current study are based on composite (GGA) mode i.e. carrying out measurements in BT as well as GPS modes simultaneously; therefore, calibration was done only for twelve river sections for ascertaining accuracy of the ADCP. The permissible limit of compass error is 1 degree (Mueller *et al.,* 2013) and all our compass errors (Table 3) are well within the permissible limit.

Table 3: Compass calibration results at the selected river sections

Site Code	Typical Heading Error (°)	Site Code	Typical Heading Error (°)	Site Code	Typical Heading Error (°)	Site Code	Typical Heading Error (°)
JEH-03	0.50	CNB-06	0.34	RV-08	0.73	SUT-02	0.46
JEH-05	0.73	CNB-07	0.29	RV-04	0.72	SUT-04	0.80
JEH-15	0.42	CNB-09	0.34			SUT-05	0.67
		CNB-13	0.89				

3.4 Moving bed test

Similar to compass calibration, moving bed (MB) test is preferred for each site of discharge measurement. However, if sufficient evidence is available that moving bed conditions does not exist, the test can be omitted (Oberg *et al.,* 2005). As the measurements pertain to low flow period, tests were conducted on a few sites for ascertaining MB conditions if any. In fact, MB tests made at some other sites were lost due to technical issues of the WinRiver II software. The admissible limit of moving bed velocity as percent of mean water velocity is 1-2% depending on anchoring stability if the test is stationary boat type (Mueller *et al.,* 2013). Under this study, the admissible limit of 2% applies, as the tests were stationary boat type for which the boat could not be stably anchored as the untrained hired boatman was engaged separately for each field trip. The MB test results are given in Table 4. It shows that the potential MB error is mostly within 1-2% except in one case at the river Ravi that was in flood at the time of measurement. It means MB conditions do not exist in the eastern tributaries during low flow period, indicating that river bottom tracking (BT mode) can be used as velocity reference for discharge measurement owing to the negligible error induced by moving bed. However, BT and GPS mode measurements can become more compatible and quality assured if compass calibration and MB test are articulately carried out and magnetic declination, deviation and multipath errors are avoided. All the data pertaining to the measurements at the sections of the river Sutlej are given in Annexure A-III. As mentioned before, the data in the annexures was post-processed using site specific magnetic declination and draft depth of 0.1 m in the playback configuration of WinRiver II.

Table 4: Moving bed test results of the selected river sections

Site Code	MB Test	Distance US/MG (m)	Duration (s)	MB Velocity (m/s)	MB Direction (°)	Water Velocity (m/s)	Average Depth (m)	% Bad Bottom Track	Potential MB Error (%)
SUT-03	Stat. 000	-0.187	632.53	0	194.85	0.064	2.72	0	-0.35
SUT-04	Stat. 000	-0.604	652.03	-0.001	160.01	0.125	0.78	0	-0.72
SUT-05	Stat. 000	-2.809	586.47	-0.005	214.46	0.149	1.41	0	-3.3
SUT-07	Stat. 001	-2.338	362.41	-0.007	10.68	0.44	2.15	1.58	-1.48
RV-08	Stat. 001	-0.837	539.52	-0.002	263.9	0.384	1.42	0	-0.39
RV-04	Stat. 000	80.479	635.66	0.148	67.11	1.13	2.52	38.78	13.07

3.5 Point seepage rates

Average of the point seepage rates of three measurements at the selected river sections are shown in Figure 20. Point measurement of seepage rate is not supposed to reflect

the seepage rate of the corresponding river reach as it represents the measurement on a very small area compared with river section. Point to point variability adds further to uncertainty. However, such measurements can give reasonable estimates of sectional seepage rates for surface-groundwater interaction.

In Figure 20, the sections 10, 11 and 12 fall upstream of Mangla dam. The upstream reach of the river Jhelum above Mangla dam is in highly mountainous region and hence, the river sections were gorge type having turbulent and violent flow conditions. Therefore, measurement of seepage rates in those sections were neither possible nor carried out. Downstream Mangla dam, seepage rate varies from 2.35 (JEH-1) mm/day to 0.264 (JEH-7) mm/day. The highest rate is at the upstream reaches and the lowest at the downstream. The reason seems that the upstream reaches have coarser bed material than the downstream as per Sternberg's law. Abrasion, fragmentation and hydraulic sorting of sediment particles in the downstream reaches makes the bed material well graded and more impervious (Bouteiller *et al.,* 2011).

In the river Chenab, the highest seepage rate is 2.23 (CNB-02) mm/day and the lowest 0.34 (CNB-09) mm/day. However, the seepage rate varies randomly along the entire length of the river. The distribution of the seepage rates along the river reach shows that the frequency of high seepage rates in the upper reach above Trimmu barrage is more than its downstream. The reason for high seepage rate at the upstream reach seems the same as the bed material at upstream is less graded than the downstream. Well graded material has wide range of particle sizes that packs well within each other thereby making the strata less permeable. Contrary to that, less graded material has narrow range of particle sizes which do not pack well and make the strata more permeable (Bouteiller *et al.,* 2011). The high seepage rate exhibited in the vicinity of Trimmu barrage may be due to the reach falling in the Thal desert having sandy strata (Khan *et al*, 2016; Malik *et al.,* 2019).

In the river Ravi, the highest and the lowest seepage rates are 1.43 (RV-03) mm/day and 0.622 (RV-01) mm/day, respectively, but both the values fall in the upper reach. In fact, limited measurements could be carried out in the river Ravi either due to the river found dry, or cluttered with sewage water.

In the river Sutlej, the highest and the lowest seepage rates are 1.70 (SUT-8) (mm/day and 0.35 (SUT-2) mm/d respectively, but seepage rate values vary randomly along the reach of the river. The Sternberg's law for particle distribution along the river reach hardly applies to the reach of the Sutlej river in Pakistan as the entire water is diverted by India in its own territory. The downstream reach carries water diverted from the rivers Jhelum and Chenab through link-canals. Furthermore, the downstream reach is adjoining

Cholistan desert where high seepage rates seem rational. Therefore, seepage rates though have mixed trends depending on local strata but are generally more in upstream reaches of all the tributaries except the river Sutlej. These findings are in line with the bed material mean particle size as discussed in section 3.8. The data pertaining to the seepage measurements at the sections of all the four rivers are given with other sectional data in Annexures A-I to A-III.

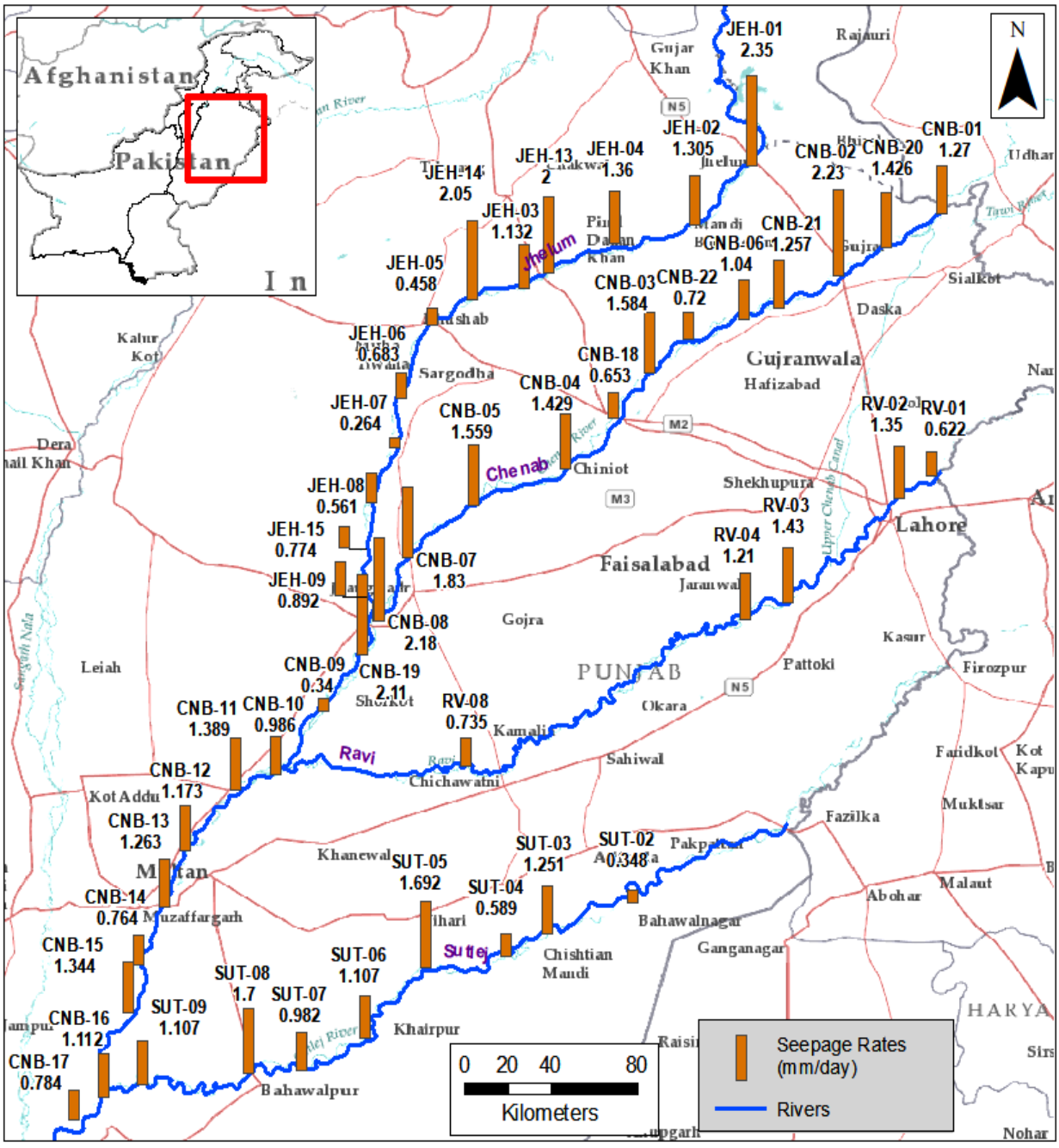


Figure 20: Seepage rates at the sections of discharge measurement in all the eastern rivers

3.6 Infiltration rates

3.6.1 Spatial coverage of Horton's steady state infiltration rates

The cumulative infiltration data were fitted on Philip (1957) and Horton (1940) equations. A comparison of the fitting in terms of R^2 on Philip and Horton cumulative infiltration equations is given in Figure 21. It shows that the fitting on Horton equation is comparatively better than on Philip equation as was also reported by Malik *et al.* (2019) for similar tests in Doabs of the Upper Indus Plain. Additional advantage of the Horton equation is that it has steady-state infiltration rate as its built-in parameter which is considered equivalent to typically required field saturation conductivity. Therefore, Horton's steady-state infiltration rates were adopted.

The so determined steady-state infiltration rates spatial coverage mapping on 20 km grids on each bank of the rivers at the sections of flow measurement at surface, 0.5 m and 1.0 m depth are given in Figures 22 to 24, respectively. The spatial coverage percentages of the area under different ranges of infiltration rates are given in Figure 25. The dominant range of steady infiltration rate at the surface and middle layers is 15-30 mm/hr, whereas it is 60-90 mm/hr at the bottom layer.

In the surface layer, the lowest infiltration rate class has the largest percentage coverage, which visibility decrease with increase in infiltration rate. Whereas in the bottom layer, the highest infiltration rate class has largest percentage of coverage, which slowly decrease with decrease in infiltration rate as is evident from the trend lines in Figure 25.

This coverage of infiltration rates is almost compatible with coverage of soil textural classes. In soil classes, as discussed in the next section, silt loam has the greatest spatial coverage at the surface and middle layers followed by loam and sandy loam. Typical infiltration rates of textural classes are silt loam< loam< sandy loam (Berhanu *et al.,* 2013).

However, infiltration rates are controlled by not only texture profile but also the role of macrospores often become dominant. Possibilities of macrospores in surface layer are normally bleak. Because in the surface layer, macrospores are frequently choked due to wind and water erosion as well as treading by humans and animals (Malik *et al.,* 2019). Contrary to that, decay of roots and living organisms create macrospores in comparatively deeper layers, which are not affected by the choking activities. When infiltration tests are performed in dug pits, macrospores normally remain intact and play crucial role in infiltration process. That is why the spatial coverage of higher infiltration rates increased with depth up to 1 meter.

The above discussion reveals that the distribution of dominant range of Horton's steady-state infiltration rate at the surface and middle layers is 15-30 mm/hr, whereas it is 60-90 mm/hr at the bottom layer showing increasing trend towards bottom layer of 1.0 m depth.

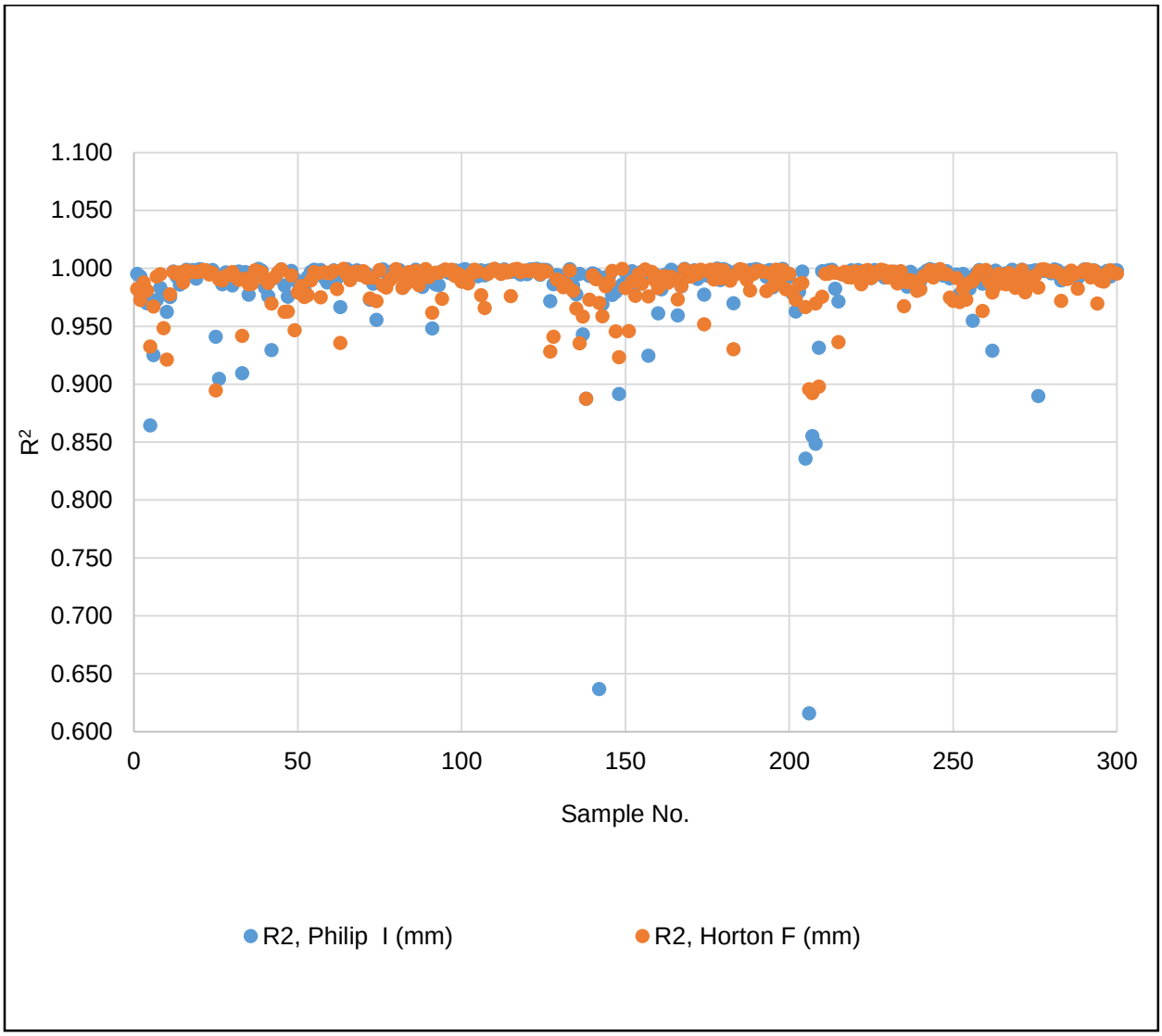


Figure 21: Comparison of R^2 of fitting cumulative infiltration data on Philip and Horton equations

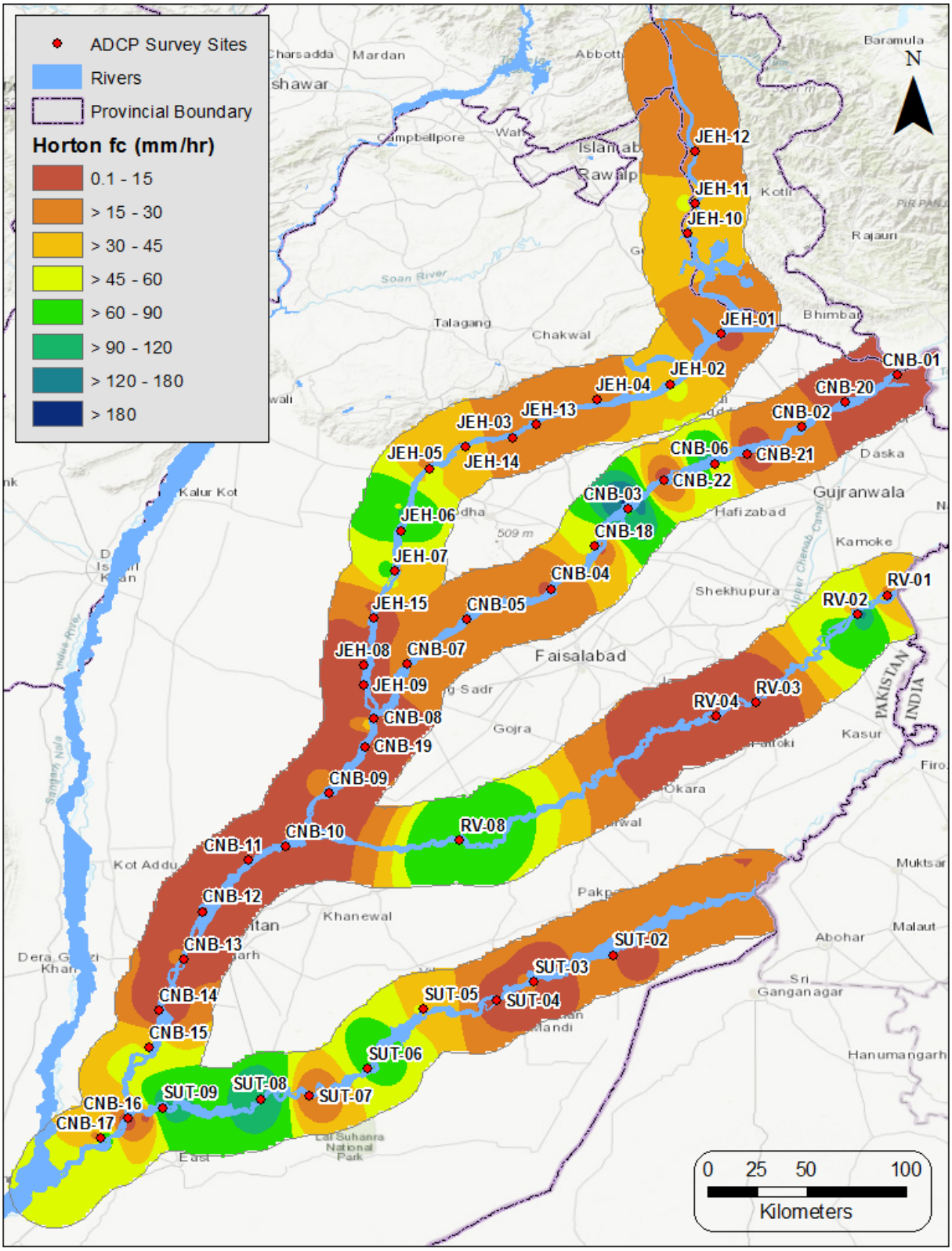


Figure 22: Spatial coverage of Horton's steady state infiltration rates in the surface layer of active flood plains (20 km each side) of the eastern rivers

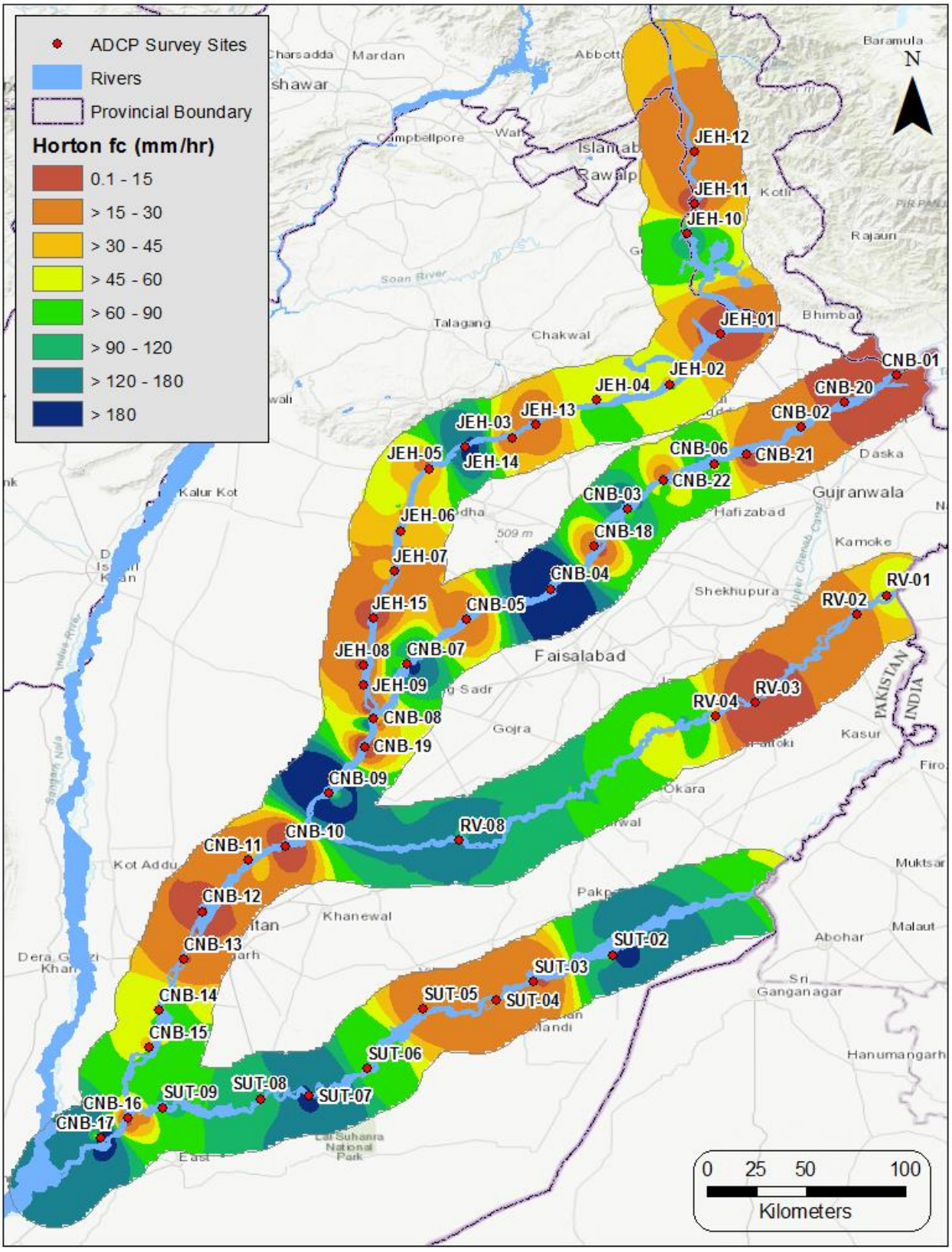


Figure 23: Spatial coverage of Horton's steady state infiltration rates in the middle layer of active flood plains (20 km each side) of the eastern rivers

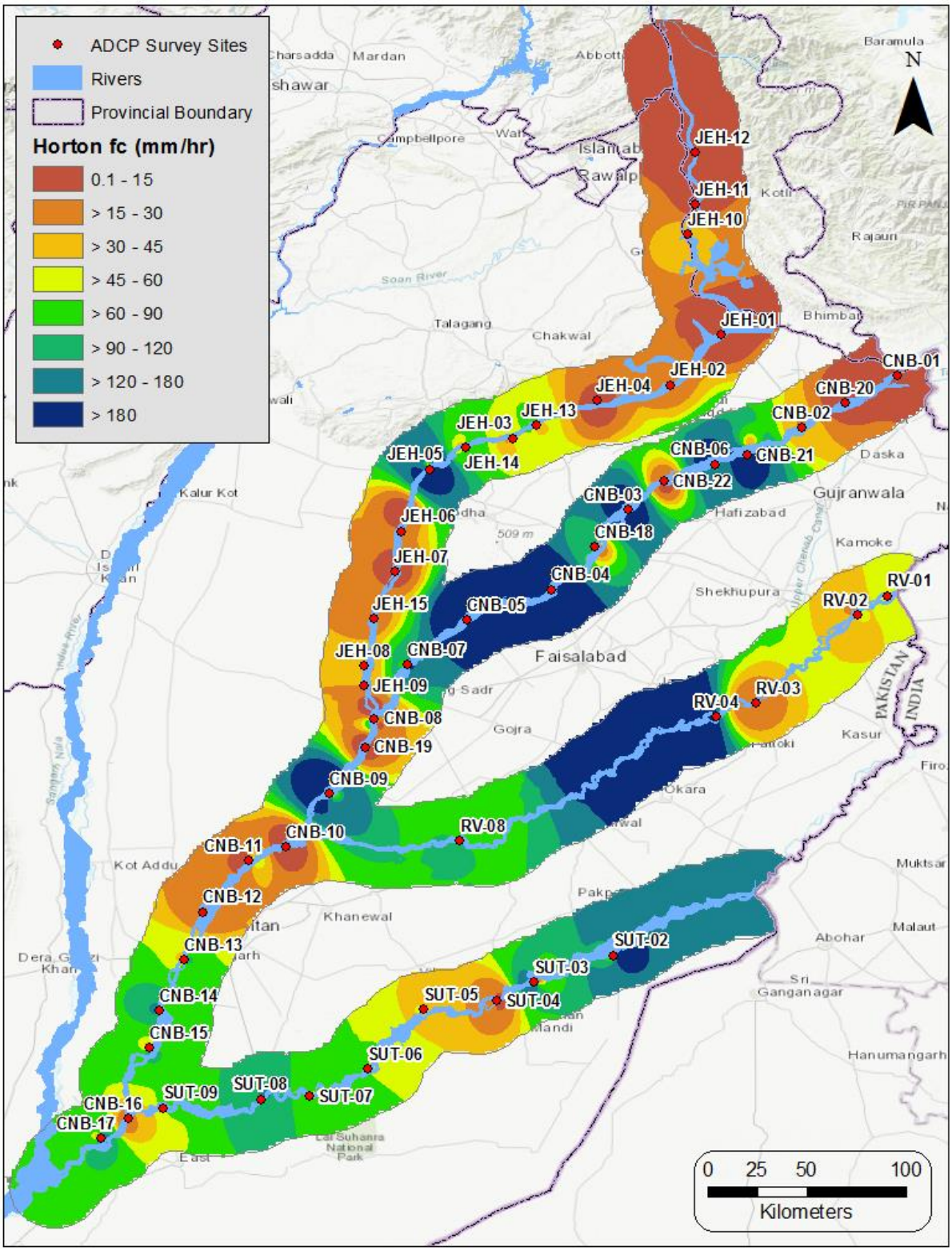


Figure 24: Spatial coverage of Horton's steady state infiltration rates in the bottom layer of active flood plains (20 km each side) of the eastern rivers

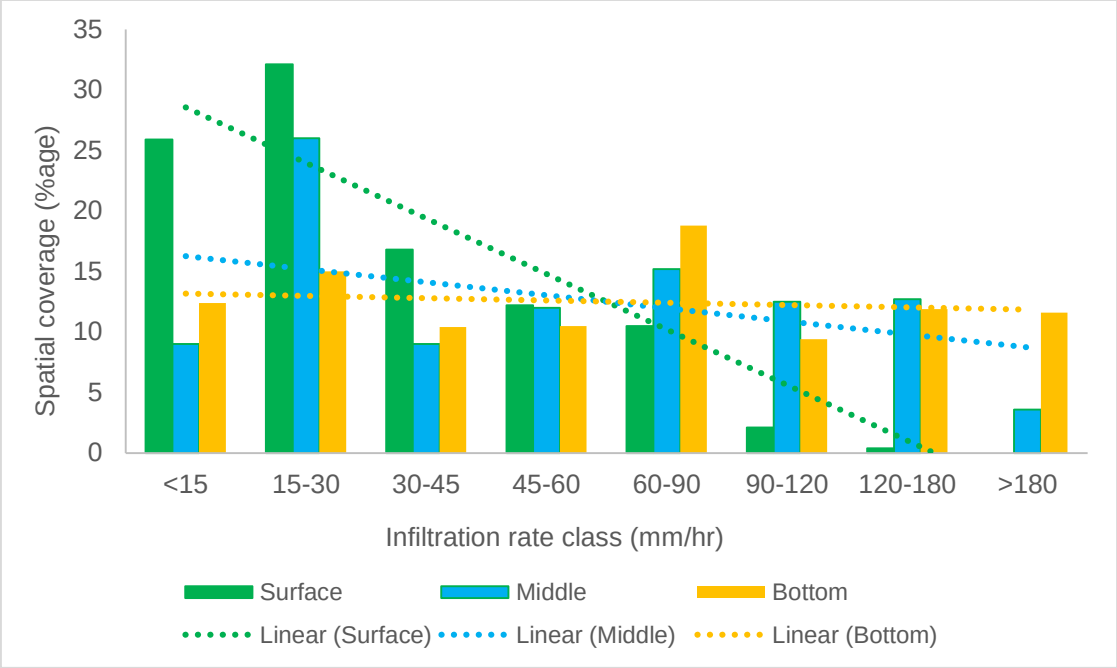


Figure 25: Spatial coverage percentages of different ranges of infiltration rates at the surface, middle and bottom layers along the banks of the eastern tributaries

3.7 Soil texture classes

Soil texture classes in the surface, middle and bottom layers of the soil pits in active flood plains both along the left and right banks of the eastern tributaries are given in Figures-26 to 28, respectively. The number of soil classes from top to bottom layers are 8, 9 and 8; respectively. Percent coverage of each of the soils class is given in Table 5. Dominant soil classes in all the three layers are silt loam, loam and sandy loam. Silt loam has the greatest spatial coverage at the surface and middle layers followed by loam and sandy loam soils. At the bottom layer, loam has the largest coverage followed by silt loam and sandy loam. With increase in depth, silt loam coverage decreases, loam remains almost stagnant and sandy loam increases.

In the active flood plains, soils along the riverbanks are typically formed due to deposition of silt and sand with floodwater or meandering rivers. Silt loam and sandy loam are the soil classes that fall at the bottom of the classification triangle and both the classes mainly comprise of sand and silt with clay fraction always less than 28%. Therefore, if the fraction of silt increases above 50%, the percentage of sand will accordingly decrease making it silty loam. Similarly, if percentage of sand increases beyond 50%, the class will shift to sandy loam. Pertinent to note that, silt loam, sandy loam and loam are adjoining classes in the triangle of soil texture. A decrease in sand and silt percentage will cause a

corresponding increase in clay content thereby changing the soil class from silt or sandy loam to loam. All the three classes represent higher percentages of sand and silt with low clay contents and fall in close proximity in the triangle. This is the peculiar composition of alluvial deposits in active flood plains comprising mostly of silt and sand. Therefore, mapping of all the three layers exhibit soil classes as expected in active flood plains.

The fraction of loam soil slightly increased with increase in depth. It may be due to washing action of water infiltrating into soil carrying with it fine clay participles thereby converting sandy loam or silty loam soil to loam soil in the context of discussion in the preceding paragraph. Studies carried out by (Malik *et al.,* 2019) in Doabs and Pothwar support this phenomenon. Therefore, the data reveals that silt loam, loam and sandy loam are dominant soil classes in all the three layers of the studied depth. However, coverage of sand dominant soil classes increase with increase in depth. The anticipated features of active flood plain as per above discussion support these findings.

Table 5: Spatial coverage percentages of different soil classes in the surface, middle and bottom layers of soil pits in active flood plains along the banks of the eastern tributaries.

Sr. No.	Soil Class	Percent Area (%)		
		Surface	**Middle**	**Bottom**
i.	Silt loam	46.504	37.283	33.882
ii.	Loam	34.401	33.556	35.893
iii.	Sandy loam	18.132	26.992	27.746
iv.	Loamy sand	0.041	0.713	1.380
v.	Sand	-	0.178	0.219
vi.	Silt	0.010	-	0.031
vii.	Clay loam	0.886	1.217	0.621
viii.	Silty clay loam	0.005	0.041	0.229
ix.	Silty clay	-	0.015	-
x.	Clay	0.020	0.005	-
	Total	**100**	**100**	**100**

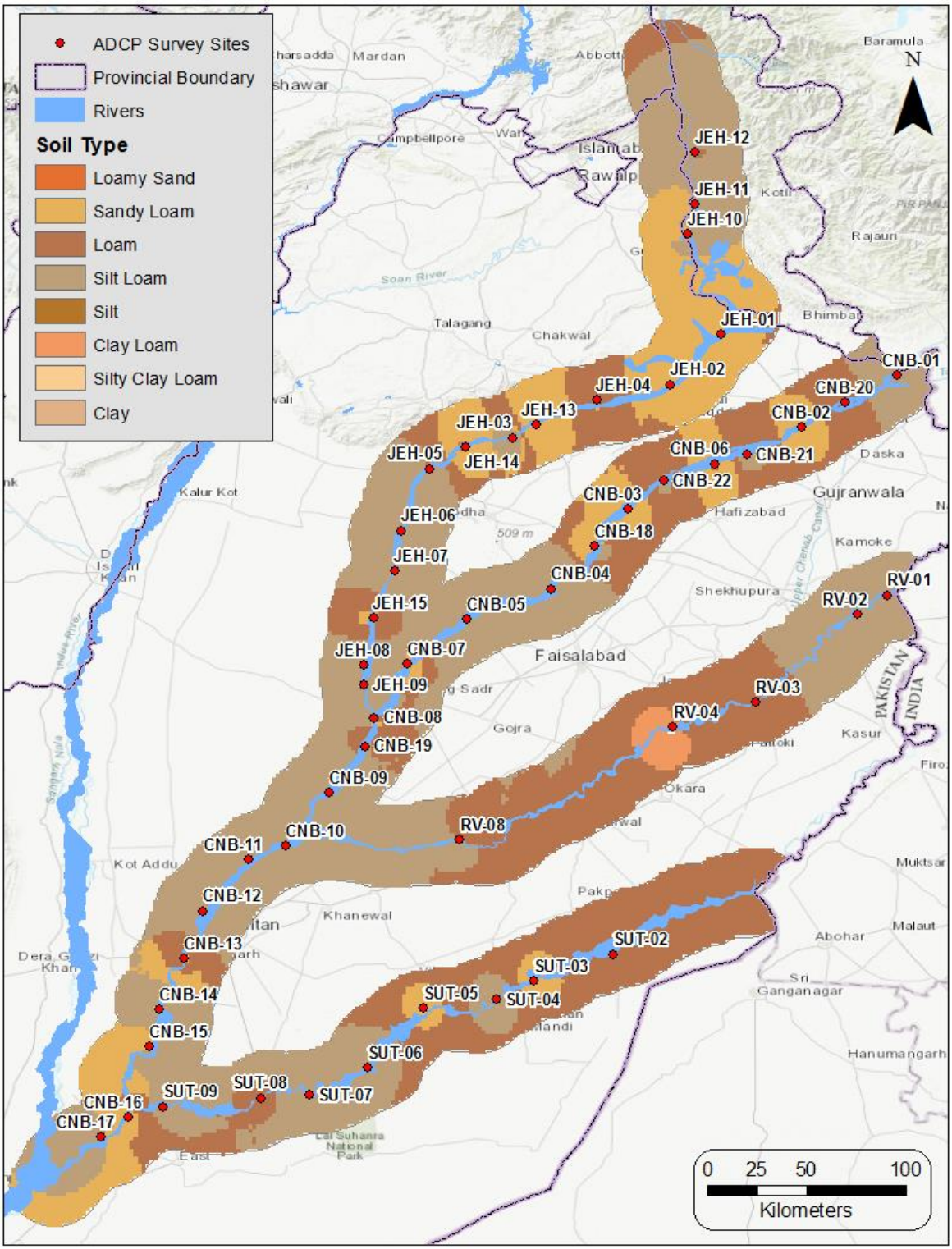


Figure 26: Spatial coverage of soil classes in the surface layer of active flood plains (20 km each side) of the eastern rivers

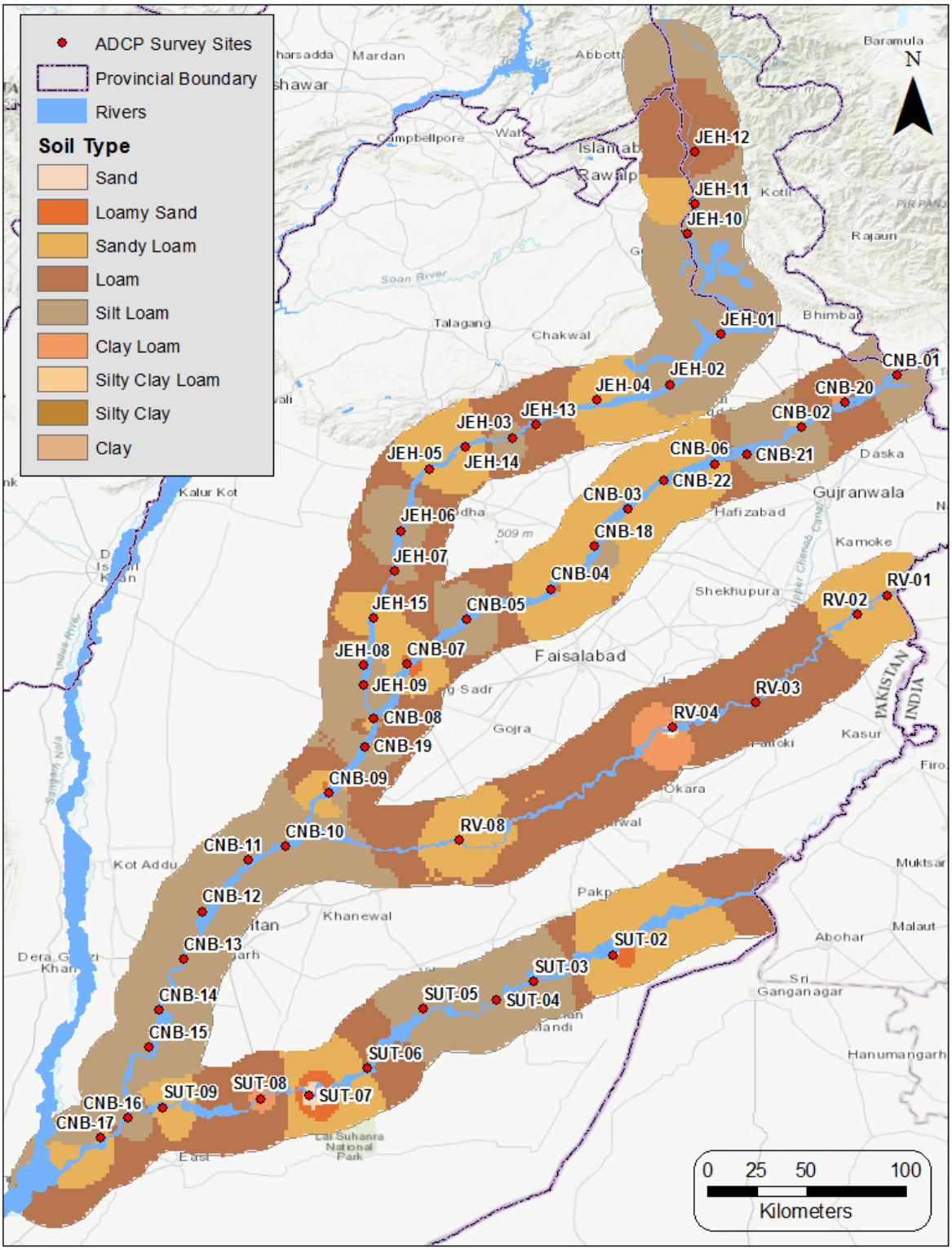


Figure 27: Spatial coverage of soil classes in the middle layer of active flood plains (20 km each side) of the eastern rivers

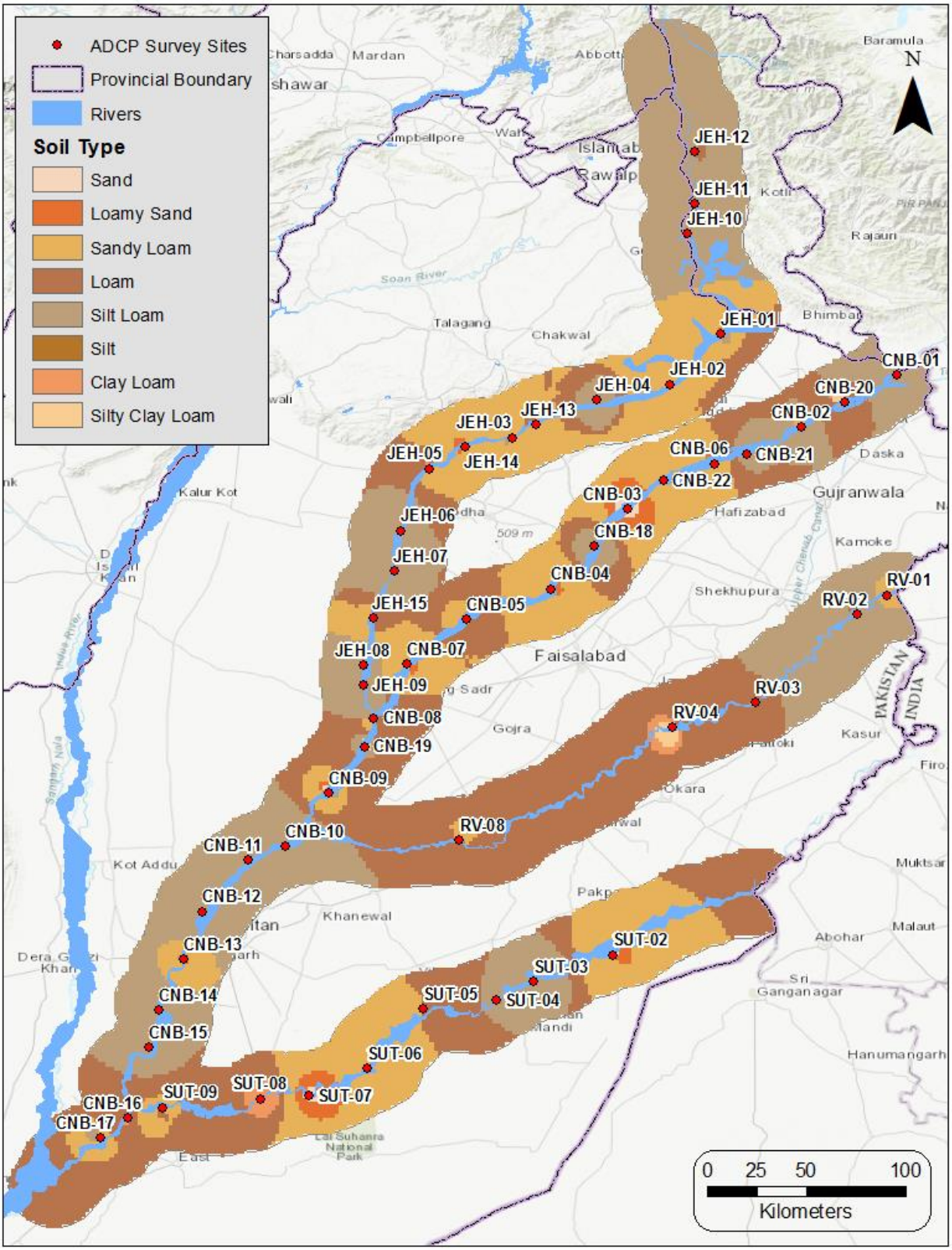


Figure 28: Spatial coverage of soil classes in the bottom layer of active flood plains (20 km each side) of the eastern rivers

3.8 Bed material of eastern rivers

3.8.1 Bed material profile of the river Jhelum

Bed material samples analysis of right and left banks of the river Jhelum is given in Figure 29. The point samples were composite of three locations in each case from the selected river sections. The sieve analysis of the composite samples was carried out and mean diameter (D_{50}) as well as Cu (D_{60}/D_{10}) determined after developing S-curves. Figure 29 shows the bed material mean diameter and Cu along each bank of the river reach from upstream to downstream. Mean particle diameter gives size of sediment having 50% of particles larger by weight, whereas uniformity coefficient (Cu) represents the distribution of particle diameters. The Cu close to 1 means particles of almost similar size. The more the Cu greater than 1, the more well distributed, or well graded, sediment particles will be.

The sediment size may depend on the sampling location whether falling on the upstream or downstream of a bridge or a diversion structure. On the upstream side of a hydraulic structures or obstructions, mean particle diameter may vary, due to increased probability of settlement of all the sizes of particles. The shift of mean particle size toward increasing or decreasing side will depend on the composition of sediment particle size profile, water velocity, settlement time becoming available, curvature of channel-bank whether concave or convex, etc. In meandering river, sediments deposit on the convex bank and erode from concave bank (Blanckaert *et al.,* 2012).

Under favorable conditions of deposition, if proportion of the large particle sizes is higher, the mean diameter shift may be towards increasing side and vice versa. This is evident from the left bank of the section JEH-1 and right bank of section JEH-3. In the former case, mean diameter is small and coefficient of uniformity is high, whereas opposite is true in case of the latter. Despite all these variabilities, the trend of mean particle size is decreasing towards the lower reaches as expected as per Sternberg's law, which states that the particle refining along the river reach is exponential function of initial grain size and distance traveled along the river (Bouteiller *et al.,* 2011). Downstream bed material size reduction occurs mainly due to particle abrasion, hydraulic sorting and fragmentation (Bouteiller *et al.,* 2011; Radoane *et al.,* 2007) involving complex interaction of mobility conditions, river aggradation, river basin concavity, lateral input of sediments, etc., which has widely been reported (Radoane *et al.,* 2007). Furthermore, the larger particles deposit earlier in the upper reaches and the finer settle later in the lower reaches after depositing coarser particles behind the hydraulic structures upstream.

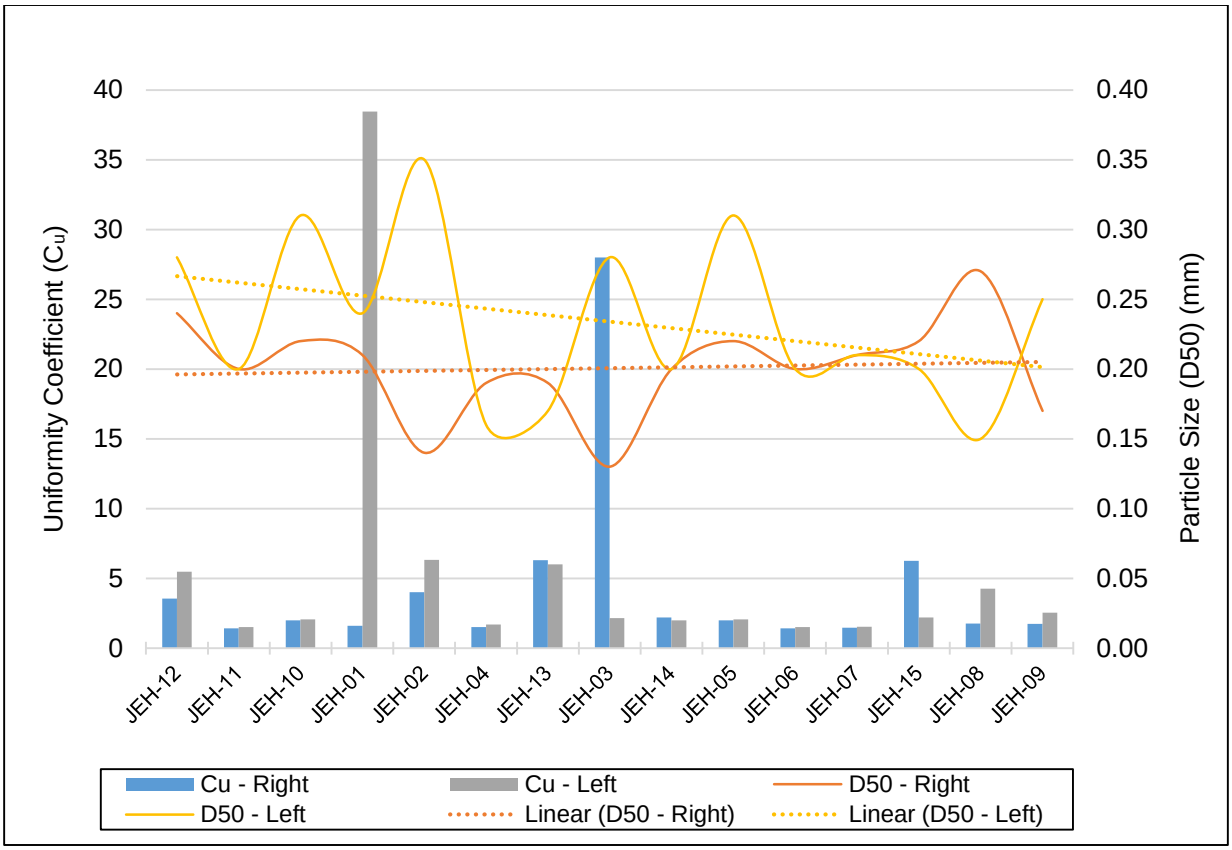


Figure 29: Bed material uniformity coefficient and mean particle size from upstream to downstream reach on both the banks of the river Jhelum

3.8.2. Bed material profile of the river Chenab

Figure 30 shows the results for the river Chenab. In case of the river Chenab, the variation of the Cu is much more compared to the river Jhelum, but this variation is in the reach below the confluence of the river Chenab and the river Jhelum at the Trimmu barrage. The highest Cu is at the section CNB-19 which is below the said confluence. The river Jhelum upstream flows through a reach adjoining the Thal desert where sediment size profile is supposed to change due to peculiar strata. Therefore, after the confluence, the sediments of different origins of the two rivers combine and broaden the spectrum of particle sizes (Radoane *et al.,* 2007). That has caused high value of Cu. Mean particle diameter of sediments has visible decreasing trend in the lower reaches as was in case of the river Jhelum in accordance with Sternberg's law narrated in the preceding paragraphs.

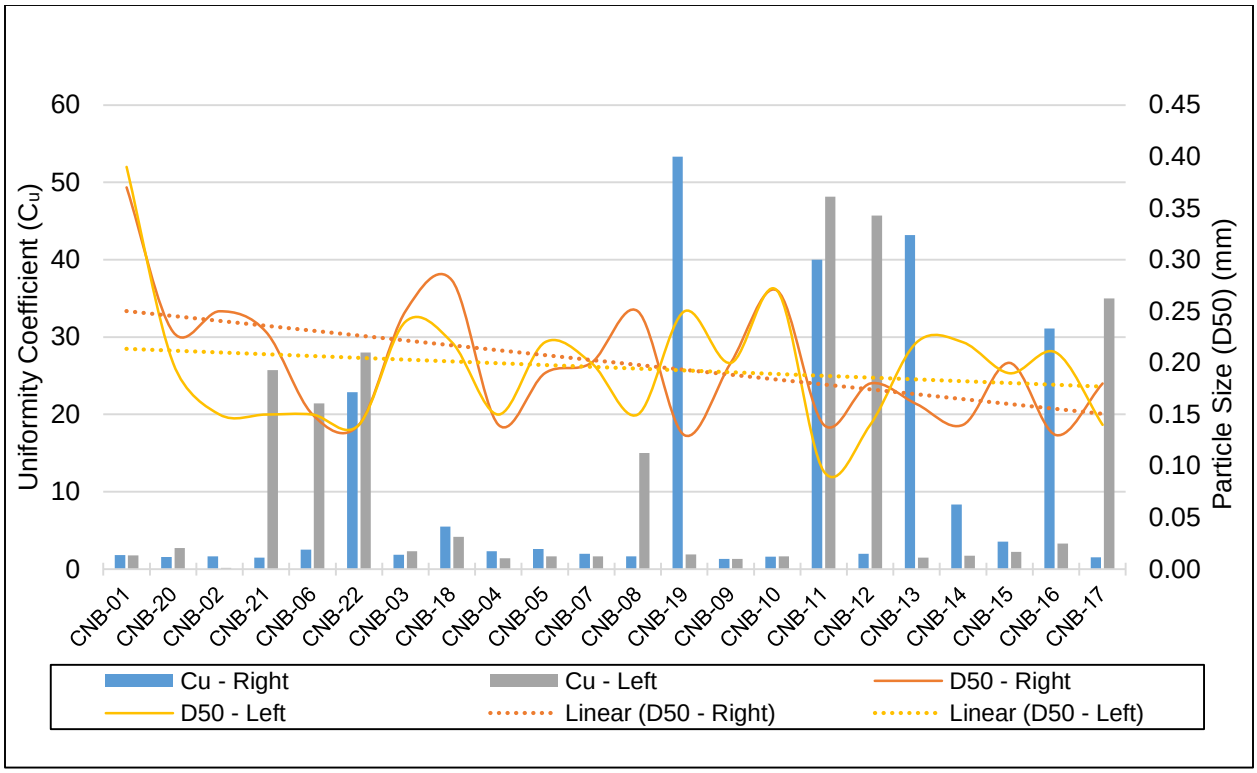


Figure 30: Bed material uniformity coefficient and mean particle size from upstream to downstream reach on both the banks of the river Chenab

3.8.3. Bed material profile of the river Ravi

The mean sediment size diameter and Cu of the river Ravi is given in Figures 31. The Cu of the river Ravi is highest in its lowest reach. Under the Indus Water Treaty (1960), India, the upper riparian, has gained full rights on waters of the rivers Ravi and Sutlej. In Pakistan's territory, these two rivers are virtually no more flowing. Several link canals supply water from the western rivers to these eastern tributaries. The eastern tributaries then divert that water into canals off-taking from several barrages. Therefore, these two eastern tributaries have lost their inherent typical features of bed material. The waters in downstream reaches are mix of waters of the rivers Chenab and Jhelum and so are the characteristics of their sediments. As such, sediment profiles of the two western rivers supplying waters to the eastern tributaries (rivers Ravi and Sutlej) broaden the particle size range in the lower reach of the river Ravi. Another important factor distorting morphology of these rivers is the sand digging for construction purpose from the upper reaches of the rivers Chenab, Ravi and Sutlej. Nevertheless, mean particle diameter has decreased toward downstream reach as in other rivers.

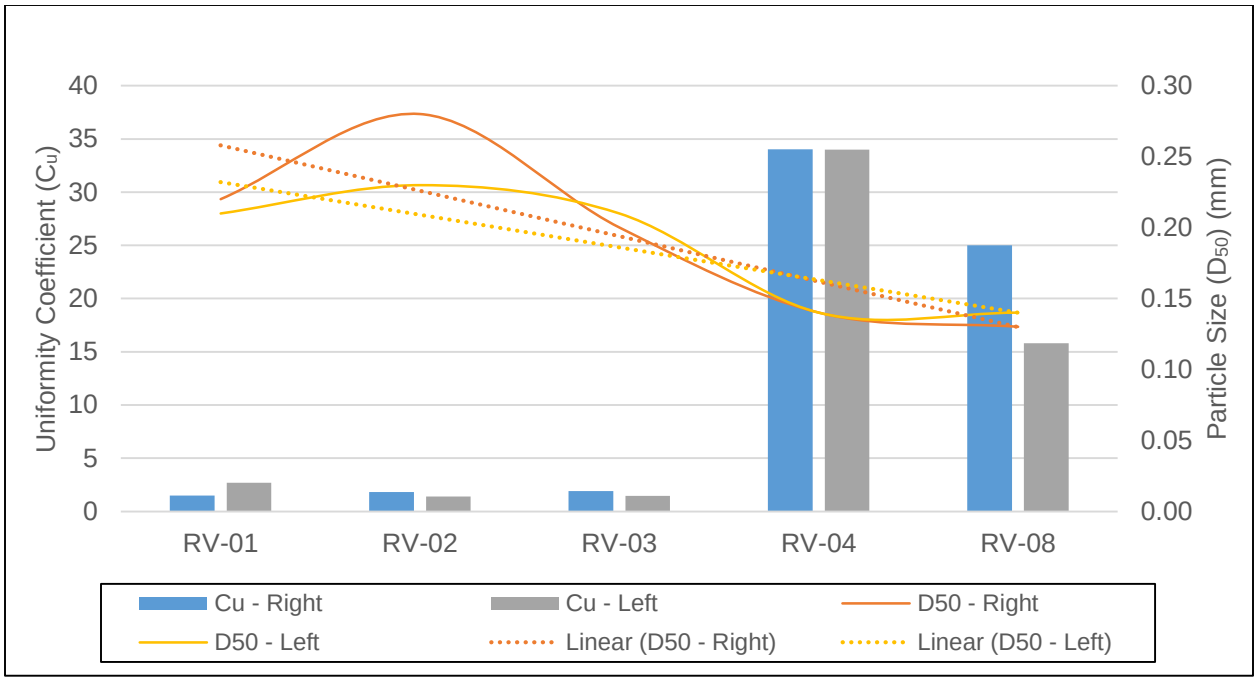


Figure 31: Bed material uniformity coefficient and mean particle size from upstream to downstream reach on both the banks of the river Ravi

3.8.4. Bed material profile of the river Sutlej

The bed material sediment profile of the river Sutlej is given in Figure 32. In case of the river Sutlej, Cu is highly variable in the upper reach than in the downstream side contrary to the other three rivers. In this river, a longer upstream reach adjoining the Cholistan Desert remains almost dry (Figure 33). Even when flowing, it is so shallow that can easily be waded. Wind erosion brings fine sand from the adjoining Cholistan desert and deposits in the bed of this river, which seems to have reduced the mean particle size of its bed material. The mean particle size increases as it escapes from the reach of wind erosion deposition and receives waters of western tributaries through link canals. Radoane *et al.,* (2007) also observed increase in mean particle size in downstream reaches of the Trotus and Siren rivers in Romania and attributed it due to contribution of tributaries. The contribution of sediments from link canals might also be contributing toward high variation of Cu in accordance with Sternberg's law.

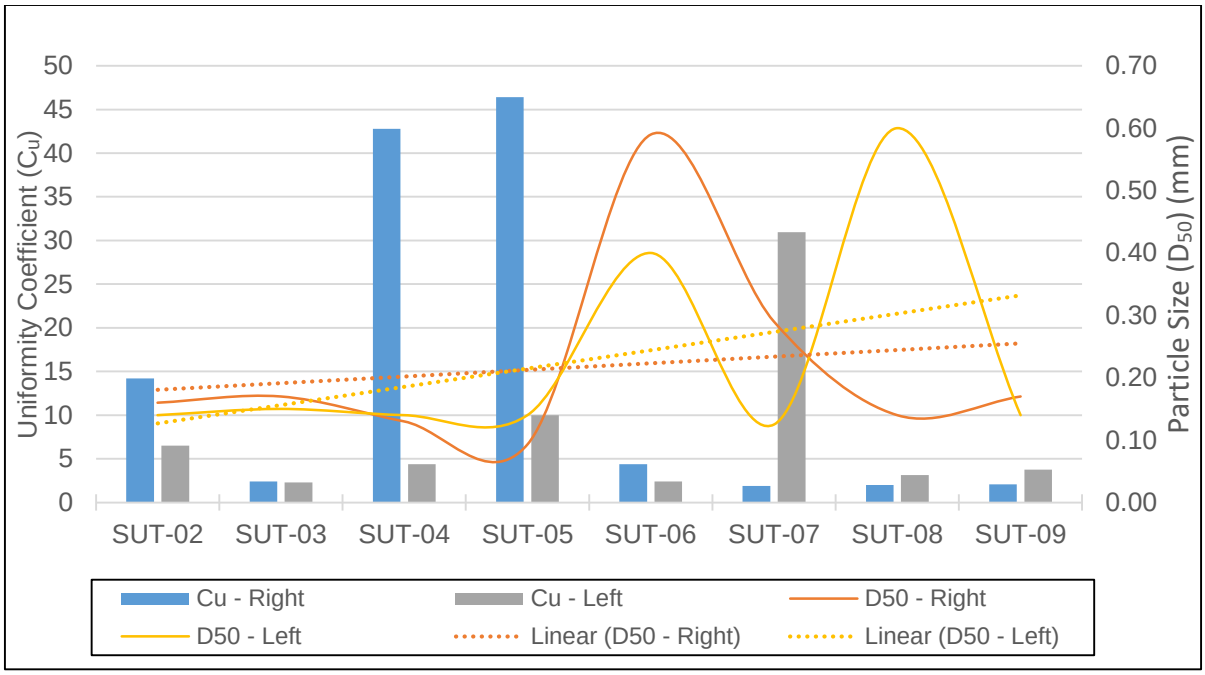


Figure 32: Bed material uniformity coefficient and mean particle size from upstream to downstream reach on both the banks of the river Sutlej



Figure 33: A view of the river Sutlej without any water at Bahawalpur Bridge

3.9. Soil moisture retention characteristics and allied parameters

Soil moisture retention curves of the soils at the surface, middle and bottom layers of the pits at the measurement sections are given in Figure 34. Altogether ten soil types were found based on texture analysis of soil samples from riverbank pits but curves are shown only for nine soils excluding clay having minor fraction. The percentage coverage of the three dominant soil classes normally increased from top to the bottom layer except for silt loam as already shown in Table 5. The numbers of soil classes from top to bottom layers are 8, 9 and 8, respectively. The soil moisture retention parameters of all the soil samples are given in Annexure B-I to B-IV. Descriptive statistics of the moisture retention and allied parameters in the active flood plains along the banks of the 50 cross-sections where ADCP measurements were carried out are given in Table 6.

Average bulk density in the studied layers varies from 1.18 to 1.90 mg/cm^3 with overall average value 1.45 mg/cm^3, which are in accordance with those reported by Malik *et al.* (2019). Meek *et al.* (1992) reported bulk density up to 1.92 mg/cm^3 of sandy loam soil due to compaction under tillage machinery and other management practices. In fact, soil bulk density is not an inherent property but depends on natural processes and anthropogenic activities (Zeng *et al.,* 2013). Coefficient of variability (CV), defined as ratio of standard deviation to mean in percent, is from 8.63 to 9.31, the latter for the surface layer. Comparatively more CV for surface may be due to changes caused by traffic and several other factors including moisture content while sampling (Meek *et al.,* 1992; Zeng *et al.,* 2013). These CV values are in the low range as per categorization by Nielsen and Bouma (1985) and are in accordance with those reported by Malik *et al.* (2019) and Dec and Dorner (2014).

The maximum values of steady-state infiltration rates in the active flood plains are 263 to 580 mm/hr, low for the surface layer and high for the middle. Hydraulic conductivity decreases with increase in bulk density due to discontinuity of pores (Dec *et al.,* 2008). Comparatively low *fc* in the top layer may be due to higher bulk density and sealing of macropores at the surface due to treading, raindrop compaction, sealing, etc. (Malik *et al.,* 2019; Chaudhari *et al.,* 2013; Iqbal *et al.,* 2005). The high value of *fc* in the middle layer may be due to dominance of roots in that layer and resultant undisturbed macropores over there (Malik *et al.,* 2019). The CV of *fc* of active flood plains is high varying from 135 to 148% and its distribution is compatible with the distribution of maximum *fc* over the depth. It should be noted that the minimum *fc* is 0.05 mm/hr which may be considered as zero. These zero values of *fc* normally pertain to those infiltration tests where some impeding layer were encountered and resultant failure of the test. Such values were not excluded as outliers because those are part of natural soil strata. The CV

values are comparatively less than those reported for Doabs by Malik *et al.,* (2019). This may be due to the reason that the active flood plains are recent alluvial deposits formed by almost similar processes and least disturbed by anthropogenic activities, and hence have less variability. However, CV values of fc are persistently high as frequently reported in literature (Riikka *et al.,* 2019; Malik *et al.,* 2019; Bodner *et al.,* 2013; Schwen *et al.,* 2011; Hu *et al.,* 2009; Das Gupta *et al.,* 2006).

Regarding the van Genuchten soil parameters, saturated moisture content (Θs) varies from 0.27 to 0.68 cm^3/cm^3 as minimum to maximum, respectively. Pertinent to note that higher the bulk density, the lower the porosity or Θs. Furthermore, Θs is always less than porosity due to entrapped air, which may be up to 10% of the bulk soil volume (Sakaguchi *et al.,* 2005). The Θs values may therefore, be seen in that context. Variability of Θs is marginally low (11.56 to 12.65%) as also similarly reported by Malik *et al.,* (2019) for Indus Plain of Pakistan and Wang *et al.,* (2014) for loess plateau of China. Trends of Θr and n are in the upper and lower margins, respectively, of the moderate range of CV categories similar to those reported for Loess Plateau of China. However, CV values of α in the present case are in moderate range similar to those reported by Malik *et al.,* (2019) for Upper Indus Plain, but are contrary to its high variability reported by Wang *et al.,* (2014). The low variability was due to better resolution of data at low suction head (Malik *et al.,* 2019). The reason of low variability is also visible from low scatter of α having standard deviation of 0.01 as compared to 0.08 reported as by Wang *et al.* (2014).

Soil organic matter is an important ingredient for various physico-chemical processes and soil water interaction. Organic matter in soils may be in elemental (charcoal, graphite, coal, etc.), inorganic (calcite, dolomite, siderite, etc.) and organic form (sugars, carbohydrates, proteins, fats, organic acids, etc.). These forms of organic matter may typically yield slightly different results depending on the method applied for its determination. Organic matter is also presented in terms of total organic carbon (TOC) and conversion factor of 1.724 is normally used (OM = 1.724xTOC). However, that conversion factor is not universal and may have values of 1.724 to 2.5 depending on soil type and depth to horizon (Schumacher, 2002).

In this study weight loss on ignition method was used and found organic matter varying from 0.09 to 3.68% with average values from 0.68 to 1.27%, the lower values pertaining to bottom layers (Table 6). The CV values are 50, 55 and 58% based on 100 samples each from top to bottom layers, respectively. Azam *et al.* (2001) reported that carbon content in soils of Pakistan varies from 0.52 to 1.38% and accordingly organic matter may be considered as 0.89 to 2.37% using the conversion factor of 1.724, which is not universal. Rizwan *et al.,* (2016) measured the organic matter in a limited region of 0.94

km^2 in Pothwar and found organic matter content varying from 0.17 to 1.51% with average value of 0.73%. As per Rizwan *et al.* (2016), the CV based on 260 samples was 39%. The reason for the higher CV is the coarse sampling resolution compared with Rizwan *et al.* (2016).

Summarizing the average range and variability of the studied soil parameters in the active flood plains in the three layers of surface, 0.5 m and 1.0 m depths: average bulk density is 1.44 - 1.45 mg/cm^3 with CV in low range of 8.63 to 9.31%. Average Horton's steady state infiltration varies from 31.86 - 76.75 mm/hr with high CV values in the range of 135 -158%.

The average van Genuchten Θs values in the three layers are 0.45 - 0.46 cm^3/cm^3 with CV in the low range of 11.56 - 12.65%, Θr is 0.05 - 0.06 cm^3/cm^3 with CV in the medium range of 86 -93%; α ranges 0.01 - 0.02 cm^{-1} with medium CV from 70 - 77%; and n have average values of 1.66 – 1.90 with CV in the medium range of 37 - 53%. Average organic matter varies in the range of 0.68 - 1.27% and have medium variability with CV ranging 50 - 58% in the in the three horizons up to 1.0 m depth.

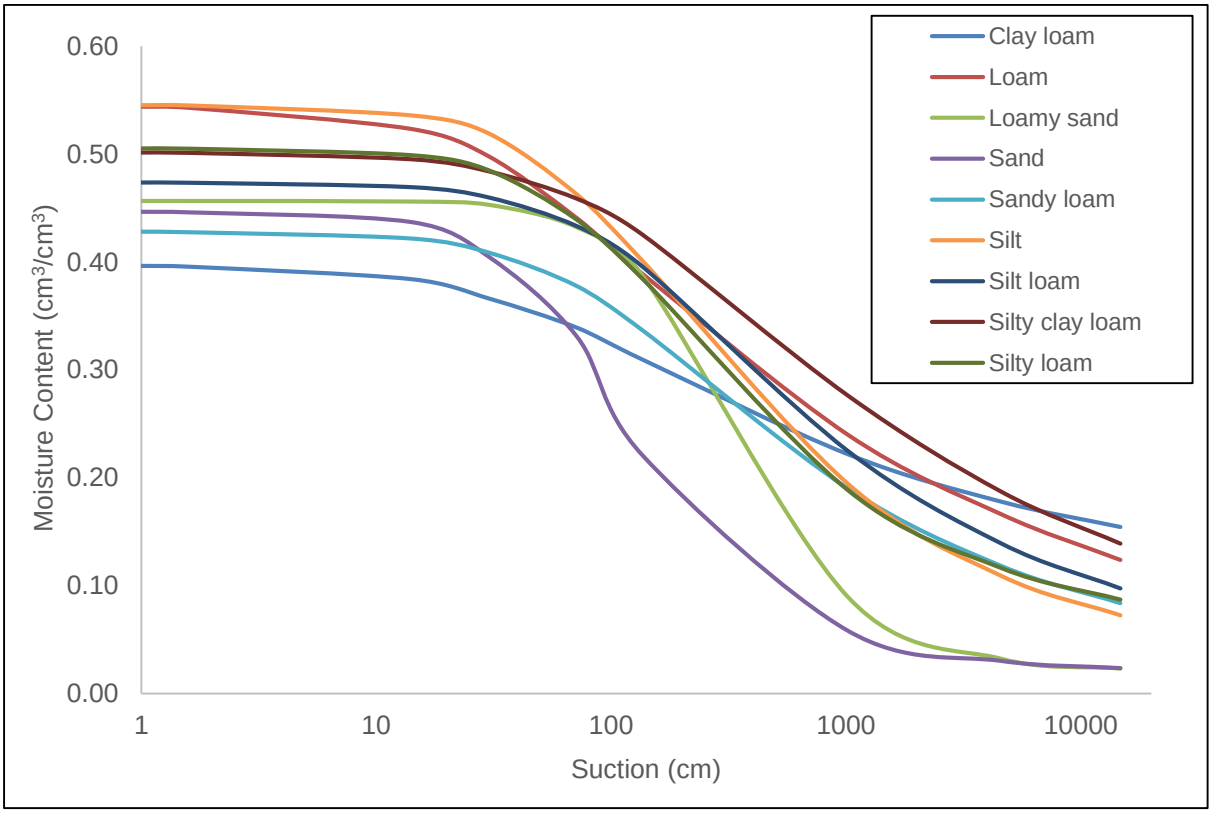


Figure 34: Soil moisture-retention curves for representative soil types of river banks

Table 6: Descriptive statistics of soil physical and hydraulic parameters along the 50 selected sections of the eastern tributaries of the river Indus

Parameter	Layer	Max	Min	Average	SD	CV percent
Avg. B.D. (g/cm^3)	S	1.90	1.21	1.45	0.13	9.31
	M	1.84	1.21	1.45	0.13	8.63
	B	1.90	1.18	1.44	0.13	8.68
fc (mm/hr)	S	263.31	0.37	31.86	43.11	135.29
	M	579.49	0.05	61.98	98.15	158.35
	B	460.71	0.71	76.75	110.47	143.93
Θs (cm^3/cm^3)	S	0.56	0.27	0.45	0.05	12.08
	M	0.68	0.31	0.46	0.06	12.65
	B	0.63	0.33	0.46	0.05	11.56
Θr (cm^3/cm^3)	S	0.21	0.02	0.06	0.05	86.54
	M	0.17	0.02	0.05	0.04	85.71
	B	0.29	0.02	0.05	0.04	92.62
α (cm^{-1})	S	0.06	0.00	0.01	0.01	69.84
	M	0.09	0.00	0.01	0.01	69.99
	B	0.08	0.00	0.02	0.01	76.89
n (dimensionless)	S	5.82	1.12	1.66	0.61	36.58
	M	5.82	1.07	1.83	0.81	44.40
	B	8.43	1.06	1.90	1.01	53.17
O.M. (%)	S	3.68	0.16	1.27	0.63	50.14
	M	2.75	0.16	0.84	0.47	55.19
	B	2.00	0.09	0.68	0.40	58.32

4. Major Findings

1. Acoustic Doppler Current Profiler provides rapid and reliable measurement of river flow regime and river morphological features. However, moving bed test, compass calibration, magnetic declination, deviation and multipath errors require special consideration.
2. Riverbed material mean particle sizes decrease towards downstream reaches in conformity with the Sternberg's law in the rivers Jhelum, Chenab and Ravi. However, mean particle size increases toward downstream reach of the river Sutlej due to anthropogenic alterations in its inherent flow regime. The rivers Ravi and Sutlej are losing their inherent characteristics due to stoppage of water by India.
3. Uniformity coefficient (Cu) of the bed material have mixed and unpredictable trends due to linkage of all the four tributaries through inter-link canals.
4. Seepage rates have mixed trends in almost all the rivers and is determined by local conditions and soil strata, but are generally more in upper reaches in line with mean particle size of the bed material.
5. Silt loam, loam and sandy loam are dominant soil classes in all the three layers of the studied depth. However, coverage of sand dominant soil classes increases with increase in depth.
6. Horton's infiltration model fits better than Philip's on the infiltration data of active-flood plains. The dominant range of Horton's steady-state infiltration rate at the surface and middle layers is 15-30 mm/hr, whereas it is 60-90 mm/hr at the bottom layer showing increasing trend towards bottom layer of 1.0 m depth.
7. Average bulk density of the active-flood plains is 1.44 - 1.45 mg/cm^3 with CV in low range of 8.63 - 9.31%. Average Horton's steady-state infiltration rate varies from 31.86 - 76.75 mm/hr with high CV in the range of 135 - 158%.
8. Average van Genuchten Θs values in the three layers are 0.45 - 0.46 cm^3/cm^3 with CV in the low range of 11.56 - 12.65%; Θr 0.05 - 0.06 cm^3/cm^3 with CV in the medium range of 86 - 93%; α ranges 0.01 - 0.02 with medium CV of 70 - 77%; and n have average values of 1.06 -1.90 with CV in the medium range of 37 - 53%.
9. Average organic matter is 0.68 -1.27% and have medium variability with CV ranging 50 - 58% in the three horizons up to 1.0 m depth.

References

Ashraf, M., (2019). Water Issues: Thinking Beyond Rhetoric. Hilal (English) – The Pakistan Armed Forces Magzine.

Azam, F., M. M. Iqbal, C. Inayatullah and K. A. Malik (2001). Technologies for sustainable agriculture. Nuclear Institute for Agriculture and Biology, Faisalabad.

Berhanu, B., A.M. Melesse and Y. Seleshi (2013). GIS-based hydrological zones and soil geo-database of Ethiopia. Catena, 104: 21-31. DOI:10.1016/ j.catena.2012.12.007.

Blanckaert, K., M.G. Kleinhans, S.J. McClelland, W.S.J. Uijttewaal, B.J. Murphy, A. Kruijs, D.R. Parsons and Q. Chen (2012). Flow Separation at the Inner (convex) and Outer (concave) Banks of Constant-width and Widening Open-channel Bends. Earth Surface Processes and Landforms. Earth Surf. Process. Landforms, John Wiley & Sons, Ltd. (wileyonlinelibrary.com) DOI: 10.1002/esp.3324.

Bodner, G., P. Scholl, W. Loiskandl, and H.P. Kaul (2013). Environmental and management influences on temporal variability of near saturated soil hydraulic properties. Geoderma, 204−205: 120−129. DOI:10.1016/j.geoderma. 2013.04. 015.

Bouteiller, C.L., F. Naaim-Bouvet, N. Mathys and J. Lavé (2011). A new framework for modeling sediment fining during transport with fragmentation and abrasion. Journal of Geophysical Research, Vol. 116 (F3), 1-15, DOI:10.1029/2010JF001926, hal-01973370.

Chaudhari, P.R., V.A. Dodha, V.D. Ahire, M. Chkravarty and S. Maity (2013). Soil bulk density as related to soil texture, organic matter content and available total nutrients of coimbatore soil. International Journal of Scientific and Research Publications, 3(2):1-4.

Das Gupta, S., B.P. Mohanty, and J.M. Köhne (2006). Soil hydraulic conductivities and their spatial and temporal variations in a Vertisol. Soil Science Society of America Journal, 70: 1872−1881. DOI: 10.2136/sssaj2006.0201.

Dec, D., J. Dörner, O. Becker-Fazekas and R. Horn (2008). Effect of bulk density on hydraulic properties of homogenized and structured soils. J. Soil Sc. Plant Nutition,. 8 (1): 1-13.

Dec, D and J. Dörner (2014). Spatial variability of the hydraulic properties of a drip irrigated andisol under blueberries. Journal of Soil Science and Plant Nutrition, Vol. 14(3): 589-601. DOI: 10.4067/S0718-95162014005000047.

Diplas, P., R. Kuhnle, J. Gray, D. Glysson and T. Edwards (2008). Sediment Transport Measurements. In: Bed Material Measurement Techniques., Sediment Engineering, ASCE, DOI: 10.1061/9780784408148.Ch05.

Fahlbusch, S. and C.D. Thathe (2004). Indus Basin History of Irrigation. Drainage and Flood Management. International Commission on Irrigation and Drainage (ICID.CIID), 48 Nyaya Marg, Chanakyapuri, New Delhi 110 021, India. 1(11), 1(14-29), 2(33), 6(122).

Gilja, G., D. Bekić and N. Kuspilić (2011). Comparison of flow velocity vectors collected by using rtk-gps and bottom-tracking as a reference on a boat mounted ADCP. Faculty of Civil Engineering, University of Zagreb, Croatia. Geography Corpus ID: 56347721.

Horton, R. E. (1940). An approach toward a physical interpretation of infiltration capacity. Proc. Soil Sci. Soc. Amer., 5: 399-417.

Hu, W., M. Shao, Q. Wang, J. Fan, and R. Horton (2009). Temporal changes of soil hydraulic properties under different land uses. Geoderma, 149: 355−366. DOI: 10.1016/j.geoderma.2008.12.016.

Iqbal, J., J.A. Thomasson, N. Johnie, P.R. Owens, and F.D. Wisher (2005). Spatial variability analysis of soil physical and properties of alluvial soils. Soil Sci. Soc. Am J. 69 (4):1338-1350.

Khan, A.D., N. Iqbal, M. Ashraf, and A.A. Sheikh (2016). Groundwater investigation and mapping in the upper Indus plain. Pakistan Council of Research in Water Resources (PCRWR), pp. 70.

Loucks, D.P. and E. van Beek (2017). Water Resource Systems Planning and Management- An Introduction to Methods, Models and Application. UNESCO-IHE, Springer Nature, Gewerbestrasse 11, 6330 Cham, Switzerland. DOI: 10.1007/978-3-319-44234-1.

Malik, M.A., M. Ashraf, A. Bahzad, and A. M. Aslam (2019). Soil Physical and Hydraulic Properties of the Upper Indus Plain of Pakistan. Pakistan Council of Research in Water Resources (PCRWR), pp. 70. DOI:10.13140/RG.2.2.21104.00008.

Meek, B.D, R. Rechel, L. M. Carter, and W. R. DeTar (1992). Bulk density of a sandy loam: traffic, tillage, and irrigation-method effects. Soil Sci. Soc. Am. J., 56(2): 562-565.

MoWR (2018). National Water Policy, Ministry of Water Resources, Government of Pakistan.

Mueller, D.S., and C.R. Wagner (2006). Application of the Loop Method for Correcting Acoustic Doppler Current Profiler Discharge Measurements Biased by Sediment Transport. U.S. Geological Survey Scientific Investigations Report 2006–5079, 26 p.

Mueller, D.S., Chad R. Wagner, Michael S. Rehmel, Kevin A. Oberg, and Francois Rainville (2013). Measuring Discharge with Acoustic Doppler Current Profilers from a Moving Boat. Chapter 22 of Book 3, Section A, Techniques and Methods 3–A22 (Version 2.0), U.S. Geological Survey, Reston, Virginia. DOI: 10.3133/tm3A22.

Nielsen D.R. and J. Bouma (1985). Soil Spatial Variability. Pudoc, Wageningen, The Netherland

Oberg, K.A., S.E. Morlock and W.S. Caldwell (2005). Quality-assurance Plan for Discharge Measurements using Acoustic Doppler Current Profilers. U.S. Geological Survey Scientific Investigations Report 2005–5183, 35 p.

Peter, A., T.R. Yuzyk and R. Harrington (1989). Bed Material Sampling Error in Sand Bed Rivers. Geography Publications Paper 293. http://ir.lib.uwo.ca/geographypub/293.

Philip, J.R. (1957). The Theory of Infiltration-1, The infiltration equation and its solution, Soil Sci., 83: 345-357.

PID, (2017). Punjuab Irrigation Department, Infographic of daily rivers and canals discharges, (www.irrigation.punjab.gov.pk).

Radoane, M., N. Radoane, D. Dumitriu and C. Miclău (2007). Downstream Variation in Bed Sediment Size along the East Carpathian Rivers: Evidence of the Role of Sediment Sources. Earth Surface Processes and Landforms, Wiley Inter Science (www.interscience.wiley.com) DOI: 10.1002/esp.1568.

Rizwan, M., M.T. Siddique, H. Ahmed, M. Iqbal and T. Ziad (2016). Spatial variability of selected physico-chemical properties and macronutrients in the shale and sandstone derived soils. Soil Environ. 35(1): 12-21, 2016 www.se.org.pk Online ISSN: 2075-1141 Print ISSN: 2074-9546.

RDI (2001). WinRiver User's Guide, International Version. RD Instruments, Acoustic Doppler Solutions, P/N 957-6171-00.

Riikka, K., J. Kaseva and J. Hyväluoma (2019). Variations in near-saturated hydraulic conductivity of arable mineral topsoils in south-western and central-eastern Finland. Agricultural and Food Science 28(2): 70-83. DOI: 10.23986/afsci.79329.

Sakaguchi, A., T. Nishimura and M. Kato (2005). The effect of entrapped air on the quasi-saturated soil hydraulic conductivity and comparison with the unsaturated hydraulic conductivity. Society. Soil Science Society of America, 4(1): 139-144. DOI:10.2136/vzj2005.0139.

Schwen, A., G. Bodner, P. Scholl, G.D. Buchan, and W. Loiskandl (2011). Temporal dynamics of soil hydraulic properties and the water-conducting porosity under different tillage. Soil & Tillage Research, 113: 89−98. DOI: 10.1016/j.still.2011.02.005.

Schumacher, B.A. (2002). Method for the determination of total organic carbon (TOC) in soils and sediments, Ecological Risk Assessment Support Center Office of Research and Development, US. Environmental Protection Agency, P.O. Box 93478 Las Vegas, NV 89193-3478. NCEA-C- 1282 EMASC-001.

Simpson, M.R. (2001). Discharge Measurements Using a Broadband Acoustic Doppler Current Profiler. US Geological Survey Open-File Report 01-1. DOI: 10.3133/ofr011.

Simpson, M.R., and R.N. Oltmann (1993). Discharge measurement using an acoustic Doppler current profiler. U.S. Geological Survey Water-Supply Paper 2395, 34p. DOI: 10.3133/wsp2395.

Teledyne RDI (2015). River ADCP Guide. Teledyne RD Instruments Inc., 14020, Stowe Drive, Poway, California 92064, USA.

World Bank, (1960). Indus Waters Treaty (http://siteresources.worldbank.org).

Wang, Y. M. Shao, Z. Liu and C. Zhang (2014). Prediction of bulk density of soils in the loess plateau region of China. Surveys in Geophysics, 35(2): 395-413. DOI: 10.1007/s10712-013-9249-8.

Wetherald, R.T. and S. Manabe, (2002): Simulation of hydrologic changes associated with global warming. J. Geophys. Res., 107(D19), 4379, DOI: 10.1029/ 2001JD001195.

Zeng, C., Q. Wang, F. Zhang and J. Zhang (2013). Temporal changes in soil hydraulic conductivity with different soil types and irrigation methods. Geoderma, 193/194:290-299. DOI:10.1016/j.geoderma.2012.10.013.

ANNEXURES

1

Annexure A-I

ADCP Measurements and River Sections Bed Material Data

River Jhelum																			
Site Code	Date	Coordinates		Mag. Declin. (°)	Total tran-sects (Nos)	MPRR (±)%	Avg. Discharge (BT) (m^3/s)	River width-BT (m)	Outliers-BT (Nos)	Actual-RR-BT(±)%	Avg. Discharge (GPS) (m^3/s)	River width-GPS (m)	Outliers-GPS (Nos)	Actual-RR-GPS (±)%	FFC Discharge (m^3/s)	Avg. Seepage Rate (mm/day)	Right Bank		Left Bank	
																	C_u	D_{50} (mm)	C_u	D_{50} (mm)
JEH-01	07/11/2017	32.907	73.722	2.38	4	5	698.57	488.9	0	-1.53	705.41	490.7	0	3.18	991.22	2.350	1.60	0.21	38.46	0.24
JEH-02	10/11/2017	32.678	73.490	2.34	6	7.5	483.53	439.4	0	-5.77	492.97	432.2	1	8.9	557.92	1.305	4.00	0.14	6.33	0.35
JEH-03	13/11/2017	32.436	72.778	2.34	4	5	552.1	499.8	2	-11.16	609.17	496.59	2	-8.07	-	1.132	28.00	0.13	2.14	0.28
JEH-04	16/11/2017	32.425	72.761	2.35	4	5	610.26	520.5	0	4.01	645.43	523.56	0	-4.26	-	1.360	1.50	0.19	1.70	0.16
JEH-05	03/01/2018	32.296	72.397	2.34	6	7.5	71.486	75.5	0	-1.53	58.016	75.88	2	-13.18	-	0.458	2.00	0.22	2.05	0.31
JEH-06	08/01/2018	32.015	72.268	2.28	4	5	83.03	140.4	0	-3.38	87.394	140.18	0	-1.12	-	0.683	1.42	0.20	1.50	0.20
JEH-07	11/01/2018	31.830	72.239	2.24	8	9.7	95.532	128.7	0	5.35	97.088	128.53	0	6.92	-	0.264	1.46	0.21	1.53	0.21
JEH-08	14/01/2018	31.405	72.099	2.15	4	5	96.853	169.5	2	-15.45	107.51	172.85	0	9.12	-	0.561	1.76	0.27	4.25	0.15
JEH-09	27/01/2018	31.173	72.149	2.10	4	5	66.94	113.4	0	-3.6	71.318	113.92	3	11.36	-	0.892	1.73	0.17	2.55	0.25
JEH-10	28/02/2018	33.360	73.568	2.52	8	9.7	188.98	127.3	0	-5.34	195.67	128.07	0	-3.9	-	-	2.00	0.22	2.05	0.31
JEH-11	04/03/2018	33.495	73.603	2.56	6	7.5	353.96	106.8	0	5.19	352.21	105.16	0	4.17	-	-	1.42	0.20	1.50	0.20
JEH-12	02/03/2018	33.731	73.602	2.61	4	5	193.66	33.8	1	5.13	177.98	32.48	2	14.11	-	-	3.54	0.24	5.47	0.28
JEH-13	06/05/2018	32.495	72.882	2.37	4	5	623.7	667.5	0	3.2	629.97	667.31	2	-7.73	-	2.000	6.29	0.19	6.00	0.17
JEH-14	08/05/2018	32.394	72.560	2.37	4	5	624.42	192.4	0	-4.69	691.85	191.11	2	-5.28	-	2.050	2.20	0.20	2.00	0.20
JEH-15	17/08/2018	31.619	72.143	2.23	2	1.7	325.48	331.3	2	-14.68	363.97	350.38	2	-20.35	-	0.774	6.25	0.22	2.20	0.20

Annexure A-II

River Chenab

Site Code	Date	Coordinates		Mag. Declin. (°)	Total transects (Nos)	MPRR(±)%	Avg. Discharge (BT) (m^3/s)	River width-BT (m)	Outliers-BT (Nos)	Actual-RR-BT(±)%	Avg. Discharge (GPS) (m^3/s)	River width-GPS (m)	Outliers-GPS (Nos)	Actual-RR-GPS(±)%	FFC Discharge (m^3/s)	Avg. Seepage Rate (mm/day)	Right Bank		Left Bank	
																	C_u	D_{50} (mm)	C_u	D_{50} (mm)
CNB-01	07/10/2017	32.721	74.516	2.27	4	5	450.67	328.2	1	5.8	486.18	344.4	1	-6.54	549.42	1.270	1.80	0.37	1.78	0.39
CNB-02	10/10/2017	32.485	74.087	2.25	6	7.5	116.839	205.8	0	-6.23	113.728	205.2	0	-5.05	113.28	2.230	1.64	0.25	0.15	0.15
CNB-03	13/10/2017	32.113	73.299	2.22	6	7.5	21.819	139.7	0	-3.89	22.083	138.4	0	-2.62	-	1.584	1.86	0.25	2.33	0.24
CNB-04	14/10/2017	31.749	72.947	2.16	3	3.5	23.48	158.1	2	-10.04	25.099	157.1	3	13.14	-	1.429	2.33	0.14	1.41	0.15
CNB-05	17/10/2017	31.611	72.567	2.15	3	3.5	20.13	43.8	2	-13.42	23.552	48.36	2	28.171	-	1.559	2.62	0.19	1.66	0.22
CNB-06	21/10/2017	32.318	73.690	2.24	4	5	304.291	581.1	0	-0.77	296.699	571	0	-3.31	331.35	1.040	2.50	0.15	21.42	0.15
CNB-07	24/10/2017	31.409	72.295	2.13	4	5	38.651	84.4	0	-2.03	38.483	84.76	0	2.7	-	1.830	2.00	0.20	1.67	0.20
CNB-08	27/10/2017	31.164	72.146	2.08	6	7.5	450.141	412.5	0	2.3	455.64	413.2	0	-2.74	113.28	2.180	1.66	0.25	15.00	0.15
CNB-09	30/10/2017	30.824	71.943	2.01	4	5	157.778	251.6	0	-2.34	160.773	251.6	0	-4.7	-	0.340	1.33	0.20	1.33	0.20
CNB-10	18/01/2018	30.582	71.746	1.99	6	7.5	223.526	189.6	0	5.52	224.587	191	3	8.95	-	0.986	1.61	0.27	1.65	0.27
CNB-11	21/01/2018	30.519	71.576	1.98	8	9.7	197.51	195.3	0	2.71	204.058	194.4	0	5.18	-	1.389	40.00	0.14	48.15	0.10
CNB-12	24/01/2018	30.288	71.369	1.94	8	9.7	232.335	227.9	0	-2.88	227.668	233.8	0	-7.44	-	1.173	2.00	0.18	45.71	0.14
CNB-13	02/02/2018	30.072	71.282	1.90	4	5	200.047	255.4	0	1.75	203.182	255.9	0	-1.65	-	1.263	43.18	0.16	1.50	0.22
CNB-14	05/02/2018	29.840	71.173	1.86	4	5	151.891	196.0	0	-2.01	154.314	196.9	0	-1.55	-	0.764	8.33	0.14	1.71	0.22
CNB-15	08/02/2018	29.670	71.128	1.82	4	5	201.164	239.6	0	1.76	199.654	239.1	0	-2.04	-	1.344	3.54	0.20	2.24	0.19
CNB-16	11/02/2018	29.350	71.029	1.76	4	5	137.475	370.0	2	8.87	131.998	371.1	2	5.79	67.97	1.112	31.10	0.13	3.30	0.21
CNB-17	14/02/2018	29.260	70.906	1.75	8	9.7	110.991	217.7	3	-17.33	110.423	216.9	4	-19.33	33.99	0.784	1.54	0.18	35.00	0.14
CNB-18	17/04/2018	31.943	73.147	2.22	4	5	12.173	222.4	4	40.7	15.8	222.6	2	-12.26	-	0.653	5.50	0.28	4.17	0.22
CNB-19	12/05/2018	31.036	72.104	2.08	6	7.5	269.107	202.6	0	-1.43	278.838	203.3	0	-6.45	286.038	2.110	53.33	0.13	1.90	0.25
CNB-20	11/08/2018	32.594	74.283	2.31	4	5	1122.97	476.5	0	1.63	1167.73	475.5	0	2.73	1537.81	1.426	1.56	0.23	2.72	0.20
CNB-21	12/08/2018	32.362	73.836	2.29	4	5	1255.71	489.6	0	-4.78	1422.4	504.9	0	1.9	1498.16	1.257	1.47	0.23	25.71	0.15
CNB-22	14/08/2018	32.241	73.459	2.29	4	5	1541.48	583.4	1	6.96	2494.15	577.9	0	-3.74	-	0.720	22.86	0.14	28.00	0.14

Annexure A-III

River Ravi

Site Code	Date	Coordinates		Mag. Declin. (°)	Total transects (Nos)	MPRR(±)%	Avg. Discharge (BT) (m^3/s)	River width-BT (m)	Outliers-BT (Nos)	Actual-RR-BT(±)%	Avg. Discharge (GPS) (m^3/s)	River width-GPS (m)	Outliers-GPS (Nos)	Actual-RR-GPS(±)%	FFC Discharge (m^3/s)	Avg. Seepage Rate (mm/day)	Right Bank		Left Bank	
																	C_u	D_{50} (mm)	C_u	D_{50} (mm)
RV-01	13/04/2018	31.721	74.471	2.07	4	5	23.406	88.38	0	-1.82	22.898	90.3	1	-6.42	-	0.622	1.50	0.22	2.71	0.21
RV-02	14/04/2018	31.635	74.337	2.06	4	5	18.331	67.66	0	-1.45	17.972	71.07	2	8.22	-	1.350	1.82	0.28	1.41	0.23
RV-03	10/05/2018	31.236	73.876	2.01	4	5	344.681	254.94	0	0.71	423.717	255.6	1	-6.84	339.847	1.430		0.20	1.47	0.21
RV-04	16/08/2018	31.221	73.857	2.02	4	5	718.191	551.43	1	-7.4	651.078	554.6	1	-6.62	560.748	1.210	34.04	0.14	34.00	0.14
RV-08	22/09/2017	30.611	72.534	1.92	10	11.7	25.644	88.68	0	-4.41	25.436	89.06	0	-8.56	-	0.735	25.00	0.13	15.80	0.14

River Sutlej

Site Code	Date	Coordinates		Mag. Declin. (°)	Total transects (Nos)	MPRR(±)%	Avg. Discharge (BT) (m^3/s)	River width-BT (m)	Outliers-BT (Nos)	Actual-RR-BT(±)%	Avg. Discharge (GPS) (m^3/s)	River width-GPS (m)	Outliers-GPS (Nos)	Actual-RR-GPS(±)%	FFC Discharge (m^3/s)	Avg. Seepage Rate (mm/day)	Right Bank		Left Bank	
																	C_u	D_{50} (mm)	C_u	D_{50} (mm)
SUT-02	03/10/2017	30.091	73.231	1.76	6	7.5	7.68	60.60	0	-6.02	7.32	59.99	0	-5.92		0.348	14.20	0.16	6.50	0.14
SUT-03	30/09/2017	29.970	72.873	1.76	6	7.5	7.64	55.80	0	5.74	7.81	56.00	1	-10.96		1.251	2.40	0.17	2.30	0.15
SUT-04	28/09/2017	29.886	72.704	1.75	8	9.7	10.23	94.59	0	-8.28	10.35	95.42	0	7.70		0.589	42.80	0.13	4.40	0.14
SUT-05	25/09/2017	29.846	72.370	1.76	4	5.0	13.94	74.98	0	3.66	13.77	75.44	1	5.19		1.692	46.40	0.09	10.00	0.14
SUT-06	16/09/2017	29.576	72.117	1.72	5	6.3	62.90	73.11	0	-2.87	60.58	72.96	1	10.60		1.107	4.37	0.59	2.40	0.40
SUT-07	16/09/2017	29.451	71.851	1.71	6	7.5	79.08	84.57	0	3.36	77.62	84.23	0	-4.70		0.982	1.88	0.29	30.95	0.13
SUT-08	13/09/2017	29.437	71.633	1.72	4	5.0	145.76	294.87	3	-22.76	94.65	218.95	4	-47.26	138.75	1.700	2.00	0.14	3.14	0.60
SUT-09	10/09/2017	29.399	71.188	1.74	8	9.7	108.59	91.72	0	-7.20	111.39	90.65	0	-2.18	325.64	1.107	2.06	0.17	3.75	0.14

Annexure B-I

Measurement Sections Banks (Active Flood Plains) Data

River Jhelum																					
Site Code		Layer	Site Location		Philips Comu. Infil.				Horton Comu. Infil.			van Genchuten Constants				Soil Texture, Bulk Density and Organic Matter					
					S	A	4hr Infil Rate	R^2	Fc	k	R^2	Ɵs	Ɵr	α	n	Avg. Bulk Density	Clay	Silt	Sand	Soil Class	Organic Matter
			Lat.	Long.	$mm/hr^{1/2}$	mm/hr	mm/hr		mm/hr			cm^3/cm^3	cm^3/cm^3			g/cm^3	%	%	%		%
JEH/01	R	S	32.914	73.722	79.69	0.006	19.93	0.995	27.81	6.19	0.982	0.424	0.043	0.047	1.251	1.56	8.6	36.7	54.8	Sandy Loam	0.81
		M			55.31	0.006	13.83	0.993	14.07	18.53	0.973	0.425	0.020	0.014	1.248	1.67	2.6	66.0	31.4	Silt Loam	0.65
		B			12.05	0.006	3.02	0.982	3.99	7.28	0.988	0.418	0.057	0.048	4.668	1.44	0.6	3.3	96.1	Fine Sand	0.21
	L	S	32.906	73.729	14.35	0.006	3.59	0.970	4.15	8.40	0.981	0.498	0.041	0.009	1.537	1.43	6.6	38.7	54.8	Sandy Loam	0.86
		M			12.52	0.692	3.82	0.864	5.40	41.93	0.932	0.470	0.064	0.009	1.335	1.72	4.6	52.7	42.8	Silt Loam	0.73
		B			4.64	0.006	1.17	0.925	1.35	6.31	0.967	0.486	0.020	0.007	1.118	1.50	10.6	80.0	9.4	Silt	1.37
JEH/02	R	S	32.680	74.492	47.26	0.006	11.82	0.973	17.77	30.47	0.993	0.474	0.020	0.020	1.332	1.34	4.6	60.0	35.4	Silt Loam	0.88
		M			32.91	0.006	8.23	0.983	9.54	4.31	0.995	0.475	0.091	0.014	1.374	1.52	0.6	74.0	25.4	Silt Loam	0.55
		B			18.96	0.006	4.75	0.979	4.78	15.98	0.948	0.500	0.036	0.026	1.368	1.50	4.6	39.3	56.1	Sandy Loam	0.46
	L	S	32.677	73.495	171.51	4.949	47.83	0.962	70.07	7.17	0.921	0.473	0.063	0.021	3.845	1.40	4.0	14.7	81.3	Loamy Sand	0.48
		M			254.94	23.974	87.71	0.975	93.18	2.59	0.978	0.492	0.020	0.021	1.407	1.55	2.0	42.0	56.0	Sandy Loam	0.46
		B			20.95	31.308	36.55	0.997	39.58	16.55	0.997	0.504	0.028	0.013	1.416	1.64	6.0	44.0	50.0	Sandy Loam	0.44
JEH/03	R	S	32.580	73.155	14.36	7.574	11.17	0.993	13.31	38.01	0.995	0.479	0.020	0.009	1.359	1.55	10.6	58.7	30.8	Silt Loam	1.10
		M			27.76	33.264	40.20	0.986	17.67	0.49	0.996	0.465	0.020	0.009	1.199	1.48	6.6	49.3	44.1	Sandy Loam	0.90
		B			22.61	7.803	13.46	0.990	14.57	3.11	0.988	0.482	0.167	0.001	8.428	1.46	6.6	46.0	47.4	Sandy Loam	1.24
	L	S	32.573	73.156	7.81	21.071	23.02	0.999	24.29	21.65	0.998	0.495	0.043	0.016	1.683	1.67	6.6	33.3	60.1	Sandy Loam	0.44
		M			74.82	80.084	98.79	0.997	104.78	3.70	0.996	0.477	0.071	0.022	1.900	1.48	0.6	28.7	70.8	Loamy Sand	0.49
		B			8.70	4.446	6.62	0.998	7.69	7.43	0.997	0.486	0.170	0.012	1.245	1.55	10.6	67.3	22.1	Silt Loam	0.60
JEH/04	R	S	32.431	72.763	19.62	13.607	18.51	0.991	21.23	27.64	0.997	0.466	0.043	0.015	1.621	1.42	4.6	52.7	42.8	Silt Loam	0.48
		M			32.12	29.082	37.11	0.999	41.95	17.09	0.997	0.500	0.060	0.008	2.016	1.44	2.6	63.3	34.1	Silt Loam	0.53
		B			28.42	63.167	70.27	0.999	74.26	11.18	0.998	0.435	0.040	0.025	4.462	1.39	0.9	3.3	95.8	Fine Sand	0.49
	L	S	32.425	72.758	0.47	14.325	14.44	0.998	14.44	47.24	0.998	0.496	0.065	0.008	1.639	1.53	4.6	71.3	24.1	Silt Loam	0.85
		M			19.44	6.448	11.31	0.996	12.52	3.16	0.995	0.445	0.020	0.004	1.449	1.64	6.6	66.7	26.8	Silt Loam	0.75
		B			13.44	10.402	13.76	0.999	15.77	16.26	0.996	0.505	0.285	0.007	1.739	1.45	0.6	81.3	18.1	Silt	0.49

River Jhelum

Site Code		Layer	Site Location		Philips Comu. Infil.				Horton Comu. Infil.			van Genchuten Constants				Soil Texture, Bulk Density and Organic Matter					
					S	A	4hr Infil Rate	R^2	Fc	k	R^2	Θs	Θr	α	n	Avg. Bulk Density	Clay	Silt	Sand	Soil Class	Organic Matter
			Lat.	Long.	$mm/hr^{1/2}$	mm/hr	mm/hr		mm/hr			cm^3/cm^3	cm^3/cm^3			g/cm^3	%	%	%		%
JEH/05	R	S	32.308	72.397	30.75	0.006	7.69	0.941	8.84	16.94	0.895	0.451	0.172	0.019	1.604	1.41	23.1	39.3	37.5	Loam	1.98
		M			31.91	0.006	7.98	0.905	5.11	4.09	0.991	0.458	0.020	0.022	1.357	1.51	9.1	20.0	70.9	Sandy Loam	1.14
		B			4.56	4.418	5.56	0.986	5.87	4.24	0.990	0.481	0.020	0.059	1.083	1.70	39.1	50.0	10.9	Silty Clay Loam	1.58
	L	S	32.296	72.405	47.91	46.682	58.66	0.996	66.01	16.19	0.994	0.463	0.020	0.010	1.246	1.84	1.1	76.7	22.2	Silt Loam	1.06
		M			0.59	54.945	55.09	0.995	55.30	1019.80	0.995	0.428	0.020	0.010	1.371	1.68	3.1	47.3	49.5	Sandy Loam	1.35
		B			1533.67	62.977	446.39	0.985	456.54	2.07	0.997	0.591	0.023	0.032	1.883	1.40	1.0	1.3	97.7	Sand	0.62
JEH/06	R	S	32.017	72.263	57.27	13.534	27.85	0.996	35.73	12.11	0.993	0.505	0.056	0.009	1.543	1.53	9.1	60.0	30.9	Silt Loam	1.29
		M			89.86	40.242	62.71	0.997	75.19	9.75	0.990	0.483	0.143	0.016	2.287	1.35	3.1	48.0	48.9	Sandy Loam	0.68
		B			18.97	4.163	8.90	0.909	11.13	15.28	0.942	0.430	0.027	0.014	1.366	1.38	1.1	54.0	44.9	Silt Loam	0.65
	L	S	32.010	72.270	126.12	77.221	108.75	0.997	126.80	11.25	0.991	0.395	0.186	0.007	1.822	1.28	5.1	74.7	20.2	Silt Loam	1.96
		M			28.22	0.006	7.06	0.977	10.79	14.11	0.986	0.452	0.099	0.011	1.681	1.41	19.1	69.3	11.5	Silt Loam	1.04
		B			18.32	1.865	6.44	0.992	7.94	3.61	0.987	0.465	0.056	0.015	1.223	1.45	29.1	64.0	6.9	Silty Clay Loam	1.14
JEH/07	R	S	31.837	72.231	36.00	87.864	96.86	0.998	97.94	2.87	0.998	0.406	0.138	0.011	1.454	1.55	11.1	62.7	26.2	Silt Loam	1.46
		M			52.42	29.151	42.25	1.000	48.56	7.06	0.997	0.420	0.020	0.007	1.413	1.52	9.1	44.0	46.9	Loam	1.19
		B			15.36	12.325	16.16	0.998	18.31	11.47	0.996	0.441	0.020	0.007	1.241	1.53	13.1	72.7	14.2	Silt Loam	1.32
	L	S	31.837	72.242	8.14	0.006	2.04	0.983	2.83	9.53	0.991	0.441	0.020	0.019	1.211	1.66	15.1	65.3	19.5	Silt Loam	0.86
		M			11.77	0.006	2.95	0.976	4.04	5.18	0.987	0.440	0.020	0.006	1.229	1.59	19.1	60.0	20.9	Silt Loam	0.49
		B			5.40	0.006	1.36	0.929	1.41	10.19	0.969	0.481	0.119	0.015	1.169	1.39	5.1	73.3	21.5	Silt Loam	0.99
JEH/08	R	S	31.406	72.098	13.19	0.413	3.71	0.992	4.63	3.19	0.992	0.414	0.045	0.014	1.591	1.49	5.1	48.7	46.2	Sandy Loam	0.81
		M			0.26	7.738	7.80	0.996	7.87	839.83	0.996	0.432	0.170	0.005	2.136	1.54	9.1	63.3	27.5	Silt Loam	1.22
		B			0.08	42.434	42.43	0.999	42.40	568.28	0.999	0.415	0.020	0.009	1.186	1.52	3.1	84.0	12.9	Silt	1.34
	L	S	31.405	72.112	9.10	1.333	3.61	0.985	4.94	12.54	0.963	0.401	0.020	0.025	1.154	1.57	1.1	83.4	15.5	Silt	1.79
		M			26.61	19.167	25.82	0.976	29.68	8.45	0.963	0.424	0.020	0.013	1.382	1.48	1.1	81.3	17.5	Silt	0.97
		B			22.08	13.694	19.21	0.998	22.44	13.46	0.994	0.425	0.049	0.011	3.369	1.33	1.1	48.0	50.9	Sandy Loam	0.67
JEH/09	R	S	31.198	72.125	8.85	0.081	2.29	0.991	3.88	19.99	0.947	0.509	0.135	0.015	1.449	1.26	13.1	64.7	22.2	Silt Loam	1.87
		M			7.78	2.602	4.55	0.988	5.37	5.85	0.979	0.444	0.083	0.011	1.288	1.62	11.1	72.0	16.9	Silt Loam	1.49
		B			7.92	4.904	6.88	0.986	7.19	2.94	0.985	0.495	0.078	0.008	1.620	1.52	5.1	80.0	14.9	Silt	0.61
	L	S	31.200	72.134	7.62	0.006	1.91	0.981	2.26	5.29	0.975	0.423	0.204	0.011	2.667	1.50	3.1	48.0	48.9	Sandy Loam	0.41

River Jhelum

Site Code		Layer	Site Location		Philips Comu. Infil.				Horton Comu. Infil.			van Genchuten Constants				Soil Texture, Bulk Density and Organic Matter					
					S	A	4hr Infil Rate	R^2	Fc	k	R^2	Ɵs	Ɵr	α	n	Avg. Bulk Density	Clay	Silt	Sand	Soil Class	Organic Matter
			Lat.	Long.	$mm/hr^{1/2}$	mm/hr	mm/hr		mm/hr			cm^3/cm^3	cm^3/cm^3			g/cm^3	%	%	%		%
		M			6.67	0.006	1.67	0.993	2.38	7.85	0.977	0.435	0.020	0.007	1.162	1.49	5.1	56.0	38.9	Silt Loam	0.47
		B			4.91	0.006	1.23	0.997	1.69	6.55	0.990	0.396	0.127	0.006	1.979	1.55	5.1	48.7	46.2	Sandy Loam	0.53
JEH/10	R	S	33.358	73.569	41.97	39.837	50.33	0.999	56.75	19.21	0.997	0.466	0.097	0.025	1.727	1.42	4.6	30.0	65.4	Sandy Loam	1.25
		M			0.08	19.993	19.99	0.996	19.97	2086.65	0.996	0.345	0.063	0.017	1.367	1.66	8.6	30.7	60.8	Sandy Loam	0.90
		B			60.36	0.006	15.10	0.998	21.70	16.57	0.975	0.431	0.101	0.018	1.719	1.63	6.6	32.0	61.4	Sandy Loam	0.92
	L	S	33.357	73.571	17.10	11.402	15.68	0.992	15.34	2.06	0.996	0.507	0.095	0.007	1.613	1.33	2.6	70.7	26.8	Silt Loam	0.49
		M			508.76	54.722	181.91	0.988	177.59	1.93	0.996	0.516	0.149	0.005	2.051	1.31	0.6	72.0	27.4	Silt Loam	0.57
		B			9.06	52.840	55.10	0.996	56.59	16.99	0.996	0.487	0.146	0.009	1.657	1.43	2.6	78.0	19.4	Silt Loam	0.57
JEH/11	R	S	33.496	73.578	7.25	49.998	51.81	0.998	52.79	7.77	0.998	0.395	0.079	0.026	1.430	1.64	0.6	26.0	73.4	Loamy Sand	1.23
		M			12.67	5.452	8.62	0.992	10.22	7.09	0.982	0.435	0.136	0.019	1.574	1.53	0.6	22.7	76.8	Loamy Sand	1.05
		B			21.42	5.801	11.16	0.967	14.60	16.27	0.936	0.424	0.020	0.024	1.259	1.63	0.6	52.4	47.0	Silt Loam	1.05
	L	S	33.495	73.604	21.40	23.593	28.94	0.997	28.16	1.69	0.999	0.563	0.020	0.010	1.312	1.23	4.6	84.0	11.4	Silt	1.65
		M			11.49	5.530	8.40	0.999	9.83	7.30	0.995	0.551	0.020	0.003	1.419	1.26	2.6	80.7	16.8	Silt	1.84
		B			7.07	0.796	2.56	0.995	3.17	4.03	0.990	0.635	0.064	0.008	1.592	1.24	2.6	84.0	13.4	Silt	1.49
JEH/12	R	S	33.731	73.601	8.19	11.535	13.58	0.995	14.70	16.75	0.996	0.340	0.020	0.044	1.166	1.90	14.6	46.0	39.4	Loam	0.61
		M			20.40	21.206	26.31	0.998	29.19	13.01	0.997	0.411	0.020	0.009	1.326	1.80	8.6	42.7	48.8	Loam	0.41
		B			7.72	4.954	6.88	0.994	7.31	3.35	0.995	0.341	0.020	0.004	1.380	1.85	10.6	44.0	45.4	Loam	0.24
	L	S	33.733	73.602	7.62	13.536	15.44	0.997	16.45	11.99	0.997	0.311	0.020	0.019	1.189	1.87	10.6	56.0	33.4	Silt Loam	0.49
		M			23.60	13.248	19.15	0.995	22.14	8.28	0.992	0.338	0.020	0.012	1.185	1.84	20.6	54.0	25.4	Silt Loam	0.57
		B			7.12	9.119	10.90	0.973	11.87	17.16	0.974	0.328	0.020	0.012	1.189	1.90	16.6	56.0	27.4	Silt Loam	0.57
JEH/13	R	S	32.498	72.873	62.75	0.006	15.70	0.987	18.42	7.56	0.992	0.345	0.059	0.020	1.445	1.68	12.9	28.7	58.5	Sandy Loam	0.96
		M			12.79	9.378	12.58	0.956	13.94	17.35	0.972	0.397	0.095	0.020	1.286	1.50	28.9	43.3	27.8	Clay Loam	1.18
		B			49.87	76.646	89.11	0.998	95.64	11.90	0.999	0.390	0.062	0.012	1.558	1.58	8.9	50.0	41.1	Silt Loam	0.64
	L	S	32.491	72.885	68.93	0.006	17.24	0.999	23.96	11.55	0.985	0.371	0.062	0.017	1.800	1.44	8.9	16.0	75.1	Sandy Loam	1.61
		M			43.78	1.735	12.68	0.996	17.29	5.48	0.984	0.335	0.039	0.011	1.525	1.40	10.9	25.3	63.8	Sandy Loam	1.38
		B			60.13	0.006	15.04	0.995	19.18	7.90	0.990	0.383	0.065	0.023	1.661	1.48	8.9	24.0	67.1	Sandy Loam	1.21
JEH/14	R	S	32.397	72.548	27.93	16.782	23.77	0.997	27.36	7.72	0.992	0.408	0.079	0.021	2.633	1.41	4.9	16.0	79.1	Loamy Sand	0.66
		M			42.33	124.717	135.30	0.999	141.36	22.22	0.999	0.411	0.086	0.027	1.601	1.35	8.9	25.3	65.8	Sandy Loam	1.37

River Jhelum

Site Code		Layer	Site Location		Philips Comu. Infil.				Horton Comu. Infil.			van Genchuten Constants				Soil Texture, Bulk Density and Organic Matter					
					S	A	4hr Infil Rate	R^2	Fc	k	R^2	Ɵs	Ɵr	α	n	Avg. Bulk Density	Clay	Silt	Sand	Soil Class	Organic Matter
			Lat.	Long.	$mm/hr^{1/2}$	mm/hr	mm/hr		mm/hr			cm^3/cm^3	cm^3/cm^3			g/cm^3	%	%	%		%
		B			62.70	9.940	25.62	0.998	33.99	10.33	0.995	0.375	0.070	0.021	2.908	1.45	2.9	6.0	91.1	Sand	1.18
	L	S	32.389	72.567	0.08	46.050	46.05	0.983	46.05	228.40	0.983	0.428	0.089	0.020	1.418	1.44	8.9	21.3	69.8	Sandy Loam	1.99
		M			117.29	183.738	213.07	0.990	228.54	6.90	0.986	0.360	0.044	0.015	1.733	1.54	6.9	21.3	71.8	Sandy Loam	0.38
		B			0.08	94.893	94.89	0.997	94.82	410.40	0.997	0.366	0.020	0.017	1.322	1.59	10.9	26.0	63.1	Sandy Loam	0.20
JEH/15	R	S	31.621	72.129	26.09	10.985	17.51	0.995	19.62	4.06	0.993	0.272	0.020	0.013	1.393	1.65	8.9	18.0	73.1	Sandy Loam	0.91
		M			4.18	12.984	14.03	0.999	14.66	11.59	0.998	0.305	0.020	0.016	1.388	1.59	8.9	17.3	73.8	Sandy Loam	0.79
		B			26.25	4.248	10.81	0.989	14.59	16.40	0.986	0.447	0.031	0.010	2.007	1.44	4.9	26.0	69.1	Sandy Loam	0.57
	L	S	31.624	72.152	21.33	0.006	5.34	0.984	4.95	1.98	0.997	0.435	0.020	0.011	1.166	1.57	30.9	51.3	17.8	Silty Clay Loam	1.60
		M			5.25	6.887	8.20	0.999	8.91	13.01	0.999	0.409	0.042	0.013	1.623	1.48	8.9	30.7	60.5	Sandy Loam	0.88
		B			15.76	20.055	24.00	0.993	26.07	9.76	0.992	0.442	0.021	0.015	1.442	1.54	10.9	47.3	41.8	Loam	0.46

Outliers

Annexure B-II

River Chenab

Site Code		Layer	Site Location		Philips Comu. Infil.				Horton Comu. Infil.			van Genchuten Constants				Soil Texture, Bulk Density and Organic Matter					
					S	A	4hr Infil Rate	R^2	Fc	k	R^2	Θs	Θr	α	n	Avg. Bulk Density	Clay	Silt	Sand	Soil Class	Organic Matter
			Lat.	Long.	$mm/hr^{1/2}$	mm/hr	mm/hr		mm/hr			cm^3/cm^3	cm^3/cm^3			g/cm^3	%	%	%		%
CNB/01	R	S	32.725	74.510	4.08	5.901	6.92	0.948	7.22	58.03	0.962	0.495	0.031	0.008	1.772	1.48	4.0	65.3	30.7	Silt Loam	0.80
		M			13.75	2.644	6.08	0.986	8.21	17.05	0.996	0.489	0.042	0.008	2.052	1.47	4.0	48.0	48.0	Sandy Loam	0.87
		B			12.76	4.654	7.84	0.985	6.11	1.22	0.996	0.479	0.020	0.016	1.410	1.43	6.0	65.3	28.7	Silt Loam	1.24
	L	S	32.721	74.523	12.81	0.087	3.29	0.998	5.06	10.89	0.974	0.485	0.022	0.004	1.679	1.38	10.0	82.1	7.9	Silt	1.22
		M			7.81	12.969	14.92	0.997	16.04	45.00	0.999	0.566	0.023	0.006	2.345	1.21	4.0	67.4	28.6	Silt Loam	0.53
		B			20.49	3.184	8.31	0.996	9.83	3.42	0.998	0.457	0.020	0.001	1.649	1.42	24.0	71.4	4.6	Silt Loam	1.00
CNB/02	R	S	32.487	74.090	53.21	4.839	18.14	0.995	24.60	7.35	0.999	0.337	0.038	0.011	1.925	1.61	1.4	24.8	73.8	Loamy Sand	0.27
		M			51.67	18.163	31.08	0.998	37.41	7.38	0.994	0.450	0.050	0.016	2.980	1.44	1.4	18.1	80.5	Loamy Sand	0.70
		B			21.30	8.804	14.13	0.995	15.04	2.78	0.995	0.500	0.049	0.008	1.785	1.29	0.6	35.5	63.9	Sandy Loam	0.29
	L	S	32.481	74.092	31.76	5.569	13.51	0.998	18.09	13.42	0.989	0.458	0.067	0.014	1.647	1.41	3.4	42.1	54.5	Sandy Loam	2.07
		M			10.09	5.488	8.01	0.999	9.68	39.76	0.992	0.537	0.020	0.013	1.318	1.42	7.4	85.4	7.1	Silt	0.58
		B			65.21	26.854	43.16	0.996	51.33	7.13	0.987	0.497	0.020	0.025	1.400	1.41	5.4	67.4	27.1	Silt Loam	0.31
CNB/03	R	S	32.120	73.297	310.73	154.280	231.96	0.998	263.31	5.35	0.995	0.465	0.029	0.031	2.648	1.33	16.0	7.4	76.6	Sandy Loam	0.16
		M			392.48	148.549	246.67	0.997	256.16	2.22	0.999	0.511	0.034	0.023	2.860	1.38	0.0	4.8	95.2	Sand	0.16
		B			240.40	196.600	256.70	0.993	244.61	1.73	0.997	0.485	0.068	0.025	4.056	1.30	0.0	3.4	96.6	Sand	0.13
	L	S	32.109	73.299	76.82	0.006	19.21	0.998	28.02	9.90	0.977	0.493	0.030	0.010	1.716	1.29	2.0	50.8	47.2	Silt Loam	1.49
		M			13.65	1.315	4.73	0.994	7.20	60.16	0.966	0.470	0.020	0.011	1.373	1.45	8.0	65.4	26.6	Silt Loam	1.26
		B			383.33	67.876	163.71	0.998	199.25	4.52	0.995	0.440	0.027	0.020	2.165	1.42	1.0	16.0	83.0	Sand	0.19
CNB/04	R	S	31.750	72.946	3.51	5.921	6.80	0.999	7.39	61.52	0.997	0.474	0.065	0.005	1.536	1.50	13.4	66.0	20.6	Silt Loam	0.50
		M			11.05	103.604	106.37	0.999	107.37	7.34	0.999	0.477	0.034	0.006	2.455	1.48	3.4	36.7	59.9	Sandy Loam	0.79
		B			0.00	139.153	139.15	0.998	139.08	725.87	0.998	0.453	0.032	0.007	2.931	1.47	1.4	43.3	55.2	Sandy Loam	0.21
	L	S	31.750	72.958	31.94	16.609	24.59	0.998	27.62	4.65	0.995	0.519	0.023	0.006	1.761	1.49	7.4	68.7	23.9	Silt Loam	0.33
		M			166.88	383.994	425.71	0.999	448.97	9.80	0.998	0.685	0.038	0.014	2.654	1.26	3.4	14.7	81.9	Loamy Sand	0.32
		B			104.94	353.586	379.82	0.997	394.79	7.35	0.996	0.515	0.035	0.017	3.694	1.26	1.4	12.7	85.9	Sand	0.18
CNB/05	R	S	31.610	72.554	44.96	0.006	11.25	0.997	14.50	12.63	0.976	0.434	0.020	0.018	1.388	1.55	4.0	88.1	7.9	Silt	2.95
		M			17.22	14.181	18.49	0.997	18.46	2.00	0.999	0.431	0.020	0.013	1.503	1.50	6.0	55.4	38.6	Silt Loam	0.33

River Chenab

Site Code		Layer	Site Location		Philips Comu. Infil.				Horton Comu. Infil.			van Genchuten Constants				Soil Texture, Bulk Density and Organic Matter					
					S	A	4hr Infil Rate	R^2	Fc	k	R^2	Θs	Θr	α	n	Avg. Bulk Density	Clay	Silt	Sand	Soil Class	Organic Matter
			Lat.	Long.	$mm/hr^{1/2}$	mm/hr	mm/hr		mm/hr			cm^3/cm^3	cm^3/cm^3			g/cm^3	%	%	%		%
		B			531.97	228.349	361.34	0.998	368.55	1.98	0.999	0.466	0.057	0.032	3.375	1.29	0.8	3.8	95.4	Sand	0.09
	L	S			27.38	15.364	22.21	0.995	22.27	2.11	0.997	0.494	0.083	0.007	2.399	1.43	30.0	52.8	17.2	Silty Clay Loam	0.80
	L	M	31.603	72.564	17.61	13.665	18.07	0.996	17.44	1.72	0.998	0.556	0.020	0.085	1.167	1.35	26.0	67.4	6.6	Silt Loam	0.87
	L	B			421.36	58.383	163.72	0.995	179.83	2.49	0.998	0.496	0.020	0.005	1.259	1.51	32.0	66.8	1.2	Silty Clay Loam	1.24
CNB/06	R	S			30.67	129.807	137.48	0.999	142.46	14.71	0.998	0.516	0.076	0.019	1.421	1.21	4.0	38.8	57.2	Sandy Loam	1.40
	R	M	32.328	73.679	90.30	108.580	131.90	0.999	142.95	9.40	0.999	0.514	0.045	0.020	2.166	1.37	0.0	18.8	81.2	Loamy Sand	0.61
	R	B			59.21	280.566	295.37	1.000	304.35	10.37	0.998	0.465	0.045	0.019	2.488	1.39	0.0	14.8	85.2	Fine Sand	0.48
	L	S			59.95	0.006	14.99	0.995	20.07	5.65	0.995	0.480	0.164	0.018	1.979	1.45	2.0	12.1	85.9	Loamy Sand	0.57
	L	M	32.315	73.688	32.80	23.118	31.59	0.999	35.69	10.81	0.998	0.468	0.026	0.014	1.907	1.36	4.0	50.8	45.2	Silt Loam	0.35
	L	B			50.60	51.488	64.14	0.999	71.57	15.45	0.997	0.477	0.119	0.025	2.155	1.47	2.0	46.8	51.2	Sandy Loam	0.25
CNB/07	R	S			18.68	3.564	8.23	0.972	11.86	643.47	0.928	0.499	0.020	0.027	1.199	1.41	6.0	66.8	27.2	Silt Loam	1.68
	R	M	31.406	72.292	18.32	0.829	5.56	0.986	8.72	806.39	0.941	0.465	0.020	0.028	1.259	1.43	2.0	29.4	68.6	Sandy Loam	0.41
	R	B			51.14	32.702	45.49	0.994	51.74	6.86	0.990	0.478	0.049	0.014	1.739	1.37	4.0	46.8	49.2	Sandy Loam	0.46
	L	S			53.76	11.509	24.95	0.993	32.29	10.01	0.989	0.465	0.072	0.017	1.621	1.50	6.0	25.4	68.6	Sandy Loam	2.07
	L	M	31.401	72.306	346.28	161.549	250.96	0.989	273.28	3.91	0.984	0.503	0.020	0.019	2.142	1.35	0.0	10.8	89.2	Fine Sand	0.23
	L	B			368.76	87.679	179.87	0.993	210.65	4.05	0.986	0.518	0.028	0.017	2.961	1.28	0.0	8.1	91.9	Fine Sand	0.30
CNB/08	R	S			47.16	28.762	40.55	0.999	45.79	6.00	0.998	0.552	0.076	0.013	1.756	1.24	6.0	51.4	42.6	Silt Loam	3.68
	R	M	31.141	72.132	157.17	136.068	176.65	0.985	189.28	4.27	0.981	0.460	0.023	0.023	1.473	1.30	2.0	20.8	77.2	Loamy Sand	0.57
	R	B			131.36	35.263	68.10	0.978	81.57	4.80	0.965	0.416	0.020	0.017	1.550	1.36	2.0	20.8	77.2	Loamy Sand	0.55
	L	S			23.12	0.006	5.79	0.995	9.58	608.27	0.935	0.559	0.079	0.027	1.319	1.41	8.0	37.4	54.6	Sandy Loam	1.70
	L	M	31.134	72.164	7.48	5.350	7.28	0.943	8.16	996.66	0.958	0.495	0.077	0.012	1.670	1.21	18.0	52.8	29.2	Silt Loam	0.93
	L	B			0.00	8.869	8.87	0.887	8.87	360.39	0.887	0.481	0.111	0.021	1.278	1.46	22.0	38.1	39.9	Loam	0.72
CNB/09	R	S			52.10	2.500	15.52	0.993	24.35	491.66	0.973	0.489	0.020	0.012	1.413	1.40	9.4	56.0	34.6	Silt Loam	1.14
	R	M	30.845	71.939	183.23	506.666	553.98	0.996	579.49	8.33	0.994	0.486	0.020	0.011	2.054	1.25	3.4	6.0	90.6	Fine Sand	0.25
	R	B			238.40	365.444	425.04	0.995	460.71	9.47	0.991	0.451	0.020	0.025	1.676	1.32	1.4	3.3	95.2	Fine Sand	0.22
	L	S			15.51	0.006	3.88	0.637	0.37	4.73	0.970	0.521	0.020	0.015	1.352	1.42	12.0	62.1	25.9	Silt Loam	1.80
	L	M	30.830	71.960	15.81	8.954	13.04	0.969	14.46	4.78	0.959	0.522	0.020	0.008	1.486	1.45	6.0	72.8	21.2	Silt Loam	0.85
	L	B			22.95	7.881	13.62	0.992	16.09	5.37	0.985	0.509	0.073	0.007	2.180	1.36	6.0	66.8	27.2	Silt Loam	0.54

River Chenab

Site Code		Layer	Site Location		Philips Comu. Infil.				Horton Comu. Infil.			van Genchuten Constants				Soil Texture, Bulk Density and Organic Matter					
					S	A	4hr Infil Rate	R^2	Fc	k	R^2	Θs	Θr	α	n	Avg. Bulk Density	Clay	Silt	Sand	Soil Class	Organic Matter
			Lat.	Long.	$mm/hr^{1/2}$	mm/hr	mm/hr		mm/hr			cm^3/cm^3	cm^3/cm^3			g/cm^3	%	%	%		%
CHB/10	R	S	30.614	71.747	6.70	0.006	1.68	0.993	2.13	15.45	0.988	0.475	0.020	0.004	1.311	1.65	9.1	76.0	14.9	Silt Loam	1.67
		M			10.32	0.006	2.58	0.977	1.68	1.28	0.998	0.440	0.091	0.005	1.646	1.59	11.1	58.7	30.2	Silt Loam	1.28
		B			11.12	1.416	4.20	0.979	5.89	11.57	0.946	0.487	0.020	0.044	1.062	1.39	21.1	68.0	10.9	Silt Loam	2.00
	L	S	30.570	71.748	10.79	0.006	2.70	0.892	2.23	7.41	0.923	0.478	0.020	0.009	1.444	1.39	3.1	60.7	36.2	Silt Loam	0.81
		M			8.47	0.945	3.06	0.986	1.98	1.10	0.999	0.503	0.020	0.009	1.561	1.38	3.1	72.0	24.9	Silt Loam	0.82
		B			8.13	0.006	2.04	0.996	3.05	13.78	0.983	0.442	0.020	0.016	1.311	1.32	5.1	66.7	28.2	Silt Loam	1.04
CHB/11	R	S	30.516	71.565	9.27	0.151	2.47	0.985	3.80	10.96	0.946	0.457	0.020	0.011	1.374	1.47	3.1	58.7	38.2	Silt Loam	1.55
		M			37.99	2.689	12.19	0.997	16.20	4.99	0.989	0.475	0.046	0.005	1.891	1.48	1.1	79.3	19.5	Silt Loam	0.81
		B			11.21	0.006	2.81	0.987	3.09	11.75	0.976	0.504	0.052	0.008	2.065	1.38	1.0	72.1	26.9	Silt Loam	0.78
	L	S	30.518	71.601	42.05	0.006	10.52	0.993	13.55	7.67	0.995	0.444	0.061	0.009	1.999	1.35	1.0	64.3	34.7	Silt Loam	1.13
		M			90.87	10.122	32.84	0.997	42.58	5.40	0.987	0.485	0.020	0.010	1.614	1.28	1.2	63.0	35.8	Silt Loam	0.69
		B			48.84	43.749	55.96	0.996	52.50	1.47	0.999	0.436	0.039	0.010	2.058	1.37	1.0	55.7	43.3	Silt Loam	0.74
CHB/12	R	S	30.292	71.371	18.28	2.401	6.97	0.924	9.33	33.38	0.976	0.433	0.055	0.013	1.413	1.50	5.1	56.0	38.9	Silt Loam	0.67
		M			2.14	9.074	9.61	0.996	9.85	199.37	0.997	0.495	0.102	0.006	2.311	1.42	1.1	72.7	26.2	Silt Loam	0.59
		B			10.49	9.631	12.25	0.995	13.62	7.29	0.990	0.375	0.060	0.002	1.593	1.59	5.1	78.0	16.9	Silt Loam	0.95
	L	S	30.293	71.388	11.95	0.006	2.99	0.961	2.95	3.69	0.983	0.485	0.148	0.008	1.883	1.40	17.1	63.3	19.5	Silt Loam	1.08
		M			23.24	8.965	14.77	0.982	12.18	1.41	0.993	0.463	0.080	0.009	3.977	1.46	1.1	44.7	54.2	Sandy Loam	0.38
		B			50.36	7.247	19.84	0.994	23.29	3.50	0.993	0.505	0.030	0.006	2.362	1.40	1.0	76.3	22.7	Silt Loam	0.25
CHB/13	R	S	30.076	71.282	51.18	0.006	12.80	0.995	18.32	17.87	0.988	0.444	0.043	0.026	1.315	1.31	8.6	46.0	45.4	Loam	1.16
		M			32.59	13.276	21.42	0.999	25.70	8.64	0.993	0.523	0.030	0.012	1.532	1.39	12.6	62.7	24.8	Silt Loam	0.65
		B			19.51	11.728	16.61	0.997	19.54	13.91	0.991	0.579	0.020	0.013	1.470	1.30	6.6	66.0	27.4	Silt Loam	0.73
	L	S	30.072	71.296	39.19	0.006	9.80	0.959	9.34	7.66	0.973	0.463	0.040	0.015	1.492	1.44	6.6	38.7	54.8	Sandy Loam	1.51
		M			17.02	5.424	9.68	0.984	12.13	16.27	0.985	0.512	0.158	0.011	4.826	1.53	22.6	68.0	9.4	Silt Loam	1.29
		B			35.49	98.141	107.01	1.000	111.27	7.11	0.999	0.498	0.020	0.019	1.780	1.33	0.6	10.0	89.4	Sand	0.50
CNB/14	R	S	29.841	71.171	22.93	0.006	5.74	0.997	7.69	4.87	0.993	0.399	0.121	0.009	2.219	1.52	4.6	40.0	55.4	Sandy Loam	1.32
		M			9.40	9.083	11.43	0.994	12.82	17.41	0.993	0.521	0.020	0.007	1.553	1.49	2.6	70.7	26.8	Silt Loam	0.46
		B			20.40	181.309	186.41	0.998	190.64	20.32	0.998	0.434	0.085	0.018	3.078	1.54	6.6	66.0	27.4	Silt Loam	0.44
	L	S	29.838	71.179	18.59	1.356	6.00	0.991	6.81	2.68	0.995	0.459	0.020	0.013	1.327	1.55	2.6	70.0	27.4	Silt Loam	1.68

River Chenab

Site Code		Layer	Site Location		Philips Comu. Infil.				Horton Comu. Infil.			van Genchuten Constants				Soil Texture, Bulk Density and Organic Matter					
					S	A	4hr Infil Rate	R^2	Fc	k	R^2	Θs	Θr	α	n	Avg. Bulk Density	Clay	Silt	Sand	Soil Class	Organic Matter
			Lat.	Long.	$mm/hr^{1/2}$	mm/hr	mm/hr		mm/hr			cm^3/cm^3	cm^3/cm^3			g/cm^3	%	%	%		%
		M			112.70	73.456	101.63	0.994	116.72	14.74	0.999	0.479	0.083	0.018	2.681	1.32	0.6	48.7	50.8	Sandy Loam	0.37
		B			11.57	1.377	4.27	0.977	5.60	6.41	0.952	0.549	0.024	0.029	1.409	1.37	2.6	55.3	42.1	Silt Loam	1.04
CNB/15	R	S	29.671	71.125	29.64	23.728	31.14	0.994	34.69	8.61	0.998	0.455	0.028	0.018	1.468	1.43	0.6	28.7	70.8	Loamy Sand	0.69
		M			39.89	9.802	19.77	0.995	22.59	3.05	0.999	0.486	0.026	0.012	1.603	1.45	2.6	50.0	47.4	Silt Loam	0.64
		B			27.28	10.195	17.01	0.996	20.21	6.33	0.990	0.460	0.020	0.019	1.414	1.54	2.6	42.0	55.4	Sandy Loam	0.30
	L	S	29.658	71.132	33.77	53.110	61.55	1.000	66.33	12.83	0.999	0.414	0.020	0.010	1.487	1.55	2.6	72.0	25.4	Silt Loam	1.23
		M			13.89	87.006	90.48	0.990	91.07	40.19	0.991	0.545	0.020	0.011	1.451	1.46	2.6	82.0	15.4	Silt	0.68
		B			56.07	107.550	121.57	0.999	128.98	8.29	0.998	0.567	0.020	0.009	1.420	1.44	10.6	81.3	8.1	Silt	0.45
CNB/16	R	S	29.350	71.016	20.29	5.112	10.18	0.998	13.17	15.68	0.992	0.544	0.020	0.021	1.282	1.39	14.6	46.0	39.4	Loam	1.93
		M			16.62	21.058	25.21	0.993	27.28	6.19	0.989	0.446	0.020	0.011	1.519	1.41	12.6	58.0	29.4	Silt Loam	1.06
		B			104.13	0.006	26.04	0.970	36.74	7.07	0.930	0.449	0.071	0.022	1.538	1.52	1.1	27.9	71.0	Loamy Sand	1.64
	L	S	29.332	71.026	6.97	8.218	9.96	0.998	10.96	11.21	0.995	0.433	0.120	0.011	1.974	1.45	8.6	22.0	69.4	Sandy Loam	1.38
		M			11.10	8.029	10.80	0.998	12.37	17.45	0.999	0.526	0.066	0.019	1.275	1.49	16.6	56.0	27.4	Silt Loam	0.87
		B			12.29	15.254	18.33	0.997	18.47	2.39	0.999	0.484	0.062	0.030	1.162	1.56	30.6	49.3	20.1	Clay Loam	0.78
CNB/17	R	S	29.266	70.896	19.63	0.006	4.91	0.995	6.04	16.66	0.990	0.479	0.077	0.007	1.363	1.36	6.6	76.7	16.8	Silt Loam	1.48
		M			36.09	0.006	9.03	0.999	13.08	9.94	0.981	0.578	0.020	0.010	1.237	1.34	2.6	90.0	7.4	Silt	0.63
		B			17.21	10.813	15.12	0.999	17.58	12.30	0.995	0.519	0.059	0.005	1.826	1.40	0.6	83.3	16.1	Silt	0.28
	L	S	29.260	70.908	79.45	69.169	89.03	0.999	96.45	4.39	0.998	0.455	0.087	0.015	2.313	1.53	0.6	34.7	64.8	Sandy Loam	0.53
		M			54.36	332.506	346.09	0.998	354.56	14.58	0.998	0.404	0.057	0.019	2.630	1.36	6.6	1.3	92.1	Sand	0.31
		B			15.15	170.069	173.86	0.997	176.05	7.03	0.997	0.478	0.020	0.020	2.374	1.41	6.6	1.4	92.0	Sand	0.42
CNB/18	R	S	31.931	73.168	24.11	0.006	6.03	0.993	8.57	9.22	0.980	0.466	0.020	0.011	1.290	1.32	8.9	64.7	26.5	Silt Loam	1.86
		M			15.90	4.525	8.50	0.999	10.33	6.54	0.996	0.499	0.020	0.012	1.307	1.45	4.9	83.3	11.8	Silt	0.75
		B			0.75	7.599	7.79	0.984	7.76	30.30	0.985	0.524	0.020	0.011	1.360	1.48	12.9	66.0	21.1	Silt Loam	0.58
	L	S	31.946	73.141	5.58	60.009	61.40	0.999	62.12	60.13	0.999	0.469	0.021	0.030	1.369	1.51	2.9	22.0	75.1	Loamy Sand	1.82
		M			67.79	0.006	16.95	0.998	25.27	13.84	0.988	0.468	0.035	0.017	3.408	1.35	6.9	17.3	75.8	Sandy Loam	0.40
		B			54.79	104.515	118.21	0.999	125.04	7.41	0.999	0.501	0.020	0.016	1.512	1.34	12.9	58.0	29.1	Silt Loam	0.76
CNB/19	R	S	31.064	72.108	19.89	0.006	4.98	0.991	6.18	6.77	0.982	0.459	0.020	0.014	1.267	1.36	20.9	44.0	35.1	Loam	1.91
		M			8.88	0.124	2.34	0.994	3.01	3.36	0.995	0.442	0.020	0.009	1.256	1.46	24.9	55.3	19.8	Silt Loam	1.68

River Chenab

Site Code		Layer	Site Location		Philips Comu. Infil.				Horton Comu. Infil.			van Genchuten Constants				Soil Texture, Bulk Density and Organic Matter					
					S	A	4hr Infil Rate	R^2	Fc	k	R^2	Θs	Θr	α	n	Avg. Bulk Density	Clay	Silt	Sand	Soil Class	Organic Matter
			Lat.	Long.	$mm/hr^{1/2}$	mm/hr	mm/hr		mm/hr			cm^3/cm^3	cm^3/cm^3			g/cm^3	%	%	%		%
		B			9.55	0.006	2.39	0.978	2.57	6.23	0.980	0.501	0.020	0.008	1.292	1.53	28.9	55.3	15.8	Silty Clay Loam	1.16
	L	S			14.26	0.006	3.57	0.963	3.26	8.73	0.973	0.430	0.020	0.012	1.279	1.31	24.9	52.0	23.1	Silt Loam	1.88
	L	M	31.036	72.113	10.47	0.006	2.62	0.980	2.91	3.42	0.986	0.651	0.020	0.017	1.315	1.49	20.9	58.0	21.1	Silt Loam	1.89
		B			15.46	0.887	4.75	0.997	6.58	6.93	0.987	0.494	0.020	0.012	1.271	1.50	28.9	53.3	17.8	Silt Clay Loam	0.87
CNB/20		S			4.28	0.006	1.08	0.836	0.54	11.01	0.967	0.399	0.022	0.018	1.300	1.52	18.2	42.7	39.1	Loam	1.78
	R	M	32.612	74.266	0.86	0.006	0.22	0.616	0.05	11.11	0.896	0.428	0.020	0.010	1.181	1.77	34.2	46.7	19.1	Silty Clay Loam	1.43
		B			4.36	0.006	1.10	0.855	0.71	10.63	0.892	0.390	0.115	0.011	1.191	1.67	36.2	53.4	10.5	Silty Clay Loam	0.97
		S			13.99	0.006	3.50	0.849	2.10	7.85	0.969	0.427	0.020	0.007	1.308	1.66	18.2	41.4	40.5	Loam	1.55
	L	M	32.578	74.296	42.53	0.006	10.64	0.931	11.90	6.84	0.898	0.398	0.020	0.002	1.540	1.59	20.2	39.4	40.5	Loam	1.39
		B			39.33	0.039	9.87	0.998	15.10	8.92	0.976	0.396	0.020	0.017	1.570	1.49	12.2	35.4	52.5	Sandy Loam	1.09
		S			8.28	9.373	11.44	0.998	12.66	12.64	0.995	0.542	0.020	0.012	1.122	1.32	18.2	47.4	34.5	Loam	1.86
	R	M	32.410	73.850	14.52	21.040	24.67	0.998	27.00	17.46	0.995	0.470	0.020	0.013	1.398	1.42	18.2	58.1	23.8	Silt Loam	1.57
		B			14.68	21.731	25.40	0.999	27.51	10.85	0.997	0.486	0.052	0.010	1.414	1.43	22.2	55.4	22.5	Silt Loam	0.66
CNB/21		S			17.36	0.006	4.35	0.982	4.60	3.46	0.996	0.448	0.043	0.008	1.516	1.48	12.2	64.1	23.8	Silt Loam	1.78
	L	M	32.363	73.846	22.79	0.006	5.70	0.971	6.33	12.40	0.936	0.485	0.061	0.013	1.399	1.40	20.2	57.4	22.5	Silt Loam	1.17
		B			0.00	304.108	304.11	0.995	304.11	1604.12	0.995	0.448	0.020	0.085	1.177	1.48	24.2	57.4	18.5	Silt Loam	0.72
		S			13.05	3.462	6.72	0.995	8.57	16.23	0.997	0.517	0.020	0.008	1.430	1.31	32.9	49.3	17.8	Silty Clay Loam	1.72
	R	M	32.247	73.464	22.66	0.006	5.67	0.995	7.86	10.95	0.992	0.435	0.020	0.028	1.404	1.44	14.9	33.9	51.2	Loam	1.46
		B			29.34	6.808	14.14	0.998	17.28	5.50	0.992	0.418	0.027	0.018	1.677	1.43	6.9	20.6	72.5	Sandy Loam	0.88
CNB/22		S			41.40	5.374	15.72	0.996	21.13	9.77	0.997	0.481	0.020	0.005	1.388	1.40	0.9	52.7	46.5	Silt Loam	1.98
	L	M	32.219	73.468	75.61	41.083	59.98	0.998	70.48	11.35	0.995	0.464	0.020	0.017	1.740	1.28	4.9	37.3	57.8	Sandy Loam	1.51
		B			10.90	5.792	8.52	0.995	10.05	9.57	0.986	0.507	0.020	0.007	1.464	1.43	2.9	31.3	65.8	Sandy Loam	0.99

Annexure B-III

River Ravi

Site Code		Layer	Site Location		Philips Comu. Infil.				Horton Comu. Infil.			van Genchuten Constants				Soil Texture, Bulk Density and Organic Matter					
					S	A	4hr Infil Rate	R^2	Fc	k	R^2	Ɵs	Ɵr	α	n	Avg. Bulk Density	Clay	Silt	Sand	Soil Class	Organic Matter
			Lat.	Long.	$mm/hr^{1/2}$	mm/hr	mm/hr		mm/hr			cm^3/cm^3	cm^3/cm^3			g/cm^3	%	%	%		%
RV/01	R	S	31.723	74.471	61.66	6.042	21.46	0.997	25.26	2.90	0.998	0.472	0.064	0.010	1.531	1.27	0.9	52.7	46.5	Silt Loam	1.69
		M			66.73	30.537	47.22	0.996	52.66	3.63	0.999	0.442	0.020	0.017	1.395	1.51	4.9	37.3	57.8	Sandy Loam	1.66
		B			0.001	40.066	40.07	0.992	39.62	22.32	0.992	0.394	0.020	0.020	1.458	1.54	2.9	31.3	65.8	Sandy Loam	0.81
	L	S	31.717	74.469	58.92	14.159	28.89	0.998	35.25	5.43	0.994	0.473	0.034	0.009	1.756	1.41	2.9	52.0	45.1	Silt Loam	2.00
		M			9.18	48.657	50.95	0.996	51.77	28.16	0.997	0.484	0.027	0.009	1.869	1.38	2.9	52.0	45.1	Silt Loam	0.78
		B			60.86	39.012	54.23	0.998	62.23	10.35	0.999	0.525	0.020	0.007	1.880	1.32	2.9	57.3	39.8	Silt Loam	0.90
RV/02	R	S	31.657	74.331	20.65	3.537	8.70	0.992	11.61	17.35	0.998	0.474	0.035	0.007	1.422	1.42	6.9	72.0	21.1	Silt Loam	1.94
		M			12.63	14.793	17.95	0.996	19.63	7.75	0.992	0.460	0.020	0.005	1.344	1.59	4.9	48.7	46.5	Sandy Loam	0.98
		B			15.82	15.101	19.06	0.995	21.05	12.09	0.997	0.553	0.020	0.008	1.553	1.41	6.9	83.3	9.8	Silt	0.89
	L	S	31.641	74.351	2.55	139.216	139.85	0.997	138.68	43.27	0.997	0.472	0.020	0.011	1.438	1.41	2.9	67.3	29.8	Silt Loam	1.94
		M			44.68	0.006	11.18	0.996	15.15	7.44	0.987	0.460	0.020	0.011	1.509	1.44	4.9	44.0	51.1	Sandy Loam	1.27
		B			45.93	33.628	45.11	0.994	51.02	12.28	0.998	0.560	0.020	0.009	1.534	1.34	4.9	76.7	18.5	Silt Loam	0.98
RV/03	R	S	31.225	73.858	16.92	0.006	4.24	0.987	5.24	9.53	0.967	0.498	0.081	0.008	1.881	1.30	20.9	46.0	33.1	Loam	1.97
		M			12.52	0.006	3.14	0.984	3.54	3.31	0.988	0.477	0.020	0.012	1.333	1.26	28.9	52.0	19.1	Silty Clay Loam	1.05
		B			22.96	3.934	9.68	0.997	12.01	5.04	0.990	0.479	0.020	0.011	1.366	1.26	24.9	51.3	23.8	Silt Loam	1.14
	L	S	31.218	73.861	25.13	3.965	10.25	0.992	12.35	4.10	0.988	0.399	0.091	0.008	1.740	1.40	8.9	48.0	43.1	Loam	2.01
		M			10.84	0.006	2.72	0.982	3.29	8.66	0.981	0.345	0.038	0.013	1.684	1.50	4.9	32.0	63.1	Sandy Loam	0.44
		B			23.69	14.362	20.28	0.989	22.95	5.51	0.982	0.424	0.074	0.013	1.846	1.45	4.9	46.0	49.1	Sandy Loam	0.30
RV/04	R	S	31.147	73.548	10.64	7.592	10.25	0.996	11.52	6.76	0.993	0.497	0.194	0.012	1.499	1.25	14.2	35.3	50.5	Loam	1.95
		M			93.80	58.426	81.88	0.998	92.68	6.03	0.994	0.483	0.071	0.027	1.346	1.52	16.2	51.3	32.5	Silt Loam	1.12
		B			299.86	358.531	433.50	0.999	457.58	3.81	0.999	0.482	0.051	0.022	1.337	1.59	14.2	41.3	44.5	Loam	0.92
	L	S	31.113	73.502	22.06	0.398	5.91	0.997	8.90	10.88	0.992	0.455	0.214	0.021	1.192	1.56	43.6	38.6	17.8	Clay	1.56
		M			94.72	6.011	29.69	0.999	41.73	8.41	0.995	0.428	0.020	0.023	1.074	1.64	43.6	39.9	16.5	Clay	1.27
		B			574.47	101.033	244.65	0.997	270.67	2.47	0.999	0.477	0.020	0.005	1.168	1.50	37.6	53.9	8.5	Silty Clay Loam	1.03
RV/08	R	S	30.615	72.534	25.69	70.931	77.35	0.994	80.22	20.87	0.996	0.438	0.062	0.010	1.978	1.32	12.9	29.3	57.8	Sandy Loam	0.44
		M			44.41	48.596	59.70	0.998	65.96	10.40	0.995	0.486	0.020	0.006	1.734	1.40	4.9	33.3	61.8	Sandy Loam	2.75
		B			22.34	0.006	5.59	0.991	7.56	6.23	0.975	0.457	0.020	0.005	2.165	1.41	4.9	16.0	79.1	Loamy Sand	0.19
	L	S	30.610	72.531	167.09	23.214	64.99	0.994	89.85	12.64	0.972	0.456	0.029	0.011	3.387	1.32	10.9	71.3	17.8	Silty Loam	0.24
		M			210.02	123.283	175.79	0.995	191.22	3.88	0.992	0.435	0.022	0.008	5.815	1.36	4.9	40.0	55.1	Sandy Loam	0.16
		B			302.49	75.305	150.93	0.978	169.02	3.53	0.971	0.473	0.025	0.012	4.487	1.29	8.9	67.3	23.8	Silt Loam	0.13

Annexure B-IV

River Sutlej

Site Code		Layer	Site Location		Philips Comu. Infil.				Horton Comu. Infil.			van Genchuten Constants				Soil Texture, Bulk Density and Organic Matter					
					S	A	4hr Infil Rate	R^2	Fc	k	R^2	Θs	Θr	α	n	Avg. Bulk Density	Clay	Silt	Sand	Soil Class	Organic Matter
			Lat.	Long.	$mm/hr^{1/2}$	mm/hr	mm/hr		mm/hr			cm^3/cm^3	cm^3/cm^3			g/cm^3	%	%	%		%
SUT/02	R	S	30.092	73.234	79.69	0.006	19.93	0.995	27.81	6.19	0.982	0.463	0.037	0.010	1.781	1.37	15.4	43.4	41.2	Loam	0.65
		M			55.31	0.006	13.83	0.993	13.97	16.90	0.973	0.473	0.089	0.014	3.216	1.37	11.4	26.1	62.6	Sandy Loam	0.38
		B			12.05	0.006	3.02	0.982	3.99	7.28	0.988	0.447	0.052	0.013	2.514	1.18	15.4	29.4	55.2	Sandy Loam	0.34
	L	S	30.090	73.253	24.31	0.006	6.08	0.955	4.67	2.32	0.989	0.381	0.020	0.017	1.292	1.46	17.4	42.7	39.9	Loam	0.59
		M			185.63	223.421	269.83	0.995	285.22	4.37	0.993	0.430	0.034	0.013	4.323	1.38	3.4	4.0	92.6	Sand	0.20
		B			118.47	266.797	296.42	0.999	307.11	4.58	0.998	0.454	0.022	0.021	2.476	1.40	1.4	4.0	94.6	Sand	0.10
SUT/03	R	S	29.970	72.867	58.37	0.006	14.60	0.987	19.97	6.27	0.963	0.364	0.030	0.020	1.523	1.31	5.4	31.3	63.2	Sandy Loam	0.90
		M			75.89	12.100	31.07	0.988	26.06	1.42	0.999	0.430	0.020	0.012	1.446	1.43	9.4	50.7	39.9	Silt Loam	1.18
		B			214.05	130.236	183.75	0.996	214.43	10.23	0.988	0.365	0.035	0.007	2.290	1.47	5.4	46.0	48.6	Sandy Loam	0.36
	L	S	29.979	72.887	29.57	0.006	7.40	0.929	5.51	5.37	0.979	0.404	0.023	0.014	1.631	1.40	7.4	36.7	55.9	Sandy Loam	0.78
		M			17.07	1.755	6.02	0.998	8.31	9.61	0.985	0.492	0.020	0.006	1.470	1.41	15.4	78.7	5.9	Silt Loam	0.20
		B			15.74	0.660	4.60	0.988	6.84	18.09	0.995	0.519	0.020	0.007	1.479	1.37	11.4	80.7	7.9	Silt	0.79
SUT/04	R	S	29.886	72.701	6.12	8.023	9.55	0.994	10.44	9.97	0.991	0.387	0.030	0.011	1.470	1.45	10.9	46.0	43.1	Loam	1.31
		M			41.62	4.990	15.40	0.996	19.59	5.12	0.986	0.452	0.075	0.012	2.792	1.36	8.9	54.0	37.1	Silt Loam	0.82
		B			16.43	0.006	4.11	0.987	4.73	6.90	0.996	0.450	0.140	0.042	1.314	1.44	18.9	48.0	33.1	Loam	0.55
	L	S	29.886	72.706	38.54	0.041	9.68	0.999	14.73	9.21	0.989	0.401	0.020	0.002	1.369	1.66	20.9	70.0	9.1	Silt Loam	2.08
		M			25.89	2.024	8.49	0.996	12.29	14.77	0.983	0.472	0.081	0.008	4.251	1.44	10.9	59.3	29.8	Silt Loam	0.79
		B			46.27	14.492	26.06	0.984	22.87	1.57	0.992	0.435	0.021	0.008	1.507	1.40	14.9	53.3	31.8	Silt Loam	0.46
SUT/05	R	S	29.845	72.373	33.10	16.370	24.64	0.999	28.25	5.81	0.999	0.380	0.051	0.015	1.795	1.35	4.9	32.7	62.5	Sandy Loam	2.27
		M			41.77	0.006	10.45	0.995	13.92	11.01	0.979	0.417	0.033	0.008	1.523	1.34	8.9	70.0	21.1	Silt Loam	1.74
		B			54.91	0.006	13.73	0.997	18.56	8.43	0.987	0.468	0.036	0.005	1.781	1.22	10.9	76.0	13.1	Silt Loam	0.88
	L	S	29.845	72.369	86.20	24.134	45.68	0.997	57.54	10.08	0.990	0.418	0.053	0.008	5.818	1.21	12.1	37.5	50.5	Loam	0.94
		M			19.68	10.122	15.04	0.998	17.70	9.04	0.994	0.428	0.020	0.008	1.581	1.39	20.1	61.5	18.5	Silt Loam	1.22
		B			494.99	0.006	123.75	0.890	64.50	2.96	0.983	0.421	0.039	0.023	3.104	1.27	8.1	2.1	89.8	Sand	0.16
SUT/06	R	S	29.658	72.169	161.54	50.234	90.62	0.998	98.53	2.60	0.999	0.441	0.020	0.014	1.375	1.53	10.9	48.0	41.1	Loam	0.61
		M			161.54	50.234	90.62	0.998	98.53	2.60	0.999	0.485	0.039	0.010	1.980	1.31	0.9	17.3	81.8	Loamy Sand	0.39

River Sutlej

Site Code		Layer	Site Location		Philips Comu. Infil.				Horton Comu. Infil.			van Genchuten Constants				Soil Texture, Bulk Density and Organic Matter					
					S	A	4hr Infil Rate	R^2	Fc	k	R^2	Θs	Θr	α	n	Avg. Bulk Density	Clay	Silt	Sand	Soil Class	Organic Matter
			Lat.	Long.	$mm/hr^{1/2}$	mm/hr	mm/hr		mm/hr			cm^3/cm^3	cm^3/cm^3			g/cm^3	%	%	%		%
		B			133.38	41.261	74.61	0.998	82.48	2.95	0.998	0.472	0.020	0.006	2.154	1.33	0.9	16.7	82.5	Loamy Sand	0.36
	L	S	29.658	72.172	82.31	7.145	27.72	0.996	33.60	3.40	0.997	0.484	0.049	0.004	2.114	1.39	6.9	58.0	35.1	Silt Loam	0.68
		M			64.71	14.040	30.22	0.999	36.81	4.83	0.998	0.499	0.020	0.010	1.361	1.34	14.9	66.0	19.1	Silt Loam	1.19
		B			79.20	8.705	28.50	0.998	35.17	3.76	0.996	0.473	0.032	0.006	1.745	1.41	0.9	54.0	45.1	Silt Loam	0.67
SUT/07	R	S	29.457	71.867	42.33	0.006	10.59	0.990	13.66	8.15	0.972	0.490	0.034	0.007	2.201	1.34	2.9	54.0	43.1	Silt Loam	0.97
		M			132.72	51.571	84.75	0.995	98.64	4.89	0.991	0.487	0.032	0.012	1.850	1.38	0.9	6.0	93.1	Sand	0.99
		B			46.10	6.470	17.99	0.996	23.45	6.69	0.991	0.483	0.020	0.015	1.556	1.27	0.9	11.3	87.8	Sand	0.99
	L	S	29.455	71.864	48.22	9.326	21.38	0.996	26.33	4.55	0.998	0.490	0.034	0.007	2.201	1.34	2.9	54.0	43.1	Silt Loam	0.70
		M			226.78	178.543	235.24	0.996	264.26	8.32	0.995	0.487	0.032	0.012	1.850	1.38	0.9	6.0	93.1	Sand	0.23
		B			355.43	0.006	88.86	0.992	122.21	5.11	0.982	0.483	0.020	0.015	1.556	1.27	0.9	11.3	87.8	Sand	0.28
SUT/08	R	S	29.446	71.653	83.61	83.023	103.92	0.995	104.46	2.45	0.997	0.342	0.186	0.065	1.404	1.45	22.6	49.3	28.0	Loam	0.47
		M			93.41	105.415	128.77	0.999	136.50	3.68	0.999	0.360	0.174	0.030	1.536	1.60	30.6	47.3	22.0	Clay Loam	0.29
		B			180.43	96.476	141.58	0.997	146.80	2.40	0.999	0.367	0.154	0.040	1.347	1.62	32.6	34.7	32.7	Clay Loam	0.26
	L	S	29.444	71.653	127.18	47.794	79.59	0.995	104.46	2.45	0.992	0.342	0.186	0.065	1.404	1.45	22.6	49.3	28.0	Loam	0.77
		M			158.49	35.468	75.09	0.998	86.29	3.34	0.998	0.360	0.174	0.030	1.536	1.60	30.6	47.3	22.0	Clay Loam	0.53
		B			118.07	38.678	68.20	0.997	91.45	1479.30	0.970	0.367	0.154	0.040	1.347	1.62	32.6	34.7	32.7	Clay Loam	0.27
SUT/09	R	S	29.396	71.195	320.06	96.707	176.72	0.994	203.51	4.16	0.989	0.486	0.020	0.014	1.505	1.63	2.9	34.0	63.1	Sandy Loam	0.77
		M			348.67	62.221	149.39	0.993	174.63	3.77	0.988	0.446	0.020	0.016	1.867	1.24	0.9	2.0	97.1	Sand	0.53
		B			202.86	41.691	92.41	0.998	109.18	3.83	0.996	0.443	0.020	0.017	1.845	1.27	0.9	11.3	87.8	Sand	0.27
	L	S	29.393	71.192	10.51	0.006	2.63	0.993	3.92	7.82	0.998	0.513	0.020	0.006	1.657	1.31	4.9	76.0	19.1	Silt Loam	0.91
		M			38.98	0.006	9.75	0.998	13.91	5.22	0.996	0.444	0.031	0.006	2.180	1.37	0.9	66.0	33.1	Loam	0.39
		B			39.06	0.006	9.77	0.998	14.08	5.77	0.995	0.459	0.020	0.004	1.348	1.47	20.9	62.0	17.1	Silt Loam	0.90

About the Authors



Dr. Manzoor Ahmad Malik has retired as Director, Pakistan Council of Research in Water Resources (PCRWR), Islamabad. He graduated in 1985 in Agricultural Engineering from University of Agriculture Faisalabad, and served for two years as lecturer in the same university. Thereafter, he worked for the Water Management Wing of Govt of Punjab. He completed his PhD in Agri. Engineering in 1995 from University of Newcastle upon Tyne, UK. Several national and international distinctions including university gold medals (UAF) and Overseas Research Student Award (UK) are to his credit. As Project Director, he has completed several research and development projects both locally funded and those from international agencies such as UNICEF, WHO, KOICA, JICA, UNESCO, etc. He has more than 16 research publications/reports to his credit.



Dr. Muhammad Ashraf is basically an Agricultural Engineer and holds a PhD from the University of Newcastle, UK. He has more than 27 years research and development experience in water resources development and management in arid and semi-arid areas and has over 100 research publications to his credit. He has been working for provincial and national organizations such as On Farm Water Management Punjab and Pakistan Council of Research in Water Resources (PCRWR). He also had the opportunity to work for international organizations such as International Water Management Institute (IWMI), International Centre for Agricultural Research in the Dry Areas (ICARDA). Currently, he is working as Chairman, PCRWR.

PCRWR

Pakistan Council of Research in Water Resources
Ministry of Science and Technology, Government of Pakistan
Khyaban-e-Johar, H-8/1, Islamabad
E-mail: info@pcrwr.gov.pk website: www.pcrwr.gov.pk